

STUDIES ON HIGH-T_c SUPERCONDUCTORS WITH INEQUIVALENT CONDUCTING LAYERS

Thesis submitted

in partial fulfilment of the requirements

for the award of the Degree of

DOCTOR OF PHILOSOPHY

RAJU K. JOHN

**DEPARTMENT OF PHYSICS
COCHIN UNIVERSITY OF SCIENCE AND TECHNOLOGY
COCHIN - 682 022, INDIA**

1999

“The significant problems we face cannot be solved at the same level of thinking we were at when we created them.”

Albert Einstein

To

The memory of my father

DECLARATION

I hereby declare that the matter embodied in this thesis entitled **Studies on High- T_c Superconductors with Inequivalent Conducting Layers** is the result of investigations carried out by me under the supervision of Dr. V.C. Kuriakose in the Department of Physics , Cochin University of Science and Technology, Cochin-22 and that this work has not been included in any other thesis submitted previously for the award of any degree or diploma of any University.



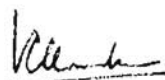
Raju K. John

Cochin-22,

6-1-1999.

CERTIFICATE

Certified that the work contained in the thesis entitled **Studies on High-T_c Superconductors with Inequivalent Conducting Layers** is the bonafide work carried out by Mr. Raju K. John under my supervision in the Department of Physics , Cochin University of Science and Technology Cochin-22 in partial fulfilment of the requirements for the award of the Degree of Doctor of Philosophy and that the same has not been included in any other thesis submitted previously for the award of any degree or diploma of any University.



Dr. V.C. Kuriakose
(Supervising Guide)

Cochin-22,

6-1-1999.

PREFACE

The work presented in this thesis has been carried out by the author as a part-time research scholar in the Department of Physics, Cochin University of Science and Technology during the period 1991-1998.

Ever since its discovery by Kammerling Onnes in 1911, the phenomena of superconductivity has proved to be of continuing interest both as a challenge to our scientific understanding and as a source of useful technology. More than a decade has elapsed since the discovery of high temperature superconductivity in layered cuprates and still there is no concensus on the microscopic mechanism responsible for high transition temperature in this class of materials. However, independent of the exact nature of the pairing mechanism within the layers, the inter layer coupling determines most of the superconducting properties of a real crystal. Hence there is a great need for a phenomenological model capable of describing the superconducting properties of these compounds.

The thesis deals with the study of superconducting properties of layered cuprates within the frame work of a modified Lawrence-Doniach (LD) model. The thesis is organized in seven chapters. Chapter I is a survey of the phenomena and theories of conventional superconductivity which can serve as a springboard for launching the study of the new class of oxide superconductors and it also includes a chronological description of the efforts made to overcome the temperature barrier. Chapter II deals with the structure and properties of the copper oxide superconductors and also the experimental constraints on the theories of high temperature superconductivity. A modified Lawrence-Doniach type of phenomenological model

which forms the basis of the present study is also discussed. In chapter III, the temperature dependence of the upper critical field both parallel and perpendicular to the layers is determined and the results are compared with d.c. magnetization measurements on different superconducting compounds. The temperature and angular dependence of the lower critical field both parallel and perpendicular to the layers is also discussed. Chapters IV, V and VI deal with thermal fluctuation effects on superconducting properties. Fluctuation specific heat is studied in chapter IV. Paraconductivity both parallel and perpendicular to the layers is discussed in chapter V. Fluctuation diamagnetism is dealt with in chapter VI. Dimensional cross over in the fluctuation regime of all these quantities is also discussed. Chapter VII gives a summary of the results and the conclusions arrived at.

A part of the present investigations has also appeared in the form of following publications

1. *Fluctuations in High- T_c Superconductors with Inequivalent Conducting Layers*, Ind.J.Phys.72A(3), 217-224 (1998).
2. *Influence of Fluctuations on the Transport Properties of Layered Superconductors with Inequivalent Conducting Layers*, Physica Scripta, 58, 656-658 (1998).
3. *Temperature Dependence of the Critical Fields H_{c2} and H_{c1} of Superconductors with Inequivalent Conducting Layers* (communicated to Physica Scripta).

and has also been presented in the following symposia/conferences

1. *Positive Curvature of the Upper Critical Field H_{c2} of Superconductors*

with Inequivalent Conducting Layers, Conference on Superconductivity, Dec.15-17,1997, University of Hyderabad.

2. *The First Critical Magnetic Field $H_{c1,z}$ of Layered Superconductors and its Dependence on Interlayer Coupling Coefficient*, Third National Conference on Phonon Physics, 20-23 Jan.1993, Cochin University of Science and Technology.

SYNOPSIS

The era of high- T_c superconductivity dawned with the discovery of superconductivity in ceramic cuprates La-Ba-Cu-O with $T_c \sim 30 - 40K$ by Bednorz and Muller in 1986. This was followed by the discovery of other cuprates with still higher transition temperatures like YBCO ($T_c \sim 90K$), BSCCO ($T_c \sim 110K$), TBCCO ($T_c \sim 130K$) etc. In all the cuprate superconductors there exist square-planar CuO_2 layers which are parallel to the ab-planes of the crystals and are sandwiched between metallic layers like the CuO chain layers in YBCO, LaO double layers in LSCO and TlO(BiO) layers in Tl(Bi) based compounds. It has been well established that the CuO_2 layers are the common features of these compounds and are the regions in the unit cell where superconductivity resides. These compounds are extremely type II superconductors and are characterised by high values of the critical temperature, very short coherence length, large anisotropy parameter and layered structure. Flux quantization and Josephson experiments indicate that the superconductivity in these materials result from pair formation, but there is still no consensus on the mechanism that enables the pairs to form. However, it does appear that whatever be the mechanism, the properties of these materials can be described by the Ginzburg-Landau concepts. But important changes arise from the extreme anisotropy, the extremely short coherence length and prominent fluctuation effects. The layered structure causes these materials to be highly anisotropic and in extreme cases to approach the two dimensional behaviour expected from a stack of decoupled superconducting film planes. A convenient model for the analysis of the consequences of layered structure in a superconducting material was proposed by Lawrence and Doniach and extensively

applied in the context of layered transition metal dichalcogenides. Several authors have employed modifications of the Lawrence-Doniach (LD) model to study the properties of layered high- T_c cuprates.

Depending on the stoichiometry the crystallographic unit cell contains varying number of CuO_2 planes. Superconductivity appears when charge carriers are doped into the CuO_2 sheets. The CuO chains in YBCO (TlO and BiO in Tl and Bi based compounds respectively) act as charge reservoirs which control the charge concentration in the CuO_2 planes. Several experiments point to the importance of the CuO chains in YBCO (TlO and BiO in Tl and Bi based compounds respectively) in enhancing the T_c although they are not required to make the material superconducting. Thus it is natural to model a ceramic superconductor as a superlattice of two dimensional superconducting (SC) sheets with multiple CuO_2 planes sandwiched between nonsuperconducting (NSC) sheets consisting of multiple metallic planes like the CuO chain layers in YBCO. Experiments by Kleiner *et al.* and also by Briceno and Zettl indicate a scenario where the strongly superconducting layers induce a finite order parameter in weakly superconducting metallic layers through proximity effect. Thus we have differing order parameter on different layers. The spatial variation of the order parameter from layer to layer in materials where NSC layers are in the proximity of SC layers gives rise to many observed phenomena. These observations necessitates the modification of the usual LD formalism with the inclusion of the inequivalency of the layers to obtain a realistic picture of cuprate superconductors. This modification was done on the lines suggested by Bulaevskii and Vagner.

We have investigated the temperature dependence of the upper critical field H_{c2} both parallel and perpendicular to the layers starting with the modified LD free

energy functional. Our calculations show a positive curvature for $H_{c2}(T)$ near T_c as is observed in D.C. magnetization measurements on single crystals of YBCO. We have showed that the curvature of $H_{c2}^\perp(T)$ not only depends on the inequivalency of the layers but also on the mass anisotropy on the chain layers. The original LD model could not explain the positive curvature of $H_{c2}^\perp(T)$ near T_c . We have also studied using our model the temperature dependence of the first critical field H_{c1} both parallel and perpendicular to the planes and also its angular dependence.

Thermal fluctuation effects in high temperature superconductors are much more pronounced than in conventional superconductors. Experimentally fluctuation contribution has been observed in conductivity, specific heat and magnetic susceptibility measurements in YBCO superconductors. The calculations based on modified LD model show that the fluctuation specific heat and parallel paraconductivity exhibit a dimensional cross over from a three dimensional regime near T_c to a two dimensional regime further away from T_c . However it is found that the temperature dependence of the c-axis paraconductivity is different from that of either the paraconductivity parallel to the layers or the specific heat, but crosses over to 0D fluctuation regime in the same temperature region. Fluctuation contribution to the London penetration depth both parallel and perpendicular to the layers and its temperature dependence has also been studied.

ACKNOWLEDGEMENTS

It gives me great pleasure to express my gratitude to Dr.V.C.Kuriakose, for his guidance and valuable suggestions. His utmost patience and constant encouragement was of immense help to me during the period of my research studies.

I am extremely thankful to Prof.K.Babu Joseph, Vice-Chancellor, Cochin University of Science and Technology and former Head, Department of Physics for his helpful suggestions and encouragement.

I thank Prof.M.Sabir, Head, Department of Physics, for allowing me to use the facilities in the Department for carrying out my research work.

I gratefully acknowledge the Principal and the Management of Union Christian College, Aluva for permitting me to carry out this work as a part-time research scholar.

I sincerely thank Mr.P.K.Suresh, Mr.R.Ganapathy and the other colleagues in the Department for extending to me their whole hearted co-operation all these years.

I remember with gratitude the encouragement and blessings received from all my teachers.

I feel a deep sense of gratitude to my mother, my wife Beena and my daughters Riya and Susan for being a constant source of inspiration in all my ventures. Their understanding, love and affection steered me through many a difficult time.

CONTENTS

PREFACE	i
SYNOPSIS	iv
ACKNOWLEDGEMENTS	vii
1 Survey of superconductivity- phenomena and theory	1
1.1 Introduction	1
1.2 Road to high temperature superconductivity	2
1.3 Early phenomenological theories	5
1.4 Ginzburg-Landau theory	7
1.5 Energy gap	12
1.6 Electron-phonon interaction and Cooper pairing	12
1.7 BCS theory	14
2 High temperature superconductivity - a phenomenological approach	22
2.1 Introduction	22
2.2 Structure and properties of copper oxide superconductors	23
2.3 Experimental constraints on theories of high- T_c superconductors	30
2.4 Anisotropic Ginzburg-Landau theory	36
2.5 Lawrence-Doniach model	41
2.6 Phenomenological model for high- T_c copper oxide superconductors	45
3 Temperature dependence of critical magnetic fields	56
3.1 Introduction	56

3.2	Upper critical field perpendicular to the layers	58
3.3	Angular dependence of H_{c2}	66
3.4	Upper critical field parallel to the layers	68
3.5	Lower critical field	70
3.6	Conclusion	73
4	Fluctuation specific heat	80
4.1	Introduction	80
4.2	Fluctuation specific heat (FSH)	82
4.3	FSH of copper oxide superconductors	85
4.4	Conclusion	89
5	Paraconductivity	90
5.1	Introduction	90
5.2	Paraconductivity of copper oxide superconductors	93
5.3	Conclusion	98
6	Superconducting fluctuation diamagnetism	100
6.1	Introduction	100
6.2	Fluctuation contribution to the London penetration depth	105
6.3	Conclusion	109
7	Summary and conclusions	111
8	References	114

CHAPTER I

SURVEY OF SUPERCONDUCTIVITY-PHENOMENA AND THEORY

1.1 Introduction

The discovery of the new oxide superconductors with transition temperatures upto 125 K or higher has generated tremendous excitement among scientists and technologists for two reasons. Firstly, the conventional electron-phonon interaction appears not to be the origin of the superconductivity in these materials leaving the fundamental physics open to investigation. Secondly they open a new temperature realm for superconducting devices which should have widespread commercial applications and these potential benefits have attracted phenomenal attention from the general public. It is becoming apparent that many of the properties of these new materials are unusual and a proper understanding will require developing and extending concepts from many areas of condensed matter physics. Nevertheless, the superconducting state appears to be associated with a pairing of charge carriers (electrons or holes as the case may be) and hence the overall superconducting behaviour of the new systems will be similar in many respects to the conventional systems. In fact, most of the familiar phenomena which are a manifestation of the superconducting state - persistent currents, Josephson tunneling, vortex lattice - have been established in the new materials. A review of the basic phenomenology of superconductivity, which can serve as a springboard for launching the study of the new class of oxide superconductors, is done in this chapter.

1.2 Road to high temperature superconductivity

The stupendous developments in the field of superconductivity all began with the liquefaction of helium by Kamerlingh Onnes in Leiden in 1908. Three years later Onnes discovered superconductivity in mercury ($T_c=4.1\text{K}$) [1]. It was observed in 1914 that superconductivity is destroyed by the magnetic field, the values of the critical field $H_c(T)$ being not very large ($H_c(0)=400\text{ Oe}$ for Hg). Until 1933 superconductivity was thought to be simply a case of vanishing electrical resistance. In that year Meissner and Ochsenfeld [2] in their landmark experiment demonstrated another basic aspect of superconductivity, perfect diamagnetism. A superconductor excludes a magnetic field except in a small penetration region near the surface where currents flow so as to balance the applied field and make the total field vanish in the interior. Superconductors known till 1937 were characterised by (1) nearly complete flux exclusion (Meissner effect) below the bulk thermodynamic critical field H_c , (2) a first order phase transition with associated latent heat in the presence of a magnetic field H , (3) near coincidence of the resistive transition with H_c and (4) except for some supercooling and superheating effects, independence of final state on magnetic and thermal history. These superconductors known as type I superconductors consisted principally of pure strain free elemental superconductors. The values of H_c are too low for these superconductors to have any useful technical application in coils for superconducting magnets. In type I superconductors critical currents are related to critical fields according to Silsbee's rule [3]. The superconducting state persists as long as the magnetic field generated by the flow of the current does not exceed the critical field. Therefore the critical

current I_c was also found to be small.

Thus even after a quarter of century after the discovery of superconductivity two obstacles remained in the path of its practical applications. The first obstacle was the temperature barrier (low values of T_c) and the second was the magnetic and current barrier (relatively weak fields H_c and currents I_c). The magnetic and current barrier was overcome in 1937 by the discovery of type II superconductivity by the Russian physicist Schubnikov [4]. Alloys and transition metals with high values of the electrical resistivity in the normal state which form the type II superconductors have superconducting electrical properties upto a field $H_{c2}(T)$. But the magnetic field first begins to penetrate the sample at much a lower field H_{c1} . Between the lower critical field H_{c1} and the upper critical field H_{c2} the flux density $\mathbf{B} \neq 0$ and the Meissner effect is incomplete (Fig.1.1). The critical fields H_{c1} and H_{c2} vary with temperature and the variation is shown in Fig.1.2. H_{c2} can assume enormous values. For example $H_{c2}(0) \simeq 200kOe$ for Nb_3Sn . As regards the critical current I_c , for high values of H_{c2} it is merely determined by the treatment of materials. Thus the current and the magnetic barriers were overcome.

In the case of type II superconductors, the onset of resistance does not come about from the destruction of superconductivity but has its roots in the phenomenon called the flux flow resistance. This mechanism results in very small critical currents for type II superconductors, but this can be eliminated by pinning the vortices in place. Imperfections in the material act as pinning centres for vortices. Superconducting wires are manufactured to be imperfect in a controlled fashion so that critical currents become quite sizeable.

Let us now outline the endeavours to overcome the temperature barrier. By 1973 the highest critical temperature $T_c \sim 23.2 - 23.9K$ was obtained for Nb_3Ge .

This remained a record till 1986. As early as 1964 superconductivity was discovered in the oxide superconductor strontium titanate at 0.7K by James Schooley at the National Bureau of Standards in Washington. David Johnston discovered in 1973 a related superconductor - lithium titanate - which superconducts at 13K. Two years later Arther Sleight [5] observed superconductivity in $BaPb_{1-x}Bi_xO_3$ at 14K for $x = 0.25$. This later led to the systematic search of the metallic oxides for superconductivity by Bednorz and Muller. They focussed their attention on metals with mixed valence states especially metal oxide compounds of copper and nickel. In 1986 they detected the appearance of superconductivity in ceramics $La_{1.85}Ba_{0.15}CuO_4$ with $T_c = 35K$ [6] heralding the era of high temperature superconductivity. In the beginning of 1987 La was replaced by Y and this led to the appearance of nitrogen superconductors with $T_c \sim 80 - 100K$. In February 1987, Maw-Kuen Wu of the University of Alabama and Ching Wu Chu of the University of Houston [7] discovered the $YBa_2Cu_3O_{7-x}$ compound (123 compound) with $T_c = 94K$. Almost one year after Maeda *et al.* [8] discovered superconductivity in $Bi_2Sr_2Cu_2O_{7+y}$ at 120 K. During a short time after that Sheng and Herman [9] synthesised three thallium oxide compounds $Tl_2Ba_2Ca_{n-1}Cu_nO_{2n+4}$ with $n=1,2$ and 3. In the same year Parkin *et al.* [10] observed superconductivity in another family of thallium oxides $Tl_1Ba_2Ca_{n-1}Cu_nO_{2n+3}$. The highest critical temperature ($T_c \sim 30K$) in non-copper oxide systems was obtained by Cava *et al.* [11] in $Ba_{1-x}K_xBiO_3$ in 1988. The bismuthates are essentially three dimensional and display none of the antiferromagnetism characteristic of the cuprates.

Superconductivity has also been reported at ~ 94 K in $HgBa_2CuO_4$ [12], the first member of the homologous series $HgBa_2Ca_{n-1}Cu_nO_{2n+2}$ with $n=1,2,3,\dots$ [13,14]. Higher transition temperature of 134 K was achieved in $HgBa_2Ca_2Cu_3O_8$ which

has three CuO_2 layers per unit cell. The T_c of this compound was found to increase continuously with pressure at an increasing rate upto 17 kbar without any sign of saturation. The thermopower shows an underdoped characteristic. These observations suggest that the T_c of HBCCO can be further enhanced with proper modulation doping without inducting any structural instabilities. Molecular solids of the buckminster fullerene C_{60} doped with K, Rb and Cs have been shown to exhibit superconductivity with critical temperatures in the range 20 K to 33 K [15,16]. Fig.1.3 shows the evolution of critical temperature since the discovery of superconductivity.

1.3 Early phenomenological theories

The discovery of Meissner effect led to the two fluid model, to the development of the thermodynamics of superconductivity by Gorter and Casimir [17] and to the classification of the superconductive-normal transition as a phase transition of the second kind. The two fluid model considers two varieties of electrons in a superconductor: superconducting and normal electrons. In 1935 F. and H. London [18] analysed the electrodynamics of superconductors using the two fluid model and proposed two equations to govern the microscopic electric and magnetic fields.

$$\mathbf{E} = \frac{\partial}{\partial t}(\Lambda \mathbf{J}_s) \quad (1.1)$$

and

$$\mathbf{h} = -c \text{curl}(\Lambda \mathbf{J}_s). \quad (1.2)$$

where the phenomenological parameter Λ is given by

$$\Lambda = \frac{4\pi\lambda_L^2}{c^2} = \frac{m}{n_s e^2}.$$

$$\mathbf{J}_s = n_s e \langle \mathbf{v}_s \rangle = -\frac{\mathbf{A}}{\Lambda c}$$

is the supercurrent, \mathbf{A} is the vector potential, n_s is the number density of superconducting electrons, \mathbf{h} is the magnetic flux density on a microscopic scale, $\langle \mathbf{v}_s \rangle$ is the local average velocity of the electrons in the presence of the field and e is the electronic charge. The second equation when coupled with Maxwell's equation

$$\text{Curl } \mathbf{h} = \frac{4\pi}{c} \mathbf{J}$$

leads to

$$\nabla^2 \mathbf{h} = \frac{\mathbf{h}}{\lambda_L^2}. \quad (1.3)$$

This implies that a magnetic field is exponentially screened from the interior of a sample with penetration depth λ_L , called the London penetration depth [Fig.1.4].

The failure of the London theory for certain superconductors led Brian Pippard [19] to propose in 1953 a non-local generalization of the London equations. He introduced the concept of coherence length (ξ_0) which is the range of correlations between the superconducting electrons in the condensed state. ξ_0 could be estimated from an uncertainty principle argument as

$$\xi_0 = a \frac{\hbar v_F}{k_B T_c}$$

where a is a numerical constant and v_F is the Fermi velocity.

The derivation of the London equations assumes that \mathbf{J}_s and hence \mathbf{h} have negligible variations over distances $\sim \xi_0$. According to equation (1.3) \mathbf{h} varies in a range λ_L . Thus London equations hold only if $\lambda_L \gg \xi_0$. In elemental superconductors like tin and aluminium λ_L is small ($\sim 300 \text{ \AA}$), the Fermi velocity v_F is large

($v_F \geq 10^8 \text{ cm/s}$) and ξ_0 is large ($\xi_0 = 10^4 \text{ \AA}$ for Al). Thus for these metals belonging to the category of type I superconductors $\xi_0 \gg \lambda_L$ London equations do not apply but they are properly described by the Pippard non-local theory. For transition metals and intermetallic compounds of the type Nb_3Sn , λ_L is large ($\sim 200 \text{ \AA}$), the Fermi velocity is small ($\sim 10^6 \text{ cm/s}$), T_c is high ($\sim 18K$ for Nb_3Sn) and ξ_0 is small ($\sim 50 \text{ \AA}$). Therefore for this class of materials belonging to the category of type II superconductors, $\lambda \gg \xi_0$ and London equations are applicable in weak fields.

1.4 Ginzburg-Landau theory

A major landmark in describing the phenomenology of the superconducting state was made by Ginzburg and Landau [20] in the year 1950. The Ginzburg-Landau (GL) theory introduces a complex pseudo wavefunction ψ as an order parameter within Landau's general theory of second order phase transitions. The order parameter ψ describes the superconducting electrons, the local density of which is given by $n_s = |\psi(x)|^2$. Then using a variational principle and working from an assumed series expansion of the free energy in powers of ψ and $\nabla\psi$ with expansion coefficients α and β , a differential equation similar to the Schroedinger equation is obtained. Following Landau, the free energy of a superconductor is written as

$$F_s = F_n + \int d\mathbf{r} \left[\alpha |\psi|^2 + \frac{\beta}{2} |\psi|^4 + \frac{1}{2m^*} \left| (-i\hbar\nabla - \frac{e^* \mathbf{A}}{c})\psi \right|^2 + \frac{\mathbf{h}^2}{8\pi} \right]. \quad (1.4)$$

F_n is the free energy in the normal state. $\mathbf{h} = \nabla \times \mathbf{A}$, where \mathbf{A} is the vector potential of the field \mathbf{h} . The coefficients α and β are regular functions of the

temperature T so that $\alpha(T)$ is negative for $T < T_c$ and vanishes at $T = T_c$ where as $\frac{d\alpha}{dT}$ remains finite at $T = T_c$. Close to T_c ,

$$\alpha(T) = (T - T_c) \left(\frac{d\alpha}{dT} \right)_{T=T_c}.$$

$\beta(T)$ is a positive quantity and close to T_c ,

$$\beta(T) \simeq \beta(T_c).$$

Minimizing the free energy for variations of the order parameter ψ and of the magnetic field \mathbf{h} ,

$$\frac{1}{2m^*} \left[-i\hbar\nabla - \frac{e^*\mathbf{A}}{c} \right]^2 \psi + \alpha\psi + \beta |\psi|^2 \psi = 0 \quad (1.5)$$

and

$$\frac{\text{Curl } \mathbf{h}}{4\pi} = \frac{\mathbf{j}}{\mathbf{c}} = \frac{e^*\hbar}{2im^*c} (\psi^*\nabla\psi - \psi\nabla\psi^*) - \frac{e^{*2}}{m^*c^2} \psi^*\psi\mathbf{A}. \quad (1.6)$$

$e^* = 2e$ and m^* is sometimes taken as $2m$. Otherwise it is left arbitrary. e and m are electronic charge and mass respectively. In principle, the GL equations (1.5) and (1.6) allow the order parameter ψ , the field \mathbf{h} and hence the currents to be calculated. However, these equations are non-linear and the calculations are rather tedious and in general purely numerical. Nevertheless, it is possible to draw from them a number of qualitative conclusions without calculating ψ or \mathbf{h} explicitly. In the case of linear problems and for certain limiting cases the complete solution can be found. With this formalism Ginzburg and Landau were able to treat two features which were beyond the scope of the London theory: (i) non-linear effects of magnetic fields strong enough to change n_s and (ii) the spatial variation of n_s .

If we consider a situation where there are neither currents nor magnetic fields and if we choose a gauge in which ψ is real, then in one dimension equation (1.5)

becomes,

$$-\frac{\hbar^2}{2m} \frac{d^2\psi}{dx^2} + \alpha\psi + \beta\psi^3 = 0 \quad (1.7)$$

There are two solutions for equation(1.7). (i) $\psi = 0$ which describes the normal state and (ii) $\psi = \psi_0 = \left(-\frac{\alpha}{\beta}\right)^{\frac{1}{2}}$ which describes the ordinary superconducting state with perfect Meissner effect. ψ_0 corresponds to the lowest free energy when $\alpha < 0$ i.e. when $T < T_c$. The thermodynamic critical field is obtained as $H_c^2(T) = \frac{4\pi\alpha^2}{\beta}$.

In the case of very weak fields, ψ is expected to vary very slowly close to the value of ψ_0 . By setting $\mathbf{A} = 0$ and $f = \frac{\psi}{\psi_0}$ in equation (1.5), we get

$$-\xi^2(T)\nabla^2 f + f - f^3 = 0 \quad (1.8)$$

where $\xi(T)$ has the dimension of length and is given by the expression $\xi^2(T) = \frac{\hbar^2}{2m|\alpha|}$. From equation (1.8) it is clear that the range of variation of f and hence that of ψ is $\xi(T)$ which is one of the two characteristic lengths of the GL scheme and is called the temperature dependent coherence length.

The second characteristic length comes into play when we introduce electromagnetic effects. In weak fields and to the first order in \mathbf{h} , $|\psi|^2$ can be replaced by ψ_0^2 , the value of $|\psi|^2$ in the absence of the field. Equation (1.6) for the current now becomes

$$\text{Curl } \mathbf{j} = -\frac{4e^2}{mc} \psi_0^2 \mathbf{h}$$

which is equivalent to the London equation with the penetration depth

$$\lambda(T) = \left[\frac{mc^2}{16\pi e^2 \psi_0^2} \right]^{\frac{1}{2}} \quad (1.9)$$

Expression (1.9) is the same as the expression for the London penetration depth λ_L where n_s , the number density of the superconducting electrons is replaced by ψ_0^2 . $\lambda(T)$ is the second characteristic length of the GL scheme and is termed temperature dependent penetration depth which determines the range of variation

of the magnetic field *i.e.* of \mathbf{h} and \mathbf{A} . In 1959, Gorkov [21] was able to show that GL theory was in fact a limiting form of the microscopic theory of Bardeen, Cooper and Schrieffer [22] valid near T_c in which ψ is directly proportional to the gap parameter Δ . According to Gorkov's derivation both $\xi(T)$ and $\lambda(T)$ vary as $(T_c - T)^{-\frac{1}{2}}$ for $T \rightarrow T_c$. However their ratio $\kappa(T) = \lambda(T)/\xi(T)$ remains finite for $T \rightarrow T_c$. The GL theory can be used to describe type I as well as type II materials in the temperature range close to T_c . Following Abrikosov [23] the distinction between type I and type II may be made as follows:

Type I superconductivity : $\kappa < \frac{1}{\sqrt{2}}$

Type II superconductivity : $\kappa > \frac{1}{\sqrt{2}}$

In 1957, Soviet physicist Alexei Abrikosov [24], using the GL scheme conceived a theory for explaining the magnetic properties of type II superconductors. The upper critical field H_{c2} of these materials is related to the thermodynamic critical field H_c by the relation $H_{c2} = \kappa\sqrt{2}H_c(T)$. For type II superconductors $\kappa > \frac{1}{\sqrt{2}}$ and hence $H_{c2} > H_c$. For applied fields H smaller than H_{c2} but greater than H_{c1} the specimen is in a mixed state. This state reduces the amount of energy that a superconductor must expend in expelling the magnetic fields by letting the field partially penetrate the material. In ordinary Meissner effect magnetic fields are kept at bay by diamagnetic screening currents that flow on the surface of the superconductor. In the mixed state magnetic field penetrates the superconductor through a number of cylindrical cores of normal material distributed across the specimen. Tiny circulating currents surround each core maintaining a magnetic field. These cores, known as vortices, each contain exactly one quantum of flux $\Phi_0 = 2 \times 10^{-7} \text{gauss} - \text{cm}^2$ whatever the value of κ . The current encircling each

vortex generates a magnetic field that interacts with the field of other vortices. As a result the vortices repel one another and therefore arrange themselves into an orderly array called the fluxon lattice. To reach the lowest energy state this lattice takes on hexagonal symmetry. An applied magnetic field thus penetrates the superconductor in a regular pattern. Since each vortex contains exactly one flux quantum increasing the magnetic field merely increases the number of vortices. The vortices themselves are quite tiny - their size is set by the superconducting coherence length so that large number of them can fit into a piece of superconductor. The superconductor finally enters the normal state when no more vortices can be packed into the material. Thus type II superconductors can remain superconducting in far greater magnetic fields than type I superconductors. Moreover type II superconductors obey the Silsbee rule only until there is enough magnetic field to drive the material into the mixed state. At that point the flux flow resistance dominates the current carrying ability of the superconductor.

The fields H_c , H_{c2} and H_{c1} were obtained from the GL theory by Abrikosov as

$$H_c = \frac{1}{2\pi\sqrt{2}} \frac{\phi_0}{\lambda(T)\xi(T)} \quad (1.10)$$

$$H_{c2} = \frac{\Phi_0}{2\pi\xi^2(T)} \quad (1.11)$$

$$H_{c1} = \frac{\Phi_0}{4\pi\lambda^2(T)} [\log \kappa + 0.08]. \quad (1.12)$$

The GL theory is now universally accepted as a master stroke of physical intuition which embodies in a simple way the macroscopic quantum mechanical nature of the superconducting state that is crucial for understanding its unique electro-

dynamic properties.

1.5 Energy Gap

One of the central features of a superconductor is that there exists an energy gap Δ of the order of $k_B T_c$ in the excitation spectrum for electrons, which was first discovered in specific heat measurements [134]. In a normal metal the specific heat at low temperatures is given by

$$C = \gamma T + B T^3$$

where the linear term is due to electron excitations and the cubic term originates from phonon excitations. Below the superconducting transition, however, the electronic contribution was found to be of the form $\exp(-\Delta/k_B T_c)$ which is characteristic of a system with a gap in the excitation spectrum of energy 2Δ . The gap is directly related to the superconducting order parameter and hence $\Delta \rightarrow 0$ as $T \rightarrow T_c$. Starting about 1953 a number of experiments yielded a measurement of Δ . The energy gap can be directly observed in tunneling measurements, in the electromagnetic absorption spectrum in the far infra-red and in the life time of the phonon excitations.

1.6 Electron-Phonon Interaction and Cooper Pairing

The first indications that the electron-phonon interaction was responsible for superconductivity came as late as 1950 with Frohlich's [25] theoretical model describing an attractive electron-electron interaction mediated by phonons and the

discovery of the isotope effect [26,27] showing the proportionality of T_c and H_c to $M^{-\frac{1}{2}}$ for isotopes of the same element.

According to classical physics, any two particles, no matter how weakly attracted, can form a bound state. In contrast, tightly bound quantum mechanical particles have large average velocities and thus large energies of motion. Unless the attractive binding energy is sufficient to overcome this kinetic energy, no bound states will be formed. The attractive interaction brought about by phonons was far too weak to produce a bound state.

Leon Cooper [28] was able to show that in the presence of an attractive interaction, no matter how weak, two electrons added to the Fermi sea will form a bound pair. Even though the kinetic energies of the added pair is higher, the overall energy of the system is lowered by the formation of the bound pair. This implies that the Fermi sea is unstable against the formation of bound pairs because the energy of the system could be lowered by taking two electrons of a given energy from the top of the sea and putting into a bound state formed from energies above the sea. The presence of the other electrons of the Fermi sea allows this to happen; two isolated electrons in the presence of a weak attractive interaction could not form a bound state. Thus pair formation is a many body effect.

The pairs of electrons in a superconductor are very weakly bound and the amount of energy needed to break up a pair is only a few thousandths of an electron volt. In comparison, the Fermi energy of the electrons in a metal is generally 5 to 10 electron volts. So the pairs should break up very easily. Under proper conditions, the pairs continually recombine in order to maintain a state of lowered energy and on the average, electrons spend their time in paired states.

The electron-phonon interaction is described as a scattering event in which the

total momentum is conserved. But the energy conservation of the electrons taking part in the process is not required. Cooper showed that the energy lowering from the formation of a bound state will overcome the additional kinetic energy of the electrons when the electrons of a pair have equal and opposite momentum. The largest number of energy lowering scattering process can occur between electrons of equal and opposite momentum. Such bound pairs of electrons of equal and opposite momenta are called Cooper pairs.

1.7 BCS Theory

Cooper considered the artificial case of two new electrons added to a metal. But the BCS theory has to deal with the case of 10^{23} electrons per cubic centimetre already present in a real metal. In order to develop a theory that could predict the behaviour of the multitude of electrons in a superconductor, BCS made a simplifying assumption. Rather than attempting to analyse the effects of interactions between three, four or more electrons at a time, they assumed that only pair interactions matter. So in considering the behaviour of a pair, the presence of all the other electrons merely limits the states into which an electron pair can scatter. Relegating the other electrons into the background role results in a mean field theory. By making the mean field assumption, the BCS theory treats all the electrons at once.

As we have seen an attractive interaction results in the Fermi sea of electrons being unstable against the formation of bound pairs of electrons formed from states above the Fermi level. Therefore it is necessary to find a new ground state of the system in which many pairs of electrons of opposite momenta are in higher energy

states than the maximum of the normal Fermi sea. The BCS ground state consists of Cooper pairs of electrons with equal and opposite momenta. The electrons in a superconductor condense into the BCS ground state. The most important property of the BCS ground state is that the pairs are completely interchangeable and indistinguishable from one another. They do not have to obey the Pauli exclusion principle that restricts individual electrons to separate quantum states. The paired electrons can all be described by a single quantum-mechanical wave function. The pair state corresponds to the macroscopic quantum state predicted by Fritz London and constitutes a highly ordered state. The pairs overlap in such a multiple fashion that the ordering propagates through out the lattice so that we have long range order in momentum space.

According to the BCS theory, the binding energy of the Cooper pairs shows up as a gap in the density of electronic states for the superconductor and a minimum energy $E_g = 2\Delta(T)$ should be required to break a pair creating two quasi particle excitations. The energy gap $\Delta(T)$ was predicted to increase monotonically from zero at T_c to a limiting value

$$\Delta(0) = 1.764 k_B T_c \quad \text{for } T \ll T_c$$

In the vicinity of the transition temperature, the theory yields

$$\Delta(T) = 1.74\Delta(0) \left[1 - \frac{T}{T_c}\right]^{\frac{1}{2}}$$

The continuous decrease of the superconducting order parameter to a value of zero is a characteristic of a second order phase transition. In the present case the behaviour is controlled by an exponent value of $\frac{1}{2}$ which is a result of mean field theory. Like the energy gap, the critical magnetic field approaches zero continu-

ously according to the relation

$$H_c(T) = H_c(0) \left[1 - a \left(\frac{T}{T_c} \right)^2 \right]$$

The electronic term in the heat capacity at low temperatures is

$$c_s = 1.34 \gamma T_c \left[\frac{\Delta(0)}{T} \right]^{\frac{3}{2}} e^{-\Delta(0)/T}$$

which is characteristic of a system which possesses an energy gap in the excitation spectrum. Most conventional superconductors actually exhibit the predicted ratio between the energy gap and the critical temperature and are known as BCS type or weakly coupled superconductors. Certain other superconductors - for example, lead - have somewhat larger values for energy gap than the theory would predict and are called strong coupled superconductors.

The existence of a gap in the low energy excitation spectrum is not a necessary condition for the occurrence of typical superconducting properties such as the Meissner effect and permanent currents. Gapless superconductivity has been shown to exist. The criterion for superconductivity seems to be the existence of a strong pairing correlation and this does not necessarily imply the existence of finite gap in the excitations. However, the existence of a gap in most superconductors has been of great importance for the establishment of the microscopic theories.

The BCS theory has been used to predict new phenomena which have been later demonstrated experimentally. One of the most important of these discoveries is that of tunneling of electrons through a thin insulating layer between a superconductor and a normal metal or between two superconductors. This was experimentally verified by Giaever [29] in 1960. A couple of years later, Josephson [30] predicted that if two superconductors are separated by a very thin insulating layer a supercurrent can tunnel between them. This phenomenon called Josephson

tunneling was first demonstrated experimentally by Rowell and Anderson [31].

The contributions of Bogoliubov, Gorkov and Eliashberg in the USSR further developed and refined the BCS theory.

The well known formula for the critical temperature in the BCS theory is

$$T_c = \Theta \exp(-1/\lambda_{eff}) \quad (1.13)$$

where Θ is the region of attraction between electrons near the Fermi surface and λ_{eff} is a dimensionless parameter characterizing the intensity of this attraction. Since equation (1.13) gives $T_c \leq 30K$ for the phonon mechanism of superconductivity, the high temperature copper oxide superconductors are left out of the ambit of the theory. However, with a reinterpretation of Θ and λ_{eff} the theory could be adapted for other type of interactions such as excitons, plasmons, etc.

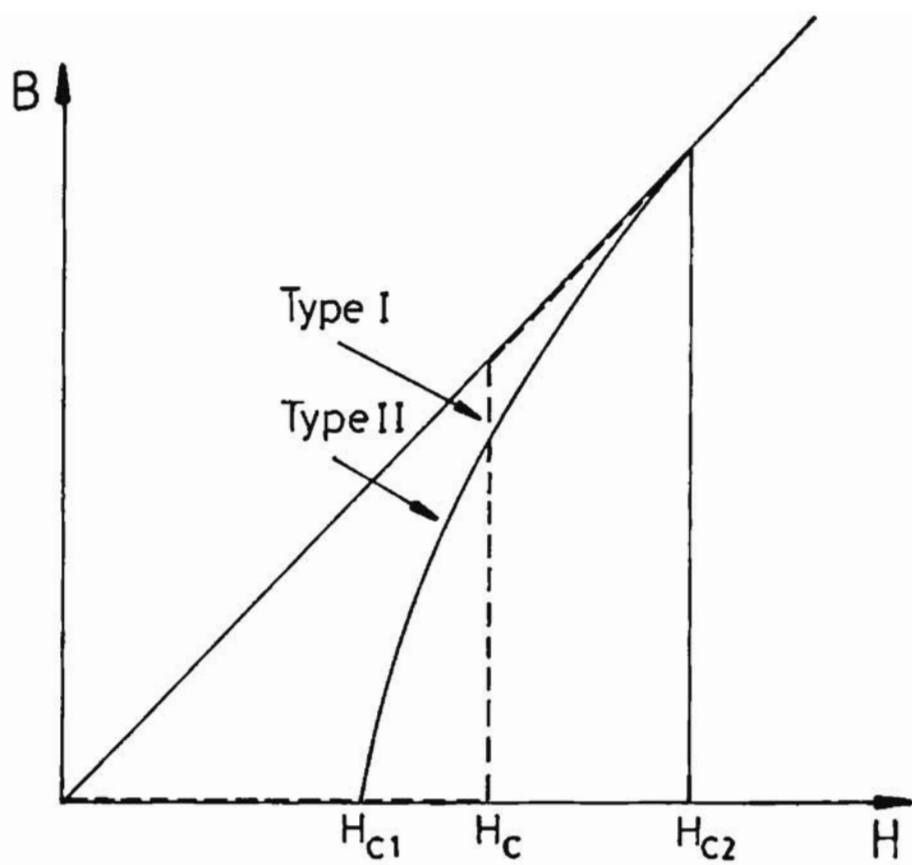


Figure 1.1 Schematic variation of the induction B versus field H in a type II superconductor.

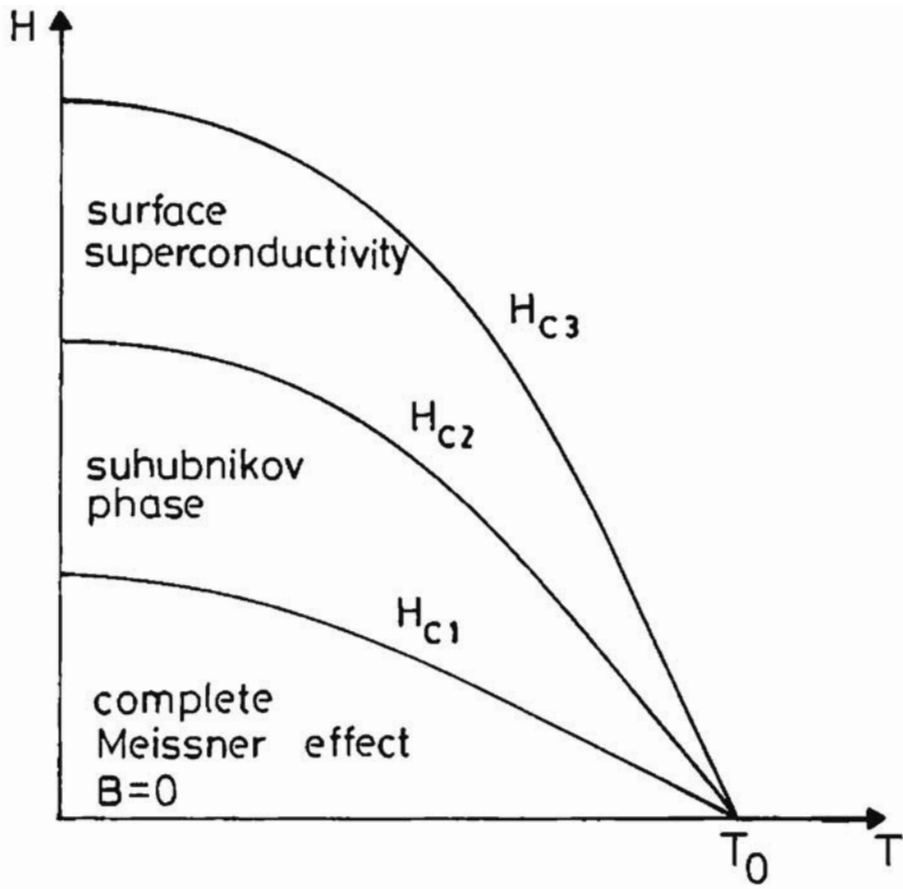


Figure 1.2 Phase diagram for a long cylinder of a type II superconductor.

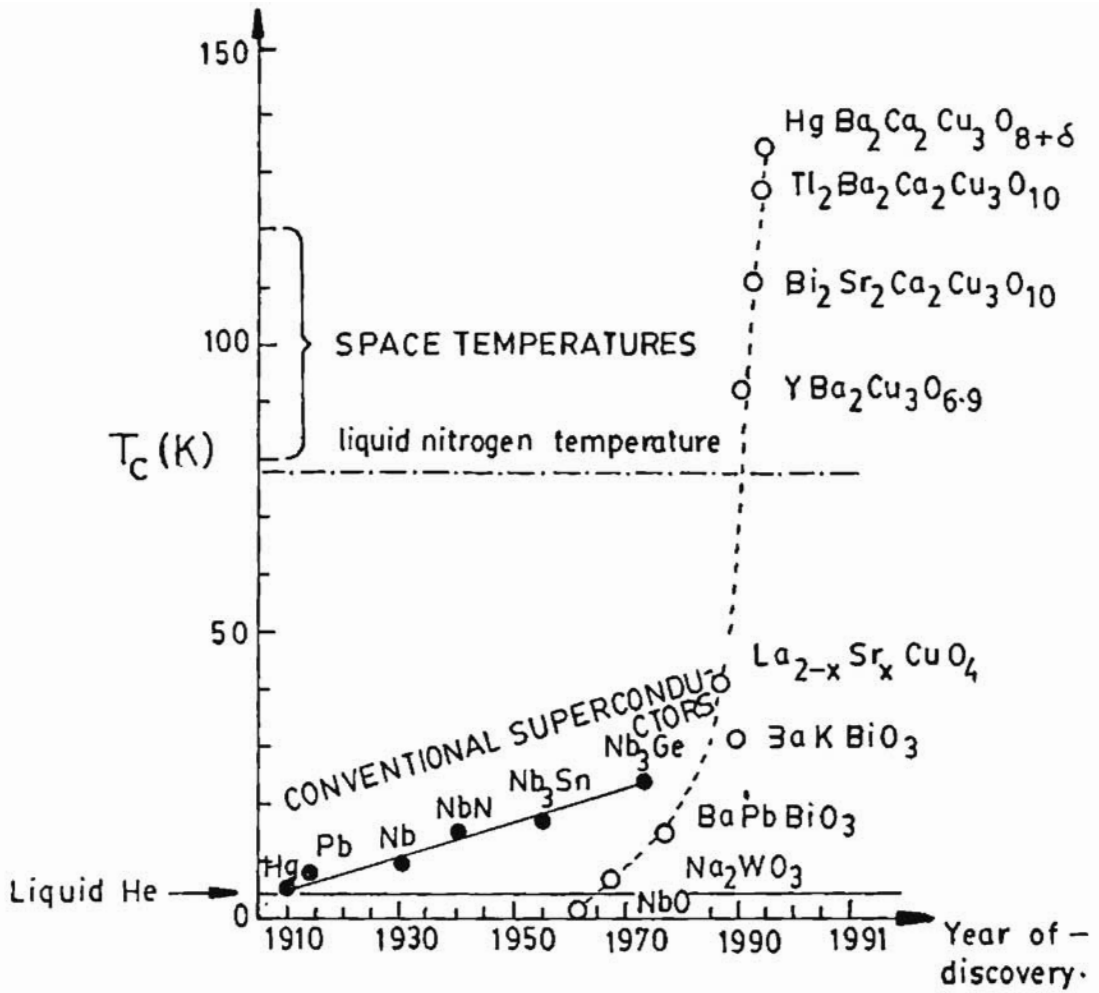


Figure 1.3 The evolution of critical temperatures since the discovery of superconductivity.

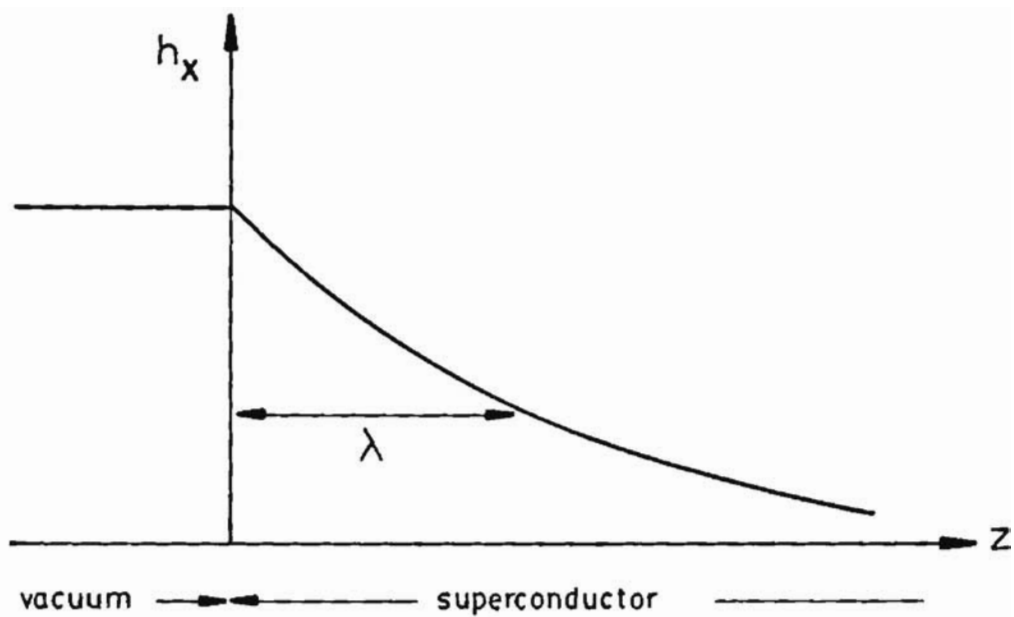


Figure 1.4 Field penetration in a superconductor.

CHAPTER II

HIGH TEMPERATURE SUPERCONDUCTIVITY - A PHENOMENOLOGICAL APPROACH

2.1 Introduction

More than a decade has elapsed since the discovery of superconductivity in cuprates by Bednorz and Muller and still there is no consensus on the microscopic mechanism responsible for high transition temperature in this class of materials. However, independent of the exact nature of the pairing mechanism within the layers, the interlayer coupling determines most of the superconducting properties of a real crystal. Hence there is a great need for a phenomenological model capable of describing the superconducting properties of these compounds. In this chapter the properties of copper oxide superconductors and phenomenological approaches to understand these properties will be discussed. Section 2.2 deals with the structure and properties of high- T_c copper oxide superconductors. Various microscopic theories put forward to explain high transition temperature in these compounds and the experimental constraints on these theories are explained in section 2.3. Ginzburg-Landau theory was extended to high- T_c superconductivity with the introduction of anisotropic mass tensor and section (2.4) deals with the anisotropic GL theory. Lawrence-Doniach (LD) model first proposed to describe anisotropic layered superconducting superlattices and intercalated dichalcogenides of transition metals is discussed in section 2.5. A modified LD model which takes into account the experimentally observed structural features of high- T_c copper oxide

superconductors with special reference to YBCO is proposed in section 2.6.

2.2 Structure and Properties of Copper Oxide Superconductors

The structure of the superconducting compounds and those of the related phases had been studied by both X-ray and neutron diffraction techniques [135]. Almost all structural refinements of these compounds were carried out using neutron powder diffraction data.

The Bednorz-Muller superconductor $La_{2-x}M_xCuO_{4-y}$ ($M = Ba, Sr$) known as 214 system has the tetragonal type structure of K_2NiF_4 at room temperature [32, 33]. The prototype compound for 214 class of layered perovskite materials is La_2CuO_{4-y} whose low temperature properties vary tremendously depending on the oxygen content and preparation techniques that affect metal sublattice stoichiometry. Oxygen vacancies promote an antiferromagnetic ground state with pronounced sensitivity. From an absence of antiferromagnetic order (Neel Temperature $T_N = 0$) at stoichiometry ($y=0$), T_N rises to room temperature at $y=0.03$ [34]. At full oxygen occupancy, long range magnetic order is absent in favour of superconductivity. La_2CuO_4 is a superconductor under special conditions [35]. A shift in the temperature dependence of the electrical resistivity of this compound from semiconducting to metallic correlates with the occurrence of superconductivity and the presence of vacancies on the La sites [36]. Thus the superconducting state is associated with vacancies on the La sublattice in conjunction with complete occupancy of the oxygen sites. When La_2CuO_4 is doped with alkaline earth elements such as Sr, Ba or Ca, the tendency to antiferromagnetism is suppressed and superconductivity becomes the dominant low temperature state. The maxi-

mum value of $T_c (\simeq 40K)$ in Sr and Ba systems is obtained for $x = 0.4$ and $x = 0.15$ respectively [37]. A tetragonal to orthorhombic phase transition for this composition occurs at about 200K. From crystallographic point of view no change can be detected between 60K and 10K *i.e.* due to superconducting transition. The structural parameters for the orthorhombic phase of $La_{1.85}Ba_{0.15}CuO_4$ at 10K are $a = 5.3430\text{\AA}$, $b = 13.2504\text{\AA}$ and $c = 5.3479\text{\AA}$. The crystal structure is remarkable because the co-ordination polyhedra of lanthanum and copper combine in a way that allows three dimensional space to be filled in a highly two dimensional manner. As a result, the two dimensional CuO_2 planes perpendicular to the c-axis interspace double layers of La/M and oxygen [Fig 2.1]. The copper oxygen plane is the microscopic region of the crystal structure where superconducting charge carriers originate.

$RBa_2Cu_3O_{6+x}$ otherwise known as 123 system with R representing trivalent rare earths such as Y, Nd, *etc* has the defect perovskite structure [38] and is highly deficient in oxygen. All physical properties of this compound are sensitive to oxygen concentration as shown in Fig. 2.2. They are orthorhombic for $x > x_{OT}$ (orthorhombic \leftrightarrow tetragonal) while they are tetragonal for $x < x_{OT}$. The structural parameters in the orthorhombic phase are $a = 3.8198\text{\AA}$, $b = 3.8849\text{\AA}$ and $c = 11.6762\text{\AA}$ [39]. The orthorhombic to tetragonal structural transition is accompanied by metal to insulator transition and it also separates the antiferromagnetic region from superconductivity. In the small x regime the compound is a tetragonal antiferromagnetic insulator while at large x and at low temperatures it is an orthorhombic superconductor. In each chemical unit cell there are three copper-oxygen layers of ions which are stacked along the c-axis. Two of these layers have oxygen ions between the copper ions in both the a and b crystallo-

graphic directions (CuO_2 planes) and the oxygen cannot be removed. The third copper layer only has oxygen ions along the b-axis (CuO chain layer) [Fig. 2.3]. The oxygen concentration in the chain layer can be readily varied from full occupancy ($x = 1$) to full depletion ($x = 0$). Detailed analysis of the charge density distribution have confirmed the one dimensional nature of the CuO chains as well as the two dimensional nature of the CuO_2 planes. In the limit $x = 1$, oxygen vacancies are due to the absence of oxygen atoms from the plane which separates the adjoining CuO_2 planes and from half of the oxygen sites in the CuO plane between the BaO layers which leads to the formation of the CuO chain. There is remarkable correlation between T_c and the oxygen concentration in the chain layer [40]. $T_c \sim 90K$ for $x \leq 1$ for all the trivalent rare earth elements R and decreases to 60K where it remains upto $x = 0.5$. Beyond this value T_c drops sharply and antiferromagnetic order sets in. In the magnetic regime there are two separate transition to antiferromagnetic order of the Cu spins which have been observed. The high temperature transition involves the ordering in the CuO_2 plane layers and has a Neel temperature $T_{N1} \sim 500K$ at $x = 0$ and monotonically decreases to zero at $x \sim x_{OT}$. At lower transition the Cu spins in the Cu chain layers also become ordered and the transition temperature T_{N2} is very sensitive to x .

The ionic Y and Ba atoms were found to act as electron donors and otherwise do not participate in superconductivity or magnetism. The lack of conduction electron density near the Y-site explains the stability of the critical temperature when isolated Y atoms are replaced by other rare earth atoms. The superconducting behaviour of the 123 - compounds do not depend on which rare earth element it contains. On the other hand, the chain layer controls all the properties of the system - magnetism, metallic behaviour and superconductivity. The rare earth atom

in 1-2-3 more or less acts like a spacer between copper oxygen planes; its chemical properties do not figure into the electrical properties of the superconductor. Thus there exists an entire family of 123-compounds that all superconduct above 90K and differ only in the identity of the rare earth element.

$YBa_2Cu_4O_8$ [41] exhibits superconductivity transition at about 80K. The main feature of this compound is the presence of two consecutive oxygen deficient CuO chain layers. The structure of this compound is otherwise similar to that of $YBa_2Cu_3O_7$.

Aside from the small orthorhombic distortion in the unit cell and the superlattice structure along the b-direction, crystal structures of both the compounds $Bi_2Sr_2CuO_6$ ($T_c \sim 22K$) and $Bi_2Sr_2CaCu_2O_8$ ($T_c \sim 84K$) are body centred tetragonal. The thallium compounds $Tl_2Ba_2Ca_{N-1}Cu_NO_{2N+4}$ have practically the same structure as that of the bismuth system. The structure of $Bi_2Sr_2CuO_6$ ($Tl_2Ba_2CuO_6$) consists of a square CuO_2 plane above which is a layer of SrO (BaO) followed by two BiO (TlO) layers and another SrO (BaO) layer before the whole structure repeats with the copper oxygen layer shifted to the body centred tetragonal position. The two layer structure differs in that the single CuO_2 layer is replaced by two CuO_2 layers separated by a layer of calcium. The three layer structure includes an additional set of Ca CuO_2 layers to the two layer structure. In the family of $Tl_1Ba_2Ca_{N-1}Cu_NO_{2N+3}$ the square planar CuO_2 layers are sandwiched between single layers of thallium oxide.

Experiments carried out in 1989 by Kikuchi *et al.* have shown that in the family of $Tl_2Ba_2Ca_{N-1}Cu_NO_{2N+4}$ T_c increases for N values from 1 to 3 (maximum $T_c=125K$ for N=3) and decreases under the passage from three to four layered specimens. They have also synthesized high- T_c superconductors $Tl_1Ba_2Ca_{N-1}Cu_NO_{2N+3}$ with

N values from 2 to 5 [43] and have shown that T_c increases with the number of layers N upto N=4 and then is lowered N equal to five and six.

All these high- T_c superconductors have the oxygen depleted layered perovskite structure which causes these materials to be highly anisotropic in their superconducting properties - critical currents, penetration depths, coherence lengths and other parameters (Table 2.1). In all of these systems copper oxide planes form a common structural element which is thought to dominate the superconducting properties. Depending on the stoichiometry the crystallographic unit cell contains varying numbers of CuO_2 planes. These planes are sandwiched between other layers which act as spacers and most important, as reservoirs of charge carriers. The electronic state of these layers determines the charge density on the copper-oxygen planes and the transition temperature of the compound.

The high- T_c cuprate superconductors are all extreme type II materials with small values for the lower critical field and exceptionally large values for the upper critical field $H_{c2}(0)$. For composition with optimal T_c , $H_{c2}(0) \geq 50T$ for polycrystalline samples of the 214 system and $H_{c2}(0)$ is as high as 340T [44] for the 123 system. Measurements of H_{c2} on single crystals of YBCO [45] reveal a high degree of anisotropy. When the applied field is parallel to the planes the slope $-(dH_{c2}/dT)_{T=T_c}$ is 3T/K. With the external field applied perpendicular to the planes the slope is reduced to about 0.6T/K. Non ideal behaviour of superconductors with strong flux pinning coupled with large demagnetization correction makes an accurate determination of H_{c1} extremely difficult. However, with these ambiguities taken into account the measure of anisotropy $(H_{c1}^\perp/H_{c1}^\parallel)$ is consistent with the expected relation $(H_{c1}^\perp/H_{c1}^\parallel)(H_{c2}^\parallel/H_{c2}^\perp) \sim 1$. These results reflect the anisotropy in the values of the coherence length and the penetration depth. The experimental

data on the anisotropic parameters are listed in Table 2.1.

The critical current J_s is determined by flux pinning strength and is a property which is quite sample dependent. As direct transport measurements of J_c on the oxide superconductors are impractical except for thin film samples, the J_c values are usually estimated from the hysteresis of the magnetization curve using the Bean model [136]. Dinger *et al.* [46] report the critical current density of a single crystal $YBa_2Cu_3O_{7-\delta}$ sample at helium temperature and zero magnetic field to be $J_c^{ab} \sim 2.9 \times 10^6 A/cm^2$ and $J_c^c \sim 4.2 \times 10^5 A/cm^2$. The temperature and magnetic field dependences are much different for J_c^{ab} and J_c^c .

A.C. Josephson experiments done by Niemeyer *et al.* for a junction between $YBa_2Cu_3O_7$ and an alloy of Pb and Sn [47] gave the value of magnetic flux quantum Φ as $hc/2e$ indicating that the charge carriers are Cooper pairs. Hall effect data for $La_{1.85}Sr_{0.15}CuO_4$ [48] gives a positive Hall constant indicating that conduction by holes dominates. The hole carrier concentration in the normal state just above T_c is low with a value of about $(5 \pm 3) \times 10^{21} cm^{-3}$. The data shows a strong correlation between T_c and hole concentration in the copper-oxygen layers providing further evidence as to the importance of the low dimensional features of these materials. The doping with alkaline earths is seen to affect T_c via a change in the hole concentration. The Hall constants of 214 systems are relatively temperature independent. The Hall effect studies on $YBa_2Cu_3O_{7-\delta}$ [49] give a Hall constant R_H which is positive and sensitive to the oxygen content increasing rapidly with increasing oxygen deficiency δ . R_H exhibits a significant temperature dependence such that the apparent carrier density $1/eR_H$ varies linearly with T extrapolating to nearly zero at T=0. Single crystal studies [50] show that Hall effect for $H \parallel c - axis$ is quite similar to that of polycrystalline samples where as R_H for

$H \parallel ab$ - plane is much smaller, is negative and seems to have quite different temperature dependence.

The resistivity of high- T_c oxides in the normal state is extremely anisotropic with metallic like behaviour along the planes and semiconducting like behaviour along the c-axis. A remarkable feature of the high- T_c cuprates is the wide range in T over which ρ_{ab} falls on a straight line passing through the origin or is linear with a positive intercept. The conspicuous absence of resistivity saturation at high temperature suggests that the electron-phonon coupling is rather weak in these oxides.

Large positive (hole-like) values of thermoelectric power have been observed in samples of $La_{2-x}Sr_xCuO_4$ and $YBa_2Cu_3O_{7-\delta}$. The approximate temperature independence contrasts with the T-linear behaviour of conventional metals.

Nearly all of the high- T_c superconducting oxides have an oxygen isotope effect according to the relation $T_c \propto M^{-\beta}$ [51]. Against the BCS value of $\beta = 1/2$, the 214 compound with $T_c \sim 34 - 37K$ has β values varying from 0.09 to 0.2 for different studies. $YBa_2Cu_3O_7$ has still smaller values for β . For bismuth compounds with $T_c = 110K$, β is only 0.026. In the case of YBCO, T_c is insensitive to the mass of the ion at the Y-site indicating that the lattice vibrations associated with the Y-sites are not contributing to the pairing in any significant way. In addition Cu and Ba isotopic studies show no measurable dependence of T_c on isotopic mass [137].

Infra-red absorption and tunneling spectroscopic studies show energy gaps which are anisotropic for the high- T_c superconductors. For the 123 compounds energy gap appears to be large in the Cu-O plane upto $6-7k_B T_c$ and smaller in the perpendicular direction of the order of $3-4k_B T_c$. Several experiments suggest that

the energy gap is not "clean" but has finite density of states all the way down to zero energy. The gap parameter does not exhibit the temperature dependence of the BCS gap width shifting down toward zero frequency as $T \rightarrow T_c$ but rather appears to fade out in intensity without a major frequency shift. The angle resolved photoemission spectroscopy (ARPES) measurements on BSCCO have shown that a gap like feature develops below T_c along the K_x or K_y directions in K-space but not along directions rotated by $\pi/4$ from them in the ab-plane.

2.3 Experimental Constraints on Theories of High- T_c Superconductors

Superconductivity in high temperature cuprate materials is also based on Cooper pairs because the usual a.c. Josephson effect frequency $2eV/h$ is observed for a junction between $YBa_2Cu_3O_7$ and an alloy of Pb and Sn [52], the observed flux quantum is of the usual size $hc/2e$ [53] and Andreev reflection along the time-reversed trajectories is seen [54] as with conventional superconductors.

If BCS theory is taken to mean the electron-phonon interaction which causes a pairing instability, then the cuprate superconductors are not BCS like. However, if the central core of the BCS theory is the pairing instability of the Fermi liquid in the presence of an attractive interaction with the source of this interaction a peripheral aspect, then the new materials may be BCS like. In this respect Eliashberg's [55] reformulation of the BCS theory is useful as it is sufficiently general to allow interactions that are not mediated by phonons alone but by other types of excitations, for example, electronic excitations.

A calculation of the size of the pair can determine whether the superconductor is of the BCS type where the pairs are formed at T_c or the Bose-Einstein type

where the pairs pre-exist and only condense at T_c (Schaforth or local pair model). The size of the pair in YBCO and LSCO determined from coherence lengths is such that several pairs will overlap one another and co-exist in the same volume. This is characteristic of the BCS model and is in contrast to the model of pre-existing tightly bound bosons.

If two electrons of wave functions $\phi_{\mathbf{K}}(\mathbf{r}_1, s_1)$ and $\phi_{\mathbf{K}'}(\mathbf{r}_2, s_2)$ are bound to form a composite particle then the pair function will have the form,

$$\psi(\mathbf{r}_1, s_1; \mathbf{r}_2, s_2) = \psi(\mathbf{R})\phi(\rho)\chi(s_1, s_2)$$

where $\mathbf{R} = (\mathbf{r}_1 + \mathbf{r}_2)/2$ is the coordinate of the centre of mass and $\rho = (\mathbf{r}_1 - \mathbf{r}_2)$ is the relative coordinate. $\psi(\mathbf{R})$, $\phi(\rho)$ and $\chi(s_1, s_2)$ are the wavefunctions of the centre of mass, relative and spin coordinates respectively. Each of these three functions contains information on the mechanism of superconductivity. The flux quantization and hence the fact that the charge carriers are pairs result from the boundary conditions on $\psi(\mathbf{R})$. We can write,

$$\phi(\rho) = \sum_{l,m} C_{lm} R(\rho) Y_{lm}(\theta, \phi)$$

where $Y_{lm}(\theta, \phi)$ are the spherical harmonics and $R(\rho)$ is a radial function. It is important to know whether the pairs are bound in s-, p-, or d-states, the spatial extent of the radial wavefunction $R(\rho)$ and whether the spins form a singlet or a triplet state. The total wave function of the pair must be antisymmetric to the exchange of the two electrons because they are fermions. Hence the singlet state must be associated with the s- or d-states and the triplet associated with the p-state.

An important question is about the nature of the pairing in these materials, whether it is of the familiar s-wave type on which the conventional BCS theory

is based or it is of the d-wave type. W.A.Little [56] has analysed several experimental results to suggest an s-wave pairing scheme just as in conventional superconductors. Niemeyer *et al.* [47] have observed d.c. Josephson effect for a junction between $YBa_2Cu_3O_7$ and a Pb/Sn alloy. Since both Pb and Sn are classic BCS superconductors in the singlet s-state, the pairs in $YBa_2Cu_3O_7$ must also be of the same symmetry as it was shown by Akhtyamov [57] in 1966 that the tunneling of the Josephson type is impossible between a triplet state and a singlet state superconductor or between any two superconductors in which the symmetry of the pair states differ. Further evidence that the pairs in cuprates are singlet pairs in s-state comes from data on the impurities on T_c . Chemical impurities depress T_c in p- and d-wave superconductors because of mixing of different lobes but have little effect on s-wave superconductors which have the same amplitude in all directions. This reduction in T_c with impurities has not been observed in YBCO and LSCO. In particular for $La_{2-x}Sr_xCuO_4$ the presence of Sr causes disorder in the lanthanum lattice, yet with increasing Sr (over a limited range) T_c goes up, not down. A careful comparison by Harshman *et al.* [138] of the temperature dependence of the depolarization rate with the predictions of the BCS theory give excellent agreement, implying that the pairs are indeed of the s-wave variety.

On the other hand a number of experimental results point to a d-wave type of pairing. Microwave measurements at ~ 1 GHz [58] and muon spin rotation experiments [59] on high quality single crystals of YBCO gave a linear temperature dependence for $n_s \propto (1 - aT)$ where $a = 7.2 \pm 0.1 \times 10^{-3} K^{-1}$ and $n_s \propto 1/\lambda^2$. At higher temperatures $\lambda(T)$ diverges as $\Delta^{-1} \sim (T_c - T)^{-\frac{1}{2}}$ as $T \rightarrow T_c$. There is general consensus that the variation of $\lambda(T)$ in YBCO at low temperatures is more rapid than would be consistent with a classic clean BCS gap and is what would be

expected from d-wave pairing. Observed deviations from the "clean gap BCS" and flux quantization measurements on superconducting SQUID rings combining films of Pb and YBCO [60] give strong support to a d-wave pairing model. Results of ARPES measurements on BSCCO are what would be expected for a $d_{x^2-y^2}$ pairing scheme.

The BCS theory predicted the rise in the nuclear relaxation rate $1/T_1$ to a Hebel-Slichter peak below T_c before an exponential drop off to zero with the freeze out of quasiparticles at lower temperatures. When NMR studies were performed on the HTSC, the striking observation was that there is no Hebel-Slichter peak in $1/T_1$, rather the relaxation rate which had been decreasing with decreasing T in the normal state above T_c simply falls more rapidly in the superconducting state. At lower temperatures $1/T_1$ was better described by a power law such as T^8 or $T^{4.5}$ than the exponential expected of a BCS energy gap. The absence of this exponential freeze out of $1/T_1$ at low temperatures indicate the absence of a clean energy gap and the power law variation is qualitatively consistent with a d-wave pairing.

To identify the excitation responsible for the attraction, it is helpful first to determine whether the coupling is weak or strong. The phenomenon of Andreev reflection and zero tunneling below $eV = \Delta$ [54] and infra- red reflectivity data give evidence for weak coupling. The observed value of $\Delta C_v/\gamma T_c$ [61] and $\gamma T_c^2/H_c^2(0)$ where γ is estimated from magnetic susceptibility χ using a free electron model are also consistent with weak coupling. On the other hand most data for HTSC suggest values of $4kT_c$ to $7kT_c$ for the gap width which are much larger than the BCS weak coupling value of $3.5kT_c$. This implies that HTSC are not weak coupling BCS superconductors, but it is possible that very strong coupling could account

for such a high $2\Delta/kT_c$ ratio. Results from Raman and infra-red spectroscopy, the temperature dependence of the thermal conductivity and Mossbauer studies are reflective of extreme strong coupling limit.

Small or negligible oxygen isotope effect, large positive values of dT_c/dp larger than that for conventional superconductors obtained from high pressure studies of YBCO and LSCO, the fact that electron-phonon superconductors all have $T_c < 23K$ and many other electronic properties indicate that the electron-phonon interaction cannot be the dominant mechanism of superconductivity in high- T_c materials. Low energy $\hbar\omega_D$ of the phonon may be responsible for the low value of T_c . It is possible that a high energy boson may act in place of or in addition to phonons yielding a higher T_c .

When a test charge is inserted in a solid three kinds of distortions occur: the lattice distorts (virtual phonons), the electrons can repopulate any partly filled band (virtual plasmons) or they can mix in components from higher unfilled bands (virtual excitons). If the test charge is time dependent (moving) then the distortions follow in time, with a lag which is larger for lattice distortion than for electronic distortions. A second test charge will feel both the direct instantaneous repulsion of the first test charge and a time dependent attraction from these dynamical distortions. The usual Eliashberg picture assumes that electronic polarization serves only to cancel part of the direct coulomb repulsion and that only phonon polarization is sufficiently strong and retarded to contribute to pair bonding. The importance of electronic correlations in high temperature superconductors is evident from the comparison of the band structure with photoemission data as well as the failure of the band theory to stabilize the antiferromagnetic ground state.

Most of the electronic polarizability of complicated materials like the cuprate

superconductors is in exciton (interband) rather than plasmon (intraband) form. There have been proposals that nearly 2D plasmons of quasi-2D metals like La_2CuO_4 are especially beneficial for superconductivity but so far there is no convincing calculation of this, even for an electron gas, let alone for a material with interband dominance. The exciton mechanism like the phonon mechanism helps to weaken the direct coulomb repulsion of electrons. But there is no simple model system which should be subjected to rigorous theoretical investigation.

Exotic forms of superconductivity could emerge in solids from highly correlated electronic states which are not describable as ordinary Fermi liquids. Bipolaronic and RVB superconductors are such proposals. In the limit $\epsilon_F \ll E_B$, $\epsilon_F \ll \Theta$ where E_B is the binding energy of the pair, electrons form mobile pairs bound by electron-phonon interactions called bipolarons provided the attraction is strong enough to support a bound state. There is no unambiguous evidence that bipolarons exist in any known solid. Scalapino *et al.* [62] argue that Cu-O based superconductivity may be electron-phonon driven and on the border between bipolaronic and BCS like.

The close proximity of antiferromagnetic state in 214 and 123 compounds with superconducting state has been the starting point for resonance valence bond theory where as other theories have involved the exchange of magnons [63] or spin fluctuation [64] to provide a more conventional BCS attractive interaction. Nuclear magnetic and quadrupole resonance experiments show no evidence of static moments on the copper sites in YBCO nor any evidence of magnetic interactions. Furo *et al.* [65] report that the relaxation rate of ^{65}Cu which has the larger magnetic moment but smaller quadrupole moment is smaller than ^{63}Cu showing that the relaxation is not of magnetic origin. Lyons *et al.* [66] have reported the results

of inelastic light scattering experiments that do give evidence of pair excitation near 0.3meV in both insulating La_2CuO_4 and $YBa_2Cu_3O_6$. However as one approaches the superconducting state the scattering cross section decreases rapidly suggesting that the magnetic terms are competing with superconductivity rather than being responsible for it.

In spite of the wide variety of measurements carried out on HTSC, there is still no consensus concerning the mechanism of high- T_c in these materials. However, it does appear that, whatever the mechanism, the superconducting properties in these materials can well be described by BCS/GL concepts.

2.4 Anisotropic Ginzburg-Landau Theory

Starting from the 1970's three new classes of superconductors were synthesized which have crystal structures quite different from the cubic one of conventional superconductors and show highly anisotropic electron properties. These are dichalcogenides of the transition metals of the $NbSe_2$ type and their intercalated compounds, the organic superconductors and copper oxide high- T_c superconductors. All of them have layered crystal structure.

The dichalcogenides of the transition metals have the chemical formula MX_2 where $M=Nb, Ta, Mo$ and $X=S, Se, Te$. In the crystal atoms M and X form a sandwich which consists of two layers of X and only a layer of M in between. The bonding of the atoms M and X inside the sandwich is strong, the inter atomic distance being 1.5\AA . But the coupling of the sandwiches is rather weak with distances of about 3\AA between the layers X of neighbouring sandwiches (Fig.2.4). The electrons move freely inside the sandwiches while the motion between the

sandwiches is characterized by a narrow band due to the weak overlap of the electron wavefunctions of different sandwiches. The anisotropy of conductivity $\sigma_{\parallel}/\sigma_{\perp}$ is about 20-50 in $NbSe_2$ and TaS_2 . The intercalation of these crystals by large insulating organic molecules arranged in between sandwiches enhances strongly the anisotropy and the ratio $\sigma_{\parallel}/\sigma_{\perp} \simeq 10^5$ was achieved in TaS_2 intercalated by the pyridin molecule C_5H_5N .

The organic superconductors $(TMTSF)_2X$ with $X = PF_6, ClO_4, AsF_6$ and $(BEDT-TTF)_2X$ with $X = I_3, AuI_2, Cu(CNS)_2$ are based on the organic molecules TMTSF and BEDT-TTF respectively which form charge transfer salts with small anion groups. The plane molecules TMTSF and BEDT-TTF with conjugated bonds form stacks which are arranged in layers. In the crystal the layers of this molecule alternate with layers of linear anions. The motion of the electrons along the layers is characterized by a broad conduction band whereas the motion of the conducting electrons via the anion layers is rather weak. The anisotropy of conductivity in $(TMTSF)_2X$ family is characterized by the ratio 1000:50:1 while in the $(BEDT - TTF)_2X$ family it is 400:200:1 where the first two values are for conductivities along the layers and the last one is for the perpendicular direction.

In the copper oxide superconductors CuO_2 layers which are responsible for superconductivity alternate with other layers and the anisotropy of conductivity in YBCO is about 100; it increases to 10^5 in Bi- and Tl-compounds.

The standard isotropic GL model (1.4) is valid for a) temperatures close to T_c i.e. $\tau = \frac{T_c - T}{T_c} \ll 1$, b) isotropic Fermi surface and c) superconducting correlation length ξ larger than the interatomic distance a_0 . The last condition can be written as $T_c \ll \epsilon_F$ which is easily fulfilled in conventional isotropic superconductors due to the large value of ϵ_F . But the layered compounds because of their extreme

anisotropy and extremely short coherence length are beyond the ambit of the isotropic GL approach. One way of describing their anisotropic electron spectrum is by introducing the anisotropic effective mass. For axial symmetry with z-axis perpendicular and (x,y) plane parallel to the layers we get the electron spectrum

$$\epsilon(\mathbf{K}) = \frac{\hbar^2 \mathbf{K}_{\parallel}^2}{2m_{\parallel}} + \frac{\hbar^2 K_z^2}{2m_z} \quad (2.1)$$

where $\hbar \mathbf{K}_{\parallel}$ is the momentum along the layers. The spectrum (2.1) corresponds to an elliptical closed Fermi surface for any concentration of conducting electrons. The model (2.1) is appropriate for compounds with intermediate degree of anisotropy but may be invalid in the case of very high anisotropy because the Fermi surface might be open there. Therefore a more general description [99] is provided by the tight binding model along z-direction for which the electron spectrum

$$\epsilon(\mathbf{K}) = \frac{\hbar^2 \mathbf{K}_{\parallel}^2}{2m_{\parallel}} + 2t \cos K_z d \quad (2.2)$$

where d is the interlayer distance and 2t is the band width for electron motion across the layers. If t is small in comparison with Fermi energy inside the layers $\hbar^2 n d / m_{\parallel}$ (where n is the three dimensional concentration of conducting electrons), the Fermi surface is open and has a cylindrical form. For $t \gg \hbar^2 n d / m_{\parallel}$ the spectrum (2.1) approaches spectrum (2.2).

In anisotropic compounds all the kinetic properties of electrons in the normal phase as well as superconducting properties can be characterized by the tensor of inverse effective mass $(m^{-1})_{i\mathbf{K}}$. In the coordinate system assumed above, we get

$$\begin{aligned} \frac{1}{m_z} &= \frac{-1}{2\epsilon_F} \left\langle \left(\frac{\partial \epsilon}{\partial K_z} \right)^2 \right\rangle_F \\ \frac{1}{m_{\parallel}} &= \frac{1}{2\epsilon_F} \left\langle \left(\frac{\partial \epsilon}{\partial K_{\parallel}} \right)^2 \right\rangle_F \end{aligned} \quad (2.3)$$

where the angular brackets mean averaging over the three-dimensional Fermi surface. The parallel component of this tensor is given by m_{\parallel}^{-1} introduced in (2.1) and (2.2) while m_z^{-1} is given by td^2/\hbar^2 in the case of closed Fermi surface ($t \gg \hbar^2 nd/m_{\parallel}$) and by $t^2 d^2/\hbar^2 \epsilon_F$ for the open Fermi surface. Ginzberg [67] generalized the isotropic GL functional to anisotropic superconductors by changing the scalar value $1/m$ in (1.4) by the tensor of inverse effective mass $(m^{-1})_{iK}$. The free energy

$$F_s = F_n + \int d\mathbf{r} \left[\sum_{i,j} \left\{ \frac{\hbar^2}{4} (m^{-1})_{ij} (\nabla_i - \frac{2ie}{\hbar c} A_i) \psi (\nabla_j - \frac{2ie}{\hbar c} A_j) \psi^* \right\} + \alpha(T) |\psi|^2 + \frac{\beta}{2} |\psi|^4 + \frac{\hbar^2}{8\pi} \right] \quad (2.4)$$

The value of the upper critical field is calculated from the linearized GL equation with anisotropic mass tensor as

$$H_{c2,z} = \frac{\Phi_0}{2\pi\xi_z^2}, \quad H_{c2,\parallel} = \frac{\Phi_0}{2\pi\xi_{\parallel}\xi_z} \quad (2.5)$$

where $\xi_i = \frac{\hbar^2}{4m_i\alpha(T)}$. Thus the expression $\frac{H_{c2,\parallel}}{H_{c2,z}} = \left(\frac{m_z}{m_{\parallel}}\right)^{\frac{1}{2}}$ can be used to calculate the mass anisotropy from H_{c2} measurements. If the magnetic field is oriented in **such** a way that the angle between \mathbf{H} and z -axis is θ , we get for $H_{c2}(\theta)$

$$H_{c2}^2(\theta) \left(\frac{\cos^2 \theta}{H_{c2,z}^2} + \frac{\sin^2 \theta}{H_{c2,\parallel}^2} \right) = 1 \quad (2.6)$$

It is interesting to compare this expression with that for angular dependence of H_{c2} in thin plate with thickness $L \ll \xi$ [68]. In this case

$$H_{c2}(\theta) \left| \frac{\cos \theta}{H_{c2,z}} \right| + H_{c2}^2(\theta) \frac{\sin^2 \theta}{H_{c2,\parallel}^2} = 1 \quad (2.7)$$

with $H_{c2,\parallel} = \sqrt{6}\Phi_0/\pi\xi L$ and $H_{c2,z} = \Phi_0/2\pi\xi^2$. θ is the angle between \mathbf{H} and the normal to the plate. The origin of the anisotropy of H_{c2} is quite different in the

two systems under consideration. In the former case, it is due to the anisotropy of the electron spectrum while in the latter it is caused by the restricted geometry of the sample. We obtain a cusp in the dependence $H_{c2}(\theta)$ near $\theta = 90^\circ$ for the plate while the cusp is absent in the anisotropic superconductor. However it is possible to observe the cross over from the dependence (2.6) to (2.7) in the superlattices which consist of alternating superconducting and insulating sheets with thickness $L_S = L_I$ as L_S increases from the atomic scale to the values L_S which fulfill the inequalities $a_0 \ll L_S \ll \xi$. At small L_S the electron effective mass m_z is rather small due to the tunneling between conducting layers. There the orbital effect due to the motion of electrons between the layers is important and formula (2.6) is valid. As L_S increases the mass m_z grows and then at some L_S the electrons stop to move between the conducting plates. Only the orbital effect inside the conducting plate is important in this case and the formula (2.7) becomes applicable. The cross over occurs at $\xi_x \simeq L_S$.

Within the frame work of the GL model (2.4), the temperature dependence $H_{c2}(T)$ is linear near T_c independently of θ .

The lower critical fields are obtained as

$$H_{c1,z} = \frac{\Phi_0}{2\pi\lambda_{\parallel}^2} \ln \frac{\lambda_{\parallel}}{\xi_{\parallel}}, \quad H_{c1,\parallel} = \frac{\Phi_0}{4\pi\lambda_{\parallel}\lambda_z} \ln \left(\frac{\lambda_{\parallel}\lambda_z}{\xi_{\parallel}\xi_z} \right)^{\frac{1}{2}} \quad (2.8)$$

For parallel field the normal core of the vortex is elliptic with half axes ξ_{\parallel} , ξ_z . It may be noted that $\xi_{\parallel} > \xi_z$ while $\lambda_{\parallel} < \lambda_z$. The Meissner screening is determined by λ_{\parallel} in the magnetic field which is perpendicular to the layers. It is stronger for this orientation than for the parallel one. Correspondingly, $H_{c1,z} > H_{c1,\parallel}$ while $H_{c2,z} < H_{c2,\parallel}$. For an arbitrary orientation of the magnetic field with respect to

the z-axis,

$$H_{c1}^2(\theta) \left(\frac{\cos^2 \theta}{H_{c1,z}^2} + \frac{\sin^2 \theta}{H_{c1,\parallel}^2} \right) = 1. \quad (2.9)$$

The approach with the anisotropic mass in GL functional is valid until condition (c) above is fulfilled. For open Fermi surface which represents actually the case of strong anisotropy ($m_z \gg m_{\parallel}$) this condition is equivalent to the inequality $t \geq T_c$. If this condition is violated, the functional (2.4) is valid in a narrow temperature interval near T_c only *i.e.* $\tau \ll (t/T_c)^2$. In the interval $\tau \gg (t/T_c)^2$ the Lawrence-Doniach (LD) [69] model discussed in section (2.5) has to be used with finite differences of the order parameter in the z-direction.

2.5 Lawrence - Doniach Model

In the layered compounds the superconducting order parameter is highly inhomogeneous in the direction across the layers. If the distance between the layers d is very large compared to ξ_z *ie* $d \gg \xi_z$, the inhomogeneous nature of the order parameter essentially affects the superconducting properties. The order parameter is rather large inside the conducting layers but very small between the layers. The situation is the same as in Josephson contacts. Therefore we can describe the order parameter in the region of space where it is strong enough and ignore the region in-between. Under such description the layered superconductors can be considered as an array of superconducting layers coupled by Josephson interaction. The necessary condition of such treatment is that the energy of layer coupling should be much smaller than the energy of superconducting condensation inside the layers. If this condition is fulfilled the currents between layers cannot in any way destroy the superconducting ordering inside the layers; they affect the phase difference

only. This condition is equivalent to the inequality $d \gg \xi_z$.

To describe this situation we introduce a discrete variable n which is the number of layers in the z -direction. The order parameter for the n^{th} layer will be $\psi_n(\rho)$ where $\rho = (x, y)$. The free energy functional for the superconducting system is now the sum of the energy inside the layers and the energy of Josephson coupling.

$$F = \sum_n \int d\rho \left[\alpha(T) |\psi_n|^2 + \frac{\beta}{2} |\psi_n|^4 + \frac{\hbar^2}{4m_{\parallel}} \left| \left(\nabla_{\parallel} - \frac{2ie}{\hbar c} \mathbf{A}_{\parallel} \right) \psi_n \right|^2 + f_j |\psi_n - \psi_{n+1} \exp(-i\chi_{n,n+1})|^2 \right] \quad (2.10)$$

where ∇_{\parallel} is the gradient along the layers, $\mathbf{A}_{\parallel} = (A_x, A_y)$, $\chi_{n,n+1} = \frac{2e}{\hbar c} \int_{n\hat{z}}^{(n+1)\hat{z}} A_z dz$, $f_j = \hbar j_c / 2e |\psi_0|^2 d$ and $|\psi_0|^2 = \alpha/\beta$. Here j_c is the critical value of the Josephson current across the layers and parameters f_j and j_c determine the strength of the Josephson coupling.

The free energy functional (2.10) was introduced by Lawrence and Doniach [69] for the analysis of the consequences of the layered structure in superconducting materials and it is a generalization of the standard GL functional to describe the case $\xi_z \ll d$. It was extensively applied in the context of layered transition metal dichalcogenides with organic molecules intercalated between the metallic layers. Although these materials had transition temperatures of only a few Kelvins, the formalism is equally useful for the high temperature superconductors.

The upper critical field $H_{c2,z}$ in this model is also given by the expression (2.5) because electrons move along the layers at such orientation of the field and $\psi_n(\rho)$ does not depend on n . The Josephson part of the energy is unessential at such orientation of H at $H = H_{c2}$.

For the parallel magnetic field, taking the vector potential in the form $A_z = Hx$,

we get the linear Mathieu equation

$$\xi_{\parallel}^2(0) \frac{d^2\psi(x)}{dx^2} + r(1 - \cos \frac{2\pi H x d}{\Phi_0})\psi(x) - \tau\psi(x) = 0 \quad (2.11)$$

where $\tau = 2\xi_z^2(0)/d^2$. The critical temperature $T_c(H)$ is given by the lowest eigen value $\tau(H)$ and the dependence $T_c(H)$ gives the dependence $H_{c2}(T)$. The solution of equation (2.11) can be found in analytical form for the cases of large and small magnetic fields.

Introducing dimensionless variables $x' = x/\xi_{\parallel}(0)$ and $h = 2\pi H\xi_{\parallel}(0)d/\Phi_0$, for $h \ll 1$ we can expand $\cos hx'$ to obtain the harmonic oscillator equation with the lowest eigen value $\tau = h(\tau/2)^{\frac{1}{2}}$. This is the same as the GL expression (2.5) for $H_{c2,\parallel}(T)$ with linear dependence in τ . The assumption $h \ll 1$ reduces to the condition $\xi_z(T) \gg d$.

For large h , equation (2.11) is the Schroedinger equation for a particle in a periodic potential $r(1 - \cos hx')$ with small periods of oscillations. The lowest eigen value is obtained using the perturbation theory in potential as $\tau = \tau - h^{-2}$ which shows that the upper critical field $H_{c2,\parallel}$ due to the orbital effect only diverges at $\tau \geq T_c = r$ i.e. at $\tau > \tau_c$ the orbital effect itself cannot destroy the superconductivity. This conclusion is natural for Josephson systems because the Josephson currents cannot destroy the superconductivity inside the layers. This unphysical situation can be overcome by taking into account the finite layer thickness, pair breaking due to Pauli paramagnetism and spin orbit coupling effects. The paramagnetic effect is accounted for by changing τ to $\tau - (H/H_p)^2$ where $H_p = 2\pi T_c/\mu_B\sqrt{7\zeta(3)}$ and $\zeta(3) = 1.2$. For $\tau \geq \tau_c$, $H_{c2,\parallel} = H_p\sqrt{\tau}$. Knowing $H_{c2,\perp}$ and $H_{c2,\parallel}$, the angular dependence of H_{c2} on θ is determined from the equation,

$$H_{c2}^2(\theta) \left[\left(\frac{\cos \theta}{H_{c2,\perp}^*(\tau^*)} \right)^2 + \left(\frac{\sin \theta}{H_{c2,\parallel}^*(\tau^*)} \right)^2 \right] = 1 \quad (2.12)$$

where $\tau^* = \tau - (\frac{H_{c2}(\theta)}{H_p})^2$ and $H_{c2,\parallel}(\tau)$ is given by equation (2.10) *i.e.* by the orbital effect alone [114]. The solution of (2.12) has the form

$$\frac{H_{c2}(\theta)}{H_{c2}^*(\theta)} = \frac{[(1 + 4x^2)^{\frac{1}{2}} - 1]}{2x^2}, \quad x = \frac{H_{c2}^*(\theta)}{H_p} \quad (2.13)$$

Near T_c ($\tau \rightarrow 0$), $x \rightarrow 0$ and $H_{c2}(\theta) = H_{c2}^*(\theta)$. At $\tau > \tau_c$, we have $1/H_{c2}^* = 0$ and $H_{c2}(\theta)$ is determined from the equation

$$H_{c2}(\theta) \left| \frac{\cos \theta}{H_{c2,z}} \right| + \frac{H_{c2}^2(\theta)}{H_{c2,\parallel}^2} = 1 \quad (2.14)$$

which does not differ practically from equation (2.7) for the value $H_{c2}(\theta)$ in the plate except for the definition of $H_{c2,\parallel}$. Thus the smooth dependence of H_{c2} on θ near $\theta = 90^\circ$ as obtained close to T_c changes by cusp anomaly at $\tau > \tau_c$

At $r \ll 1$ the dependence $H_{c2,\parallel}(T)$ has a positive curvature while $H_{c2,z}(T)$ is linear. The dependence of H_{c2} on θ and T indicates that the essential parameter of layered compounds for cross over from 3D-anisotropic GL regime to Josephson coupling of layers is $r = 2\xi_z^2(0)/d^2$.

Near T_c *i.e.* at $\tau \ll \tau_c$ we get the standard effective mass expression (2.8) for $H_{c1}(\theta)$. At $\tau > \tau_c$, in the Josephson regime, the expression for $H_{c1,z}$ is standard while the structure of vortex in the parallel field differs slightly from the usual one. The parallel vortex has a large periphery with dimensions of the order of λ and λ_z with weak perpendicular currents $j_z \ll j_c$. The periphery part is defined by linear GL effective-mass tensor equations. The centre of vortex with dimensions of the order d is described by non-linear equations of LD model because the perpendicular currents between the layers j_z are of the order of j_c . Thus the non-linear core of the vortex determines the logarithmic factor in $H_{c1,\parallel}$ and hence

$$H_{c1,\parallel} = \frac{\phi_0}{4\pi\lambda_{\parallel}\lambda_z} \ln \frac{\lambda_{\parallel}}{d} \quad (2.15)$$

For an arbitrary angle θ between \mathbf{H} and z-axis we again get the expression (2.9) with logarithmic accuracy assuming $\ln(\frac{\lambda_{\parallel}}{\xi_{\parallel}}) \gg \ln(\frac{\lambda_{\parallel}}{d})$. Here again the main contribution is given by the periphery part and so with logarithmic accuracy the results of the GL model with anisotropic effective mass is valid. Generally the vortex lattice structure in layered compounds with Josephson coupling can be described by GL effective mass equations upto a limiting parallel field. However, since effects such as pinning of the vortices and lattice excitations which determine the distortions of the lattice from the ideal Abrikosov lattice depend on core energy, such effects as lattice melting due to thermal excitations and disordering of vortices due to imperfections of the crystal should be quite different in GL effective mass model and LD model.

2.6 Phenomenological Model for High- T_c Copper Oxide Superconductors

More than a decade has elapsed since the discovery of superconductivity in cuprates by Bednorz and Muller and still there is no consensus on the microscopic mechanism responsible for high transition temperature in this class of materials. However, independent of the exact nature of the pairing mechanism within the layers, the interlayer coupling determines most of the superconducting properties of a real crystal. Hence there is a great need for a phenomenological model capable of describing the superconducting properties of these compounds. Since the cuprates are extremely anisotropic and possess layered structure, an appropriate model for them can be formulated on the lines of the celebrated Lawrence-Doniach theory.

In all high- T_c cuprate systems copper oxide planes form a common structural

element which dominates the superconducting properties. Depending on the stoichiometry the crystallographic unit cell contains varying number of CuO_2 planes. In addition the $YBa_2Cu_3O_{7-x}$ compound contains CuO chains which are thought to serve largely as reservoirs to control the charge density in the planes. The CuO chain layers dope the CuO_2 planes even in the limit $x = 0$. Yu *et al.* [70] have shown that if the nearest neighbour plane-plane interactions are turned off in YBCO, the transition temperature becomes 72K which is higher than 60K for the case with the nearest neighbour chain-plane interaction quenched. This means that the CuO chain between the CuO_2 planes play an important role in enhancing T_c although it is not required to make the material superconducting. Raman scattering results and the temperature dependence of $\lambda(T)$ obtained by muon spin resonance experiments [139] also point to the possibility of the CuO chains in YBCO having an influence on the coupling strength between superconducting charge carriers. The other evidence of the role of the CuO chains in superconductivity comes from the experimentally observed $\lambda_{ab}(0)$ values for Y:124, 60K Y:123 and 90K Y:123 which are all different [140]. Since all of these systems are almost identical except for the number of CuO chains, we must expect to see the same $\lambda_{ab}(0)$ if we could neglect the role of the CuO chains in the superconductivity. The clear difference among the three $\lambda_{ab}(0)$ values could therefore be interpreted as showing that the CuO chain is related to the superconductivity in yttrium based compounds.

Electronic band structure calculations [141] show that the planes composed of CuO chains in $YBa_2Cu_3O_{7-x}$ provide along with the CuO_2 planes conduction bands intercepting the Fermi level. As oxygen vacancies are introduced, the metallic nature of the chain layer bands begins to vanish along with decreasing T_c ($T_c \sim 90K$ for $0 < x < 0.2$ and $T_c \sim 60K$ for $0.2 < x < 0.5$). For x around 0.5 to 0.7 the chain

layer becomes insulating and the material ceases to superconduct. The metallic nature of the CuO chain layers is thus directly tied to the hole content in the CuO_2 planes since they arise from charge transfer from one another. The CuO chain layer provides a metallic intervening layer that enhances the interlayer coupling among the CuO_2 layers and therefore raises T_c significantly. Superconductivity has been observed in single CuO_2 layer with a T_c of 10K, but interlayer coupling along the c-axis is required to activate T_c of 90K.

The other structural element in $YBa_2Cu_3O_{7-x}$ like the Y and Ba atoms were found to act as electron donors and do not otherwise participate in the superconductivity. There is no conduction electron density near the Y site. T_c remains constant when other elements from the rare earth series are substituted for Y indicating that these magnetic ions have minimal interaction with the conduction electrons. Therefore the ions Y and Ba act as spacers which stipulate the space structure of the unit cell.

In thallium based compounds multiple CuO_2 plane layers are sandwiched between single or double TlO layers, the neighbouring CuO_2 layers in the sandwich being separated by Ca ions. Electronic band structure studies [71] show charge transfer from the CuO_2 bands to the TlO bands indicating that T_c correlates with the metallic nature of the intervening TlO bands. Like the CuO chains in YBCO the intervening metallic layers in TBCCO play the dual role of doping the CuO_2 layers and enhancing the interlayer coupling between the CuO_2 layers. Significant frequency shifts of thallium nuclear magnetic resonance have been observed in the superconducting state of the high temperature superconductor $Tl_2Ba_3Ca_3Cu_4O_{10+x}$ which suggests that the TlO bilayers participate directly in the superconductivity [142].

Bismuth based superconductors have similar structures as thallium based ones. Sterne and Wang [72] calculated the electronic structure for the one and two layer bismuth compounds and found essentially identical CuO_2 bands in both compounds. But they found the BiO planes which lie between the CuO_2 layers to be metallic in the high- T_c compound where as they are almost insulating in the low- T_c compound. Hence they proposed that the metallic nature of the layers between the CuO_2 planes could enhance T_c significantly. The role of the structural elements other than the CuO_2 planes and TlO(BiO) layers in the superconductivity of the thallium (bismuth) based compounds can be ignored.

The experimentally measured coherence length normal to the CuO_2 planes ξ_c and the CuO_2 interlayer spacing d_{Cu-Cu} for the $La_{2-x}Sr_xCuO_4$, $YBa_2Cu_3O_7$ and $Bi_2Sr_2CaCu_2O_8$ systems shown in Table 2.2 emphasize the role of interlayer coupling since in these compounds ξ_c is shorter than the distance between the CuO_2 planes [142]. In YBCO and BSCCO, however, ξ_c is comparable to the distance d_{Cu-M} from the CuO_2 layer to the metallic chain or BiO layer as the case may be so that supercurrents can flow between CuO_2 layers by taking advantage of the metallic states on intervening layers. Considering all these facts, it is natural to model a cuprate superconductor as a superlattice of the 2D conductive sheets with N CuO_2 planes and M metallic planes per unit cell with Josephson coupling which occurs through a proximity effect [73]. Experimental indications for the of this proximity effect in Bi 2:2:1:2 high- T_c superconductors have been reported by Briceno and Zettl [74]. Experiments on intrinsic Josephson effects carried out by Kleiner *et al.* [75] on single crystals of YBCO, BSCCO and TBCCO support a model of a cuprate superconductor as a stack of superconducting sheets (S) consisting of multiple CuO_2 layers (CuO_2 bilayers in the case of YBCO) separated by

weakly superconducting (S') metallic layers (chain layers in YBCO). The strongly superconducting S sheets induce a finite order parameter in weakly superconducting S' layers through proximity effect. We assume no intrinsic superconductivity in S' layers so that the order parameter in these layers is solely due to the proximity effect of S layers below T_c . The experimental results of Kleiner *et al.* [75] points to an $S - S'$ structure for YBCO with different order parameters for the S and S' layers. These observations necessitates the modification of the usual LD formalism including the inequivalence of the layers to obtain a realistic picture of cuprate superconductors. Hence we introduce two order parameters: $\psi_{1,n}^{(\rho)}$ for the multiple CuO_2 S -sheets and $\psi_{2,n}^{(\rho)}$ for the weakly superconducting S' -layers in the n^{th} unit cell as was done by Bulaevskii and Vagner [143]. Here $\rho=(x,y)$ and z is the axis perpendicular to the layers. In the case of $YBa_2Cu_3O_7$ we have to take into account the anisotropy of the effective mass due to the chain structure assuming $m_y \gg m_x$. The expression for Gibb's free energy can be written as,

$$\begin{aligned}
G = \sum_n \int & \left[a_1 |\psi_{1,n}^{(\rho)}|^2 + \frac{b_1}{2} |\psi_{1,n}^{(\rho)}|^4 + \frac{\hbar^2}{2m_{\parallel}} \left| (\nabla_{\parallel} - \frac{2ie}{\hbar c} \mathbf{A}_{\rho,n}) \psi_{1,n}^{(\rho)} \right|^2 \right. \\
& + a_2 |\psi_{2,n}^{(\rho)}|^2 + \frac{b_2}{2} |\psi_{2,n}^{(\rho)}|^4 + \frac{\hbar^2}{2} \sum_{l=z,y} \frac{1}{m'_l} \left| \left(\frac{\partial}{\partial l} - \frac{2ie}{\hbar c} \mathbf{A}_{l,n} \right) \psi_{2,n}^{(\rho)} \right|^2 \\
& \left. + t |\psi_{1,n}^{(\rho)} - \psi_{2,n}^{(\rho)} e^{i\chi_n}|^2 + t |\psi_{1,n}^{(\rho)} - \psi_{2,n+1}^{(\rho)} e^{-i\chi_n}|^2 \right] d\rho \\
& + \int \left[\frac{\mathbf{h}^2}{8\pi} - \frac{\mathbf{H} \cdot \mathbf{h}}{4\pi} + \frac{\mathbf{H}^2}{4\pi} \right] d\rho dz. \quad (2.16)
\end{aligned}$$

where $\chi_n = \frac{2ed}{\hbar c} \mathbf{A}_{x,n}$ and d is the separation between the inequivalent layers.

The modified LD model described by the free energy expression (2.16) is used in the following chapters to study the temperature dependence of the critical magnetic fields and the fluctuation effects of cuprate superconductors with special reference to $YBa_2Cu_3O_7$.

Compound	T_c K	$\xi_{ }(0)$ \AA°	$\xi_c(0)$ \AA°	Anisotropy parameter ($m_z/m_{ }$)	$H_{c2}^{\perp}(0)$ T	$H_{c2}^{\parallel}(0)$ T
$\text{La}_{2-x}\text{Sr}_x\text{CuO}_4$	36	33	7.8	18	30.2	85.4
$\text{YBa}_2\text{Cu}_3\text{O}_7$	90	15	3	25	173	960
$\text{Tl}_2\text{Ba}_2\text{CaCu}_2\text{O}_x$	100	31	6.8	20.25		
$\text{Bi}_2\text{Sr}_2\text{Ca}_2\text{Cu}_3\text{O}_x$	110	29	0.93	31	39	1210

Table 2.1. Various parametric values for some high temperature superconductors

Compound	$d_{\text{Cu-Cu}}$	$d_{\text{Cu-M}}$	ξ_c
$\text{La}_{2-x}\text{Sr}_x\text{CuO}_4$	6.6		7 - 13
$\text{YBa}_2\text{Cu}_3\text{O}_7$	8.2	4.1	4.8 - 7.0
$\text{Bi}_2\text{Sr}_2\text{CaCu}_2\text{O}_8$	12.1	4.4	4.0
$\text{Bi}_2\text{Sr}_2\text{CuO}_6$	12.3	4.5	

Table 2.2 Interlayer separations and coherence lengths in \AA for a number of high temperature superconductors

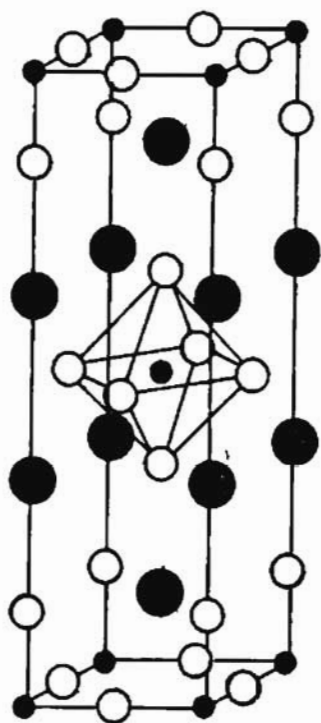


Figure 2.1 Crystal structure of La_2CuO_4 , the parent material for hole superconductors.

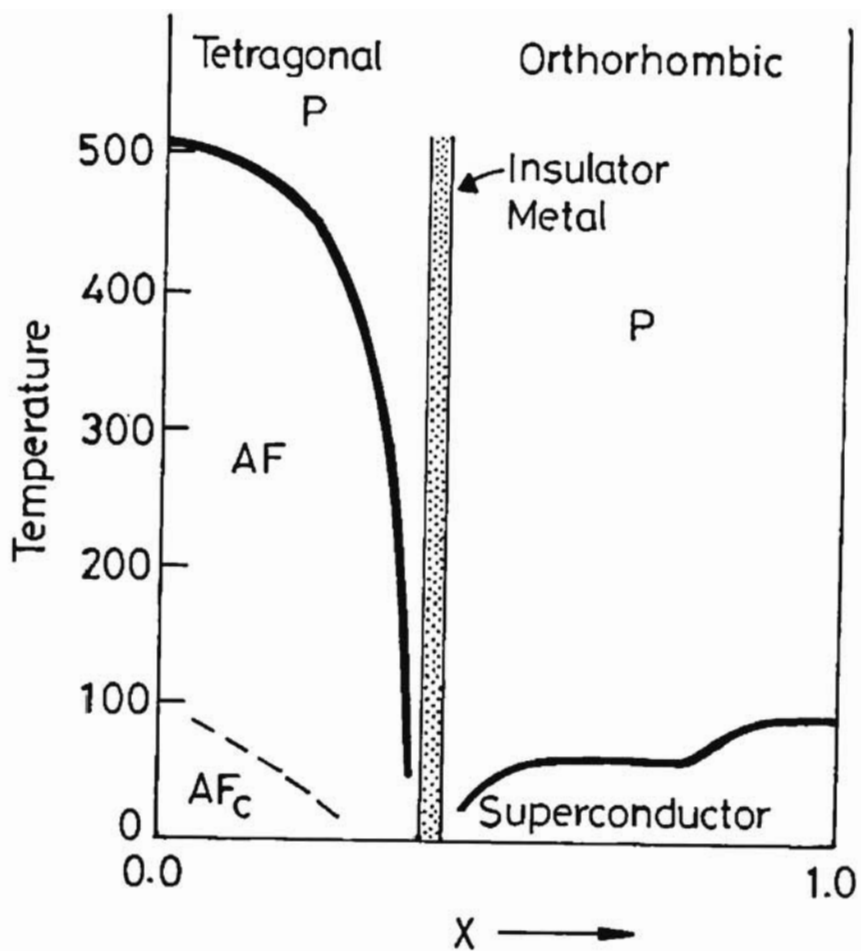


Figure 2.2 Schematic phase diagram for $RBa_2Cu_3O_{6+x}$ as a function of oxygen concentration x on the chain sites. The paramagnetic (P) and antiferromagnetic (AF) phases are shown, as well as an anti ferromagnetic phase found at lower temperatures (AF_c), where the spins on the Cu chains order [144].

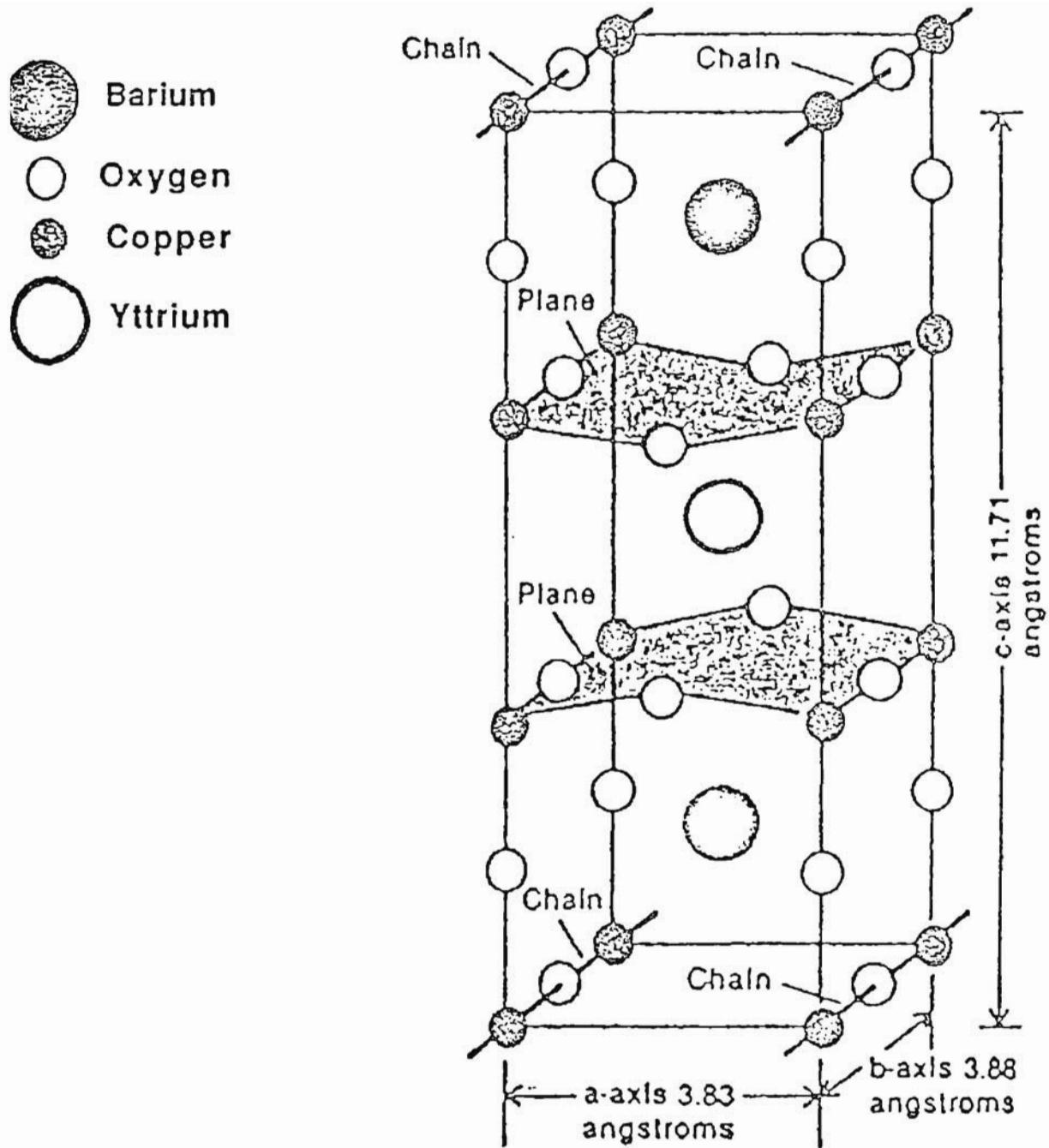


Figure 2.3 YBaCuO unit cell

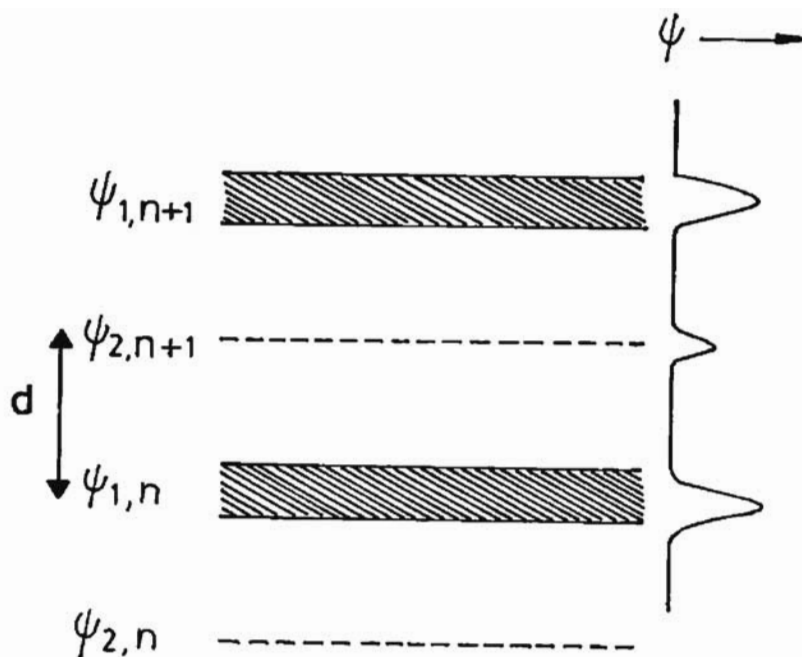


Figure 2.4 Superconducting and non-superconducting planes in YBaCuO. Shaded area represents CuO_2 double layers and dotted lines the CuO chain layers. The relationship between the order parameter on the SC layer and that on the NSC layer induced by the proximity effect is schematically indicated.

CHAPTER III

TEMPERATURE DEPENDENCE OF CRITICAL MAGNETIC FIELDS

3.1 Introduction

The metallic nature of the CuO chains and the importance of the chain-plane interactions on the superconducting behaviour of $\text{YBa}_2\text{Cu}_3\text{O}_7$ has been established in section 2.6. It is then natural to model a cuprate superconductor as a superlattice of 2D conducting sheets with N CuO_2 planes and M metallic planes per unit cell with Josephson coupling which occurs through a proximity effect, experimental evidence for which is available for Bi 2:2:1:2 [74]. Pathbreaking experiments by Kleiner *et al.* [75] on the intrinsic Josephson effects on single crystals of YBCO, BSCCO and TBCCO strongly support a model of cuprate superconductors as a stack of superconducting sheets (S) consisting of CuO_2 layers (CuO_2 bilayers in the case of YBCO) separated by weakly superconducting (S') metallic layers (chain layers in YBCO). According to Kleiner *et al.* superconducting S sheets induce a finite order parameter in the S' sheets which have no intrinsic superconductivity through a proximity effect and their experimental results support an $S - S'$ structure for YBCO with different order parameters for the S and S' sheets. The modified LD free energy functional (2.16) written on the lines suggested earlier by Bulaevskii and Vagner [143] describes this scenario fully. Other authors [145] have also considered the proximity effect between the planes and the chain layers, but introduced two coupling coefficients, one between the multiple CuO_2 planes

and another between the planes and the chain layers. However experiments by Kleiner *et al.* [75] clearly show that the multiple CuO_2 layers can be equated to single superconducting sheet and that it is not necessary to consider two coupling coefficients and instead it is sufficient to consider the $S-S'$ coupling arising due to proximity effect. It was shown in section 2.6 that the modified LD model (2.16) is applicable to bismuth and thallium based compounds also with the metallic BiO and TlO layers in these compounds playing the role of the chain layer in YBCO.

DC-magnetization measurements on single crystals of $YBa_2Cu_3O_7$ [76] of the upper critical field has established the positive curvature of H_{c2} near T_c for all field orientations. Such curvature has also been observed in low- T_c layered superconductors [77]. At lower temperatures $H_{c2}(T)$ becomes a straight line with negative slope intercepting the T-axis at about 1K below T_c [76]. The Ginzburg-Landau (GL) theory predicts linear temperature dependence for H_{c2} for all field orientations near T_c . The Lawrence-Doniach (LD) model of identical Josephson coupled layers [5], on the other hand, predicts a positive curvature near T_c for the upper critical field parallel to the layers ($H_{c2}^{\parallel}(T)$). But in this model $H_{c2}^{\parallel}(T)$ diverges at low temperatures. The positive curvature of $H_{c2}^{\perp}(T)$ however is not explained in this model.

In this chapter the modified LD model described by the free energy (2.16) is employed to study the temperature dependence of the upper and lower critical magnetic fields both parallel and perpendicular to the layers. In section 3.2 an effective free energy functional is obtained which is a modification of (2.16) with the help of newly defined parameters and rescaled order parameters. This functional (3.10) is used to obtain the temperature dependence of the upper critical field perpendicular to the layers. The results obtained therein are compared with

the experimental data for $YBa_2Cu_3O_7$ and $La_{1.87}Ca_{1.13}Cu_2O_6$. Another possible model for superconductors with inequivalent conducting layers is also discussed in this section. Temperature dependence of upper critical field parallel to the layers is considered in section 3.4. An attempt is made in section 3.5 to explain the anomalous upturn obtained by some authors in the temperature dependence of H_{c1} .

3.2 Upper critical field perpendicular to the layers

The discretized magnetic field H_n on each layer is generally defined as

$$H_n = \hat{z} \left(\frac{\partial A_{yn}}{\partial x} - \frac{\partial A_{xn}}{\partial y} \right) + \hat{x} \left(\frac{\partial A_{zn}}{\partial y} - DA_{yn} \right) + \hat{y} \left(DA_{xn} - \frac{\partial A_{zn}}{\partial x} \right) \quad (3.1)$$

Df_n is the discretized derivative across the layers and $Df_n = (f_{n+1} - f_n)/d_{n,n+1}$ where $d_{n,n+1}$ is the distance between the n^{th} and $(n+1)^{\text{th}}$ layers. H_n is invariant under the discrete gauge transformation

$$A_n \rightarrow A_n + \nabla_{\parallel} \chi_n + \hat{z} D\chi_n$$

where $\chi_n(x, y)$ is an arbitrary function of x and y . We also have $\psi_n \rightarrow \psi_n \exp(-\frac{2ie\chi_n}{\hbar c})$ under the gauge transformation. Near H_{c2} the order parameters will have small values and hence the quartic terms in (2.16) can be neglected. Also $\hbar=H$ and the free energy expression becomes,

$$\begin{aligned} G = \sum_n \int & \left[a_1 |\psi_{1,n}^{(\rho)}|^2 + \frac{\hbar^2}{2m_{\parallel}} \left| \left(\nabla_{\parallel} - \frac{2ie}{\hbar c} A_{\rho,n} \right) \psi_{1,n}^{(\rho)} \right|^2 \right. \\ & + a_2 |\psi_{2,n}^{(\rho)}|^2 + \frac{\hbar^2}{2} \sum_{\ell=x,y} \frac{1}{m'_{\ell}} \left| \left(\frac{\partial}{\partial \ell} - \frac{2ie}{\hbar c} A_{\ell,n} \right) \psi_{2,n}^{(\rho)} \right|^2 \\ & \left. + t |\psi_{1,n}^{(\rho)} - \psi_{2,n}^{(\rho)} e^{i\chi_n}|^2 + t |\psi_{1,n}^{(\rho)} - \psi_{2,n+1}^{(\rho)} e^{-i\chi_n}|^2 \right] d\rho. \quad (3.2) \end{aligned}$$

We shall assume the magnetic field on each layer as

$$H_n = H(\hat{z} \cos \theta + \hat{x} \sin \theta \cos \phi + \hat{y} \sin \theta \sin \phi). \quad (3.3)$$

Then the vector potential

$$A_n = H \left[-\hat{x} \frac{y \cos \theta}{2} + \hat{y} \frac{x \cos \theta}{2} + \hat{z} (-x \sin \theta \sin \phi + y \sin \theta \cos \phi) \right] \quad (3.4)$$

and

$$\chi_n = 2Kd \sin \theta (-x \sin \phi + y \cos \phi)$$

where $K = eH/\hbar c$. When the magnetic field is applied perpendicular to the layers, $\theta = 0$,

$$H_n = H\hat{z}, \quad A_n = \frac{H}{2}(-y\hat{x} + x\hat{y})$$

and $\chi_n = 0$. The free energy (3.2) is minimized with respect to the variations in $\psi_{1,n}^*$ and $\psi_{2,n}^*$ and the real and imaginary parts of the resulting LD equations are separately equated to zero to obtain the following equations.

$$a_1 \psi_{1,n}^{(\rho)} - \frac{\hbar^2}{2m_1} \left[\frac{\partial^2 \psi_{1,n}^{(\rho)}}{\partial x^2} + \frac{\partial^2 \psi_{1,n}^{(\rho)}}{\partial y^2} - K^2 (x^2 + y^2) \psi_{1,n}^{(\rho)} \right] + t [2\psi_{1,n}^{(\rho)} - \psi_{2,n}^{(\rho)} - \psi_{2,n+1}^{(\rho)}] = 0 \quad (3.5a)$$

$$y \frac{\partial \psi_{1,n}}{\partial x} = x \frac{\partial \psi_{1,n}}{\partial y}$$

$$a_1 \psi_{2,n}^{(\rho)} - \frac{\hbar^2}{2m_{2x}} \frac{\partial^2 \psi_{2,n}^{(\rho)}}{\partial x^2} - \frac{\hbar^2}{2m_{2y}} \frac{\partial^2 \psi_{2,n}^{(\rho)}}{\partial y^2} - \frac{\hbar^2 K^2}{2} \left(\frac{x^2}{m_{2y}} + \frac{y^2}{m_{2x}} \right) \psi_{2,n}^{(\rho)} + t [2\psi_{2,n}^{(\rho)} - \psi_{1,n}^{(\rho)} - \psi_{1,n-1}^{(\rho)}] = 0 \quad (3.5b)$$

and

$$\frac{y}{m_{2x}} \frac{\partial \psi_{2,n}}{\partial x} = \frac{x}{m_{2y}} \frac{\partial \psi_{2,n}}{\partial y}.$$

$m_1 = m_{\parallel}$ We sum equations (3.5) over all n , defining $\psi_j = \sum_n \psi_{j,n}/\sqrt{N}$ for $j = 1, 2$ where N is the number of layers considered. The equations for ψ_1 and ψ_2 which have the form

$$a_1\psi_1 - \frac{\hbar^2}{2m_1} \left[\frac{\partial^2 \psi_1}{\partial x^2} + \frac{\partial^2 \psi_1}{\partial y^2} - K^2(x^2 + y^2)\psi_1 \right] + 2t[\psi_1 - \psi_2] = 0 \quad (3.6a)$$

$$a_1\psi_2 - \frac{\hbar^2}{2m_{2x}} \frac{\partial^2 \psi_2}{\partial x^2} - \frac{\hbar^2}{2m_{2y}} \frac{\partial^2 \psi_2}{\partial y^2} - \frac{\hbar^2 K^2}{2} \left(\frac{x^2}{m_{2y}} + \frac{y^2}{m_{2x}} \right) \psi_2 + 2t[2\psi_2 - \psi_1] = 0 \quad (3.6b)$$

Reconstructing an effective free energy functional from equations (3.6a) and (3.6b), we get,

$$G_{eff} = \int \left[a_1 |\psi_1|^2 + \frac{\hbar^2}{2m_1} \left(\left| \frac{\partial \psi_1}{\partial x} \right|^2 + \left| \frac{\partial \psi_1}{\partial y} \right|^2 \right) + \frac{\hbar^2 K^2}{2m_1^2} (x^2 + y^2) |\psi_1|^2 \right. \\ \left. + a_2 |\psi_2|^2 + \frac{\hbar^2}{2m_{2x}} \left| \frac{\partial \psi_2}{\partial x} \right|^2 + \frac{\hbar^2}{2m_{2y}} \left| \frac{\partial \psi_2}{\partial y} \right|^2 + \frac{\hbar^2 K^2}{2} \left(\frac{x^2}{m_{2y}} + \frac{y^2}{m_{2x}} \right) |\psi_2|^2 \right. \\ \left. + 2t |\psi_1 - \psi_2|^2 \right] dx dy. \quad (3.7)$$

Let us put $x=y=0$ and $T = T_c$ in equations (3.6). Near T_c , ψ_1 and ψ_2 will be very small and hence the spatial variations of these functions can be neglected. Therefore we get,

$$a_1(T_c)\psi_1 + 2t\psi_1 - 2t\psi_2 = 0 \quad (3.8a)$$

and

$$a_2(T_c)\psi_2 + 2t\psi_2 - 2t\psi_1 = 0 \quad (3.8b)$$

Equations (3.8) have nontrivial solutions only when

$$a_1(T_c) + 2t - \frac{4t^2}{a_2 + 2t} = 0 \quad (3.9a)$$

Let us assume $a_1(T) = \alpha_1(T - T_0)/T_c$ and $a_2(T) = \alpha_2$ where T_0 is some phenomenological temperature and α_1 and α_2 are positive constants. Here it is assumed that

the temperature dependence appears only in the coefficient associated with the CuO_2 planes. From (3.9a), we obtain the relation

$$\frac{T_0}{T_c} = 1 + \frac{2t}{\alpha_1} - \frac{4t^2}{\alpha_1(\alpha_2 + 2t)}. \quad (3.9b)$$

The free energy functional (3.7) may be written in terms of

$$\lambda = \frac{4t^2}{\alpha_1(\alpha_2 + 2t)}, \quad \xi^2 = \frac{\hbar^2}{2m_1\alpha_1}$$

$$\ell_x^2 = \frac{\lambda^2 \hbar^2 \alpha_1}{8m_{2x}t^2}, \quad \ell_y^2 = \frac{\lambda^2 \hbar^2 \alpha_1}{8m_{2y}t^2}.$$

and the rescaled order parameters $\psi'_1 = \alpha_1\psi_1$ and $\psi'_2 = \frac{2t}{\lambda}\psi_2$. After dropping the primes for convenience the effective free energy can be written as

$$G_{eff} = \int \left[\left(\frac{T}{T_c} - 1 \right) |\psi_1|^2 + \xi^2 \left(\left| \frac{\partial \psi_1}{\partial x} \right|^2 + \left| \frac{\partial \psi_1}{\partial y} \right|^2 \right) + \xi^2 K^2 (x^2 + y^2) |\psi_1|^2 \right. \\ \left. + \ell_x^2 \left| \frac{\partial \psi_2}{\partial x} \right|^2 + \ell_y^2 \left| \frac{\partial \psi_2}{\partial y} \right|^2 + K^2 (\ell_y^2 x^2 + \ell_x^2 y^2) |\psi_2|^2 \right. \\ \left. + \lambda |\psi_1 - \psi_2|^2 \right] dx dy \quad (3.10)$$

The equations that minimize G_{eff} are

$$\xi^2 \left(\frac{\partial^2 \psi_1}{\partial x^2} + \frac{\partial^2 \psi_1}{\partial y^2} \right) = \xi^2 K^2 (x^2 + y^2) \psi_1 + \left(\frac{T}{T_c} - 1 \right) \psi_1 + \lambda [\psi_1 - \psi_2] \quad (3.11a)$$

and

$$\ell_x^2 \frac{\partial^2 \psi_2}{\partial x^2} + \ell_y^2 \frac{\partial^2 \psi_2}{\partial y^2} = K^2 (\ell_y^2 x^2 + \ell_x^2 y^2) \psi_2 + \lambda [\psi_2 - \psi_1]. \quad (3.11b)$$

The solutions to eqns.(3.11a) and (3.11b) in the limit $\lambda \rightarrow 0$ and $T \rightarrow T_c$ can be written as

$$\psi_1 = \psi_{10} e^{-\gamma(x^2 + y^2)}$$

and

$$\psi_2 = \psi_{20} e^{-\gamma(\frac{\ell_x}{\ell_c} x^2 + \frac{\ell_y}{\ell_c} y^2)} \quad (3.12)$$

where $\gamma = \frac{K}{2}$. Substituting (3.12) back into (3.11), we get,

$$\left(\frac{T}{T_c} - 1 + \lambda + 2K\xi^2\right)\psi_{10} - \lambda\psi_{20} = 0 \quad (3.13)$$

and

$$\lambda\psi_{10} - (\lambda + 2K\ell^2)\psi_{20} = 0 \quad (3.14)$$

where $\ell^2 = \ell_x \ell_y$. Equations (3.13) and (3.14) have nontrivial solutions only if

$$1 - \frac{T}{T_c} = \lambda + 2K\xi^2 - \frac{\lambda^2}{(2K\ell^2 + \lambda)} \quad (3.15)$$

Equation(3.15) determines the temperature dependence of H_{c2}^\perp . As

$$H \rightarrow \infty, \quad 1 - \frac{T}{T_c} = \lambda + 2K\xi^2.$$

At large H-values, $H_{c2}^\perp(T)$ becomes a straight line which cuts the T-axis at $T = T_c(1 - \lambda)$. In SI units $H_{c2}^\perp(T)$ can be written as

$$H_{c2}^\perp(T) = \frac{(1 - \lambda)\hbar}{2e\xi^2} - \frac{1}{T_c} \frac{\hbar}{2e\xi^2} T \quad (3.16)$$

Comparing this with the linear fit for critical field data on single crystal $YBa_2Cu_3O_7$ for fields perpendicular to the layers given in ref.[76]

$$H_{c2}^\perp = 173.1689 - 1.8919T$$

we obtain $\xi = 13.725A^\circ$ and $\lambda = 0.0098$. For small values of H ,

$$\frac{dH}{dT} = -\frac{1}{T_c} \frac{\hbar c}{2e L^2}$$

where $L^2 = \xi^2 + \ell^2$. Low field critical field data on $YBa_2Cu_3O_7$ single crystals [78] yields $\frac{dH}{dT} = 80G/K$. This is smaller than the critical field slope observed at higher

fields by a factor of 100. From the expression for $\frac{dH}{dT}$ we get $\ell = 210.5\text{\AA}$. The curvature

$$\frac{1}{R} = \frac{\hbar c}{2e} \frac{2\ell^2}{\lambda T_c^2 L^4 [1 + \frac{\hbar^2 c^2}{4e^2 T_c^2} L^{-4}]}$$

is positive. Experimental data on single crystal $YBa_2Cu_3O_7$ [76,78] show that the curvature is present for H-values upto 18G, depends on the mass anisotropy in the CuO chain layers and is enhanced by it.

Reliable H_{c2} data is also available for the $La_{1.87}Ca_{1.13}Cu_2O_6$ [79] for which the double CuO_2 planes in the crystallographic unit cell constitutes the S layer and the double metallic LaO planes form the S' layer. Our calculations based on the experimental data in ref.[79] give $\lambda = 0.1694$, $\xi = 30.1\text{\AA}$ and $\ell = 233\text{\AA}$ for this compound. This value of ξ compares favourably with the experimental value of 33\AA . The fairly strong coupling coefficient obtained from the calculations agrees with the rather small anisotropy of the coherence length which implies a fairly isotropic electronic structure for the compound inspite of its quasi two dimensional crystal structure.

From equation (3.14),

$$\frac{\psi_{20}}{\psi_{10}} = \frac{\lambda}{\lambda + 2K\ell^2}. \quad (3.17)$$

As

$$H \rightarrow 0, \quad \frac{\psi_{20}}{\psi_{10}} \rightarrow 1.$$

But as H increases $\frac{\psi_{20}}{\psi_{10}} \rightarrow 0$ (see Fig.3.1). Therefore the linear region of $H_{c2}^{\perp}(T)$ is precisely the region where the order parameter becomes zero on the S' layers.

The temperature dependence of H_{c2}^{\perp} can also be obtained by a variational

method. We try the solution

$$\psi_1 = b e^{-\gamma(x^2+y^2)}$$

and

$$\psi_2 = e^{-\gamma(x^2+y^2)} \quad (3.18)$$

where b and γ are variational parameters. We now make use of the fact that G_{eff} given by (3.10) should vanish at the transition from the superconducting to the normal state. Substituting equation (3.18) in (3.10), performing the integration with the help of standard integrals [100] and setting $G_{eff} = 0$, we get

$$\left[\left(\frac{T}{T_c} - 1 + \lambda \right) \gamma + 2\xi^2 g_1 \right] b^2 - 2b\lambda\gamma + \left[(\ell_x^2 + \ell_y^2) g_1 + \lambda\gamma \right] = 0 \quad (3.19)$$

where $g_1 = \gamma^2 + \frac{K^2}{4}$. Maximizing $T_c(H)$ given by equation (3.19) with respect to b , we obtain

$$1 - \frac{T}{T_c} = \lambda + 2\xi^2 g_1 - \frac{\lambda^2}{[(\ell_x^2 + \ell_y^2) g_1 + \lambda]}$$

Since λ is small, $T_c(H)$ can be maximized with respect to γ neglecting the term in λ^2 . Then we get $\gamma = \frac{K}{2}$ and

$$1 - \frac{T}{T_c} = \lambda + 2\xi^2 K - \frac{\lambda^2}{[(\ell_x^2 + \ell_y^2) K + \lambda]} \quad (3.20)$$

Equation (3.20) is similar to equation (3.15) and validates all the features of the $H_{c2}^{\perp}(T)$ discussed earlier. In the case of thallium and bismuth based compounds and the 214 compound S^v layers are square planar. Therefore $\ell_x = \ell_y$ and equations (3.15) and (3.20) are identical. In the LD case of identical superconducting planes, $\psi_2 = 0$. If we set $\lambda = 0$,

$$\psi_1 = \psi_{10} e^{-\frac{K}{2}(x^2+y^2)}.$$

The temperature dependence of the upper critical field in this case is obtained from equation (3.13) as

$$1 - \frac{T}{T_c} = 2K\xi^2.$$

For small λ , the correction to H_{c2} can be obtained by evaluating G_{eff} with the above unperturbed functional forms for ψ_1 and ψ_2 and equating the result to zero. This yields

$$1 - \frac{T}{T_c} = \lambda + 2K\xi^2. \quad (3.21)$$

When $H=0$, $T \neq T_c$ and hence this result is not valid near T_c . However it agrees with the large H -limit of equation (3.15). The situation here is identical to the LD model with equidistant identical superconducting layers.

Another possible model for $YBa_2Cu_3O_7$ with inequivalent conducting layers [150] is obtained by ignoring the proximity effect and the contribution of the S' layers and considering the two CuO_2 layers in the elementary cell separately [Fig.3.5]. The distance between the CuO_2 layers in the same elementary cell is $d_1 = 3.3A^\circ$ and that between layers in the neighbouring cells is $d_2 = 8.4A^\circ$. This entails the introduction of two different coupling coefficients t_1 and t_2 and two different order parameters ψ_1 and ψ_2 to represent the inequivalently placed CuO_2 layers. The Gibb's free energy for this model is

$$\begin{aligned} G = d \sum_n \int & \left[a(|\psi_{1,n}|^2 + |\psi_{2,n}|^2) + \frac{b}{2}(|\psi_{1,n}|^4 + |\psi_{2,n}|^4) \right. \\ & + \frac{\hbar^2}{2m} \left| \left(\nabla_{\parallel} - \frac{2ie}{\hbar c} A_{\parallel} \right) \psi_{1,n} \right|^2 + \frac{\hbar^2}{2m} \left| \left(\nabla_{\parallel} - \frac{2ie}{\hbar c} A_{\parallel} \right) \psi_{2,n} \right|^2 \\ & + t_1 \left| \psi_{1,n} - \psi_{2,n} e^{-i \frac{2ed_1}{\hbar c} A_m} \right|^2 + t_2 \left| \psi_{1,n} - \psi_{2,n-1} e^{-i \frac{2ed_2}{\hbar c} A_m} \right|^2 \right] d\rho \\ & + \int \left[\frac{\mathbf{h}^2}{8\pi} - \frac{\mathbf{h} \cdot \mathbf{H}}{4\pi} + \frac{\mathbf{H}^2}{4\pi} \right] d\rho dz. \quad (3.22) \end{aligned}$$

where $d = d_1 + d_2$, $a_1 = a_2 = a$, and $m_{2x} = m_{2y} = m_1 = m$. Proceeding as before,

we find:

$$1 - \frac{T}{T_c} = 2\ell_1^2 K \quad (3.23)$$

The $H_{c2}^\perp(T)$ graph is a straight line which cuts the T-axis at $T = T_c$ and there is no curvature for low values of H. Comparison of the results (3.21) and (3.23) show conclusively that the positive curvature which is a generic property of high- T_c superconductors can be explained only if the contribution from the S' layers which are structurally different from the S layers are also included in the free energy expression. The inequivalency of the CuO_2 layers as described by (3.22) alone does not suffice to explain the positive curvature of $H_{c2} \perp (T)$.

3.3 Angular dependence of H_{c2}

When the magnetic field is applied in the x-z plane, $\phi = 0$,

$$H_n = H(\hat{z} \cos \theta + \hat{x} \sin \theta)$$

and

$$A_n = yH(\hat{z} \sin \theta - \hat{x} \cos \theta).$$

In this case the order parameters have no explicit x -dependence and proceeding as in section 3.2, we get

$$\begin{aligned} G_{eff} = \int & \left[\left(\frac{T}{T_c} - 1 \right) |\psi_1|^2 + \xi^2 \left| \frac{\partial \psi_1}{\partial y} \right|^2 + 4\xi^2 K^2 \cos^2 \theta y^2 |\psi_1|^2 + \ell_y^2 \left| \frac{\partial \psi_2}{\partial y} \right|^2 \right. \\ & + 4K^2 \ell_x^2 y^2 \cos^2 \theta |\psi_2|^2 + \frac{\lambda}{2} |\psi_1 - \psi_2 \exp(i2Kdy \sin \theta)|^2 \\ & \left. + \frac{\lambda}{2} |\psi_1 - \psi_2 \exp(-i2Kdy \sin \theta)|^2 \right] dy \quad (3.10a) \end{aligned}$$

Using trial solutions

$$\psi_1 = b \exp(-\gamma y^2) \quad \text{and} \quad \psi_2 = \exp(-\gamma y^2), \quad (3.18a)$$

G_{eff} is evaluated with the help of standard integrals [100] and it is set equal to zero at the transition from the superconducting to the normal state *i.e.* when $H = H_{c2}$. In the resulting expression $T_c(H)$ is maximized with respect to b and we get

$$1 - \frac{T}{T_c} = \lambda + \xi^2 g_2 - \frac{\lambda^2 \exp(-\frac{e^2 d^2 H^2 \sin^2 \theta}{\hbar^2 c^2 \gamma})}{[\ell_y^2 \gamma + \ell_x^2 \frac{K^2 \cos^2 \theta}{\gamma} + \lambda]} \quad (3.24)$$

where $g_2 = \gamma + \frac{K^2 \cos^2 \theta}{\gamma}$. In the general case maximization of this expression with respect to γ can be done only numerically. However for large fields when $(\ell_y^2 \gamma + \ell_x^2 \frac{K^2 \cos^2 \theta}{\gamma}) > \lambda$, the last term in λ^2 becomes negligible and $\gamma = K \cos \theta$. In the large H limit, the temperature and angular dependence of H_{c2} is given by

$$1 - \frac{T}{T_c} = \lambda + 2K\xi^2 \cos \theta - \frac{\lambda^2}{(\ell_x^2 + \ell_y^2)K \cos \theta} \exp(-\frac{Kd^2 \sin^2 \theta}{\cos \theta}). \quad (3.25)$$

For $\theta = 0$ equation (3.25) reduces to equation (3.20). In the opposite limit, when $\lambda > (\ell_y^2 \gamma + \ell_x^2 \frac{K^2}{4\gamma})$ the exponential in equation (3.24) is expanded to the first order in the argument and then maximized with respect to γ to obtain

$$\gamma = \frac{eH}{\hbar c} (\cos^2 \theta + \epsilon \sin^2 \theta)^{\frac{1}{2}} \quad (3.26)$$

where $\epsilon = \lambda d^2 / \xi^2$. In this limit, the temperature and angular dependence of H_{c2} is obtained as

$$1 - \frac{T}{T_c} = \frac{2eH\xi^2}{\hbar c} [\cos^2 \theta + \epsilon \sin^2 \theta]^{\frac{1}{2}} \quad (3.27)$$

Equation (3.27) is the θ -dependence obtained from the GL anisotropic theory and was experimentally verified in ref.[80].

3.4 Upper critical field parallel to the layers

Our results (3.25) and (3.27) cannot be relied upon for $\theta = 90^\circ$ since in this case the order parameters are oscillatory Mathieu functions as we will see later in this section. Setting $\theta = 90^\circ$, equation (3.27) yields

$$1 - \frac{T}{T_c} = 2\sqrt{\lambda} \frac{ed\xi}{\hbar c} H$$

which represents a straight line with negative slope passing through $T = T_c$. We can also calculate the temperature dependence of H_{c2}^{\parallel} by the variational method. G_{eff} given by (3.10a) is evaluated after setting $\theta = 90^\circ$, using the ansatz (3.18a) and is set equal to zero. This gives us $T_c(H)$ as a function of variational parameters. The maximization of $T_c(H)$ with respect to b can be done analytically whereas the same with respect to γ can be done only in certain limiting cases. In the limit $\lambda > \ell_y^2 \gamma$,

$$1 - \frac{T}{T_c} = \lambda + \frac{\xi^2 dK}{L_y} - \frac{\lambda^2(1 - L_y dK)}{[\frac{\ell_y^2 dK}{L_y} + \lambda]} \quad (3.28)$$

where $L_y^2 = (\xi^2 + \ell_y^2)/\lambda$. At large values of H , $H_{c2}^{\parallel}(T)$ is a straight line which on extrapolation cuts the T -axis at $T^* = T_c(1 - 2\lambda)$. It is interesting to consider the case when $\psi_2 = 0$ and only identical equispaced double CuO_2 planes are consid-

ered. The situation is identical to the LD formalism. In this case $T_0 = T_c$. The free energy expression for determining H_{c2}^{\parallel} in this case becomes

$$F_S = \sum_n \int dx \left[a |\psi_n|^2 + \frac{\hbar^2}{2m_{\parallel}} \left| \frac{\partial \psi_n}{\partial y} \right|^2 + t |\psi_n - \psi_{n-1} e^{i\chi_n}|^2 \right]$$

$\psi_n(y) = \psi(y) \exp(-ikn)$. Differentiating F_S with respect to ψ^* we obtain the Mathieu equation

$$-\frac{\hbar^2}{2m_{\parallel}} \frac{\partial^2 \psi}{\partial y^2} + 2t\psi \left[1 - \cos \frac{2edH}{\hbar c} y \right] = -a\psi. \quad (3.29)$$

If $E(H)$ is the lowest eigen value of this equation, then transition to the normal state occurs when $E(H) \geq |a|$. For small values of H the cosine term is expanded to the first order in the argument. We obtain the Schrodinger equation for the harmonic oscillator solving which

$$H_{c2}^{\parallel} = \left(\frac{mc^2 \alpha^2}{2e^2 d^2 t} \right)^{\frac{1}{2}} \frac{T - T_c}{T_c}. \quad (3.30)$$

At large H , $E(H) \geq |a| > t$. For $t < E < 2t$ equation (3.29) can be solved to obtain

$$H_{c2}^{\parallel} = \left[\frac{mc^2 t^2}{e^2 d^2 \alpha} \frac{T_c - T^*}{T_c} \right]^{\frac{1}{2}} \quad (3.31)$$

where $T^* = T_c(1 - 2\lambda)$. When $|a| > 2t$, $E(H)$ is always smaller than $|a|$ and H_{c2}^{\parallel} becomes infinite. Thus $H_{c2}^{\parallel}(T)$ exhibits positive curvature even if we consider a system of identical layers. This shows that while inclusion in the free energy of the contributions from the non superconducting layers arising from the proximity effect is essential for explaining the positive curvature of $H_{c2}^{\parallel}(T)$, the LD model with its equidistant identical superconducting layers can also explain the positive curvature of $H_{c2}^{\parallel}(T)$.

The preceding procedure can be extended to $La_{2-x}Sr_xCuO_4$ superconductor with ψ_1 and ψ_2 representing the CuO_2 mono layers and LaO bilayers respectively and also to the thallium and bismuth based superconductors. Figure 3.3 is a graphical representation of equations (3.20) and (3.28) for $YBa_2Cu_3O_7$ compound whereas figure 3.4 is the same for $La_{1.87}Ca_{1.13}Cu_2O_6$ superconductor. Equation (3.28) is valid upto 2.6T for $YBa_2Cu_3O_7$ and upto 37T for $La_{1.87}Ca_{1.13}Cu_2O_6$.

3.5 Lower Critical Field

In this section the temperature dependence of the lower critical field is studied using the high field approximation employed in refs.[99,146] in the case of superconducting intercalated layered compounds. The quartic terms in equation (2.16) are retained while evaluating H_{c1} . For magnetic fields parallel to the layers

$$H_n = H \hat{x} \quad \text{and} \quad A_n = Hy \hat{z}.$$

In the region close to T_c , $\frac{v_{zn}}{v_{zn}} \rightarrow 1$ (section 3.3) and H_{c1} has the usual isotropic GL form for a continuous medium [146]. $H_{c1}^{\parallel} = \frac{H_c}{\kappa\sqrt{2}} \ln \kappa$ where $H_c = \sqrt{\frac{4\pi}{b}} |a|$ and $\kappa\sqrt{2} = \frac{c}{4ed} \left(\frac{2m_{\parallel}b}{\pi\hbar^2t}\right)^{\frac{1}{2}}$. Hence

$$H_{c1}^{\parallel} \propto \left(\frac{T_0 - T}{T_c}\right)^{\frac{1}{2}}. \quad (3.32)$$

$\frac{T_0}{T_c}$ could be different from that given by equation (3.9b) as the quartic terms were not considered in deriving the same.

In the low temperature region characterised by two dimensional behaviour, $t \ll |a|$ and the Josephson coupling term can be treated as a perturbation. For $t = 0$, the minimum of G is obtained for $h = H$, $\psi_{1n} = |\psi_{10}| \exp(i\frac{2\pi}{\Phi_0} Hnyd)$, $\psi_{2n} = |\psi_{20}| \exp(i\frac{2\pi}{\Phi_0} Hnyd)$ with $|\psi_{10}|^2 = -a_1/b_1$ and $|\psi_{20}|^2 = -a_2/b_2$. By

substituting these unperturbed values into (2.16), the free energy per unit volume is obtained as

$$g = \frac{H^2}{8\pi} - \frac{|a_1|^2}{2b_1} - \frac{|a_2|^2}{2b_2}.$$

Introducing the perturbation term,

$$g = \frac{H^2}{8\pi} - \frac{|a_1|^2}{2b_1} - \frac{|a_2|^2}{2b_2} + 2t \frac{|a_1|}{b_1} + 2t \frac{|a_2|}{b_2} - 2t \left(\frac{a_1 a_2}{b_1 b_2} \right)^{\frac{1}{2}}. \quad (3.33)$$

In the Meissner state where $h = 0$ and $A_x = A_y = A_z = 0$ the free energy density

$$g = \frac{H^2}{4\pi} - \frac{|a_1|^2}{2b_1} - \frac{|a_2|^2}{2b_2} + 2t \frac{|a_1|}{b_1} + 2t \frac{|a_2|}{b_2} - 4t \left(\frac{a_1 a_2}{b_1 b_2} \right)^{\frac{1}{2}}. \quad (3.34)$$

Comparing equations (3.33) and (3.34) we get

$$H_{c1}^{\parallel} = 4 \left(\frac{\pi^2 t^2 \alpha_1 \alpha_2}{b_1 b_2} \right)^{\frac{1}{4}} \tau^{\frac{1}{4}}. \quad (3.35)$$

From equations (3.32) and (3.35) we see that the temperature dependence of $H_{c1}^{\parallel}(\tau)$ changes from τ linear near T_c to $\tau^{\frac{1}{4}}$ at low temperatures. Fitting equation (3.35) to the low temperature data in ref.[81], we get H_{c1}^{\parallel} at $T=10K$ to be $49.1mT$ which is comparable to the experimental value of $56mT$. We obtain $H_{c1}^{\parallel}(0) = 54.13mT$ where as a parabolic fit attempted in ref. [81] gives $60mT$. Figure (3.4) shows the temperature variation of H_{c1} according to equations (3.32) and (3.34) for $YBa_2Cu_3O_7$. The figure shows the anomalous upturn at low temperatures observed by several authors in the $H_{c2}^{\parallel}(\tau)$ graph of copper oxide superconductors[81,84].

H_{c1}^{\perp} can be evaluated by a similar procedure by setting

$$\begin{aligned} H_n &= H \hat{z}, & A_n &= \frac{H}{2} (-y \hat{x} + x \hat{y}), \\ \psi_1 &= \psi_{10} \exp - \frac{K}{2} (x^2 + y^2), & \psi_2 &= \psi_{20} \exp - \frac{K}{2} (x^2 + y^2), \\ h &= h(0) \exp - \left(\frac{\rho}{\lambda} \right) & \text{and} & \quad \int h d\rho = \Phi_0. \end{aligned}$$

λ is the penetration depth and $\Phi_0 = 2 \times 10^{-7} \text{gauss} - \text{cm}^2$ is the superconducting flux quantum. We now obtain

$$H_{c1}^{\perp} = \frac{\Phi_0}{8\pi\lambda_x(\tau)\lambda_y(\tau)} + \frac{\pi\hbar^2\alpha_1}{4m_1b_1\Phi_0}\tau + \frac{\pi\hbar^2\alpha_2}{8b_2\Phi_0}\left(\frac{1}{m_{2x}} + \frac{1}{m_{2y}}\right) \quad (3.36)$$

For copper oxide superconductors it has been shown experimentally by several authors [82] that the BCS clean limit approximation holds for the temperature dependence of the inplane London penetration depth near T_c so that

$$\frac{1}{\lambda_{ab}^2(T)} = \frac{1}{\lambda_{ab}^2(0)}\left(1 - \frac{T}{T_c}\right).$$

Thus H_{c1}^{\perp} has a τ -linear behaviour near T_c . Experimental data of ref.[83] point to a linear T-dependence for both $\lambda_{ab}(T)$ and $\lambda_c(T)$ below 25K for $Bi_2Sr_2Cu_2O_{8+y}$. If this behaviour is general to other copper oxide superconductors also, the change over from τ -linear dependence near T_c to τ^{-2} dependence for the low temperature regime as given by equation (3.36) explains the upturn in $H_{c1}^{\parallel}(T)$ graph at low temperatures observed by several authors [81,84].

For applied field in the x-z plane,

$$H_{c1}^{\theta} = \frac{\Phi_0}{8\pi\lambda_{\theta}^2(0)} + \frac{\pi}{\Phi_0(\cos^2\theta + \epsilon\sin^2\theta)} \left[\frac{\hbar^2\alpha_1\cos^2\theta}{4m_1b_1}\tau + 2td^2\sin^2\theta\left(\frac{\alpha_1\alpha_2}{b_1b_2}\right)^{\frac{1}{2}}\tau^{\frac{1}{2}} + \frac{\hbar^2\alpha_2\cos^2\theta}{8b_2}\left(\frac{1}{m_{2x}} + \frac{1}{m_{2y}}\right) \right] \quad (3.37)$$

where ϵ is an anisotropy parameter[7]. When $\theta = 0$ equation (3.37) reduces to (3.36).

3.6 Conclusion

We have theoretically studied the temperature dependence of the critical magnetic fields of $YBa_2Cu_3O_7$ superconductor by employing the free energy functional (2.16). For temperatures close to T_c , $H_{c2}^\perp(T)$ has a positive curvature and becomes a straight line with negative slope at large H values. The theoretical expression (3.16) was fitted to the experimental data for $YBa_2Cu_3O_7$ and $La_{1.87}Ca_{1.13}Cu_2O_4$. The values of the parameter ξ obtained in these two cases agree with the respective experimental values. $H_{c2}^\parallel(T)$ also exhibits positive curvature. Our treatment shows that the curvature depends not only on the inequivalency of the order parameters but also on the mass anisotropy of the CuO chain layers. Comparisons of models (2.16) and (3.22) show conclusively that the non-zero value of the order parameter on the NSC layers which are structurally different from the SC layers is essential to explain the positive curvature of $H_{c2}^\perp(T)$ whereas the positive curvature of $H_{c2}^\parallel(T)$ can be explained even on the standard LD model. This is also borne out by the calculations in ref.[145] where the authors obtain a positive curvature for H_{c2}^\perp considering the proximity effect between the CuO_2 planes and the CuO chain layers and by introducing two different coupling coefficients. The large H-limit of H_{c2} given by (3.16) and the parameters deduced therein are exactly identical to those of ref.[145] which is nothing but the expression (3.21) obtained for the LD model. However the experiments of Kleiner *et al.* substantiates the simpler model that we have considered in arriving at the results (3.15), (3.16), (3.20), (3.25), (3.26) and (3.28).

Calculations carried out in section 3.5 shows that the temperature dependence of $H_{c1}^\parallel(T)$ changes from a τ -linear dependence given by equation (3.32) near T_c

to a τ^4 dependence given by equation (3.35) further away from T_c . A fit of the experimental data of ref.[81] for $YBa_2Cu_3O_7$ according to equations (3.32) and (3.35) is shown in Fig.(3.4). The $H_{c1}(T)$ graph shows a positive curvature. The estimated value for $H_{c1}^{\parallel}(0)$ is 54.13mT which compares favourably with the value of 60mT obtained from a parabolic fit attempted in ref.[81]. Equation (3.36) gives the temperature dependence of $H_{c1}^{\perp}(T)$. The different temperature dependence of λ_{ab} experimentally observed by several authors [82,83] near T_c and at lower temperatures when substituted in equation (3.36) gives an upturn in the $H_{c1}^{\perp}(T)$ graph at low temperatures which has been observed experimentally [81,84] for copper oxide superconductors.

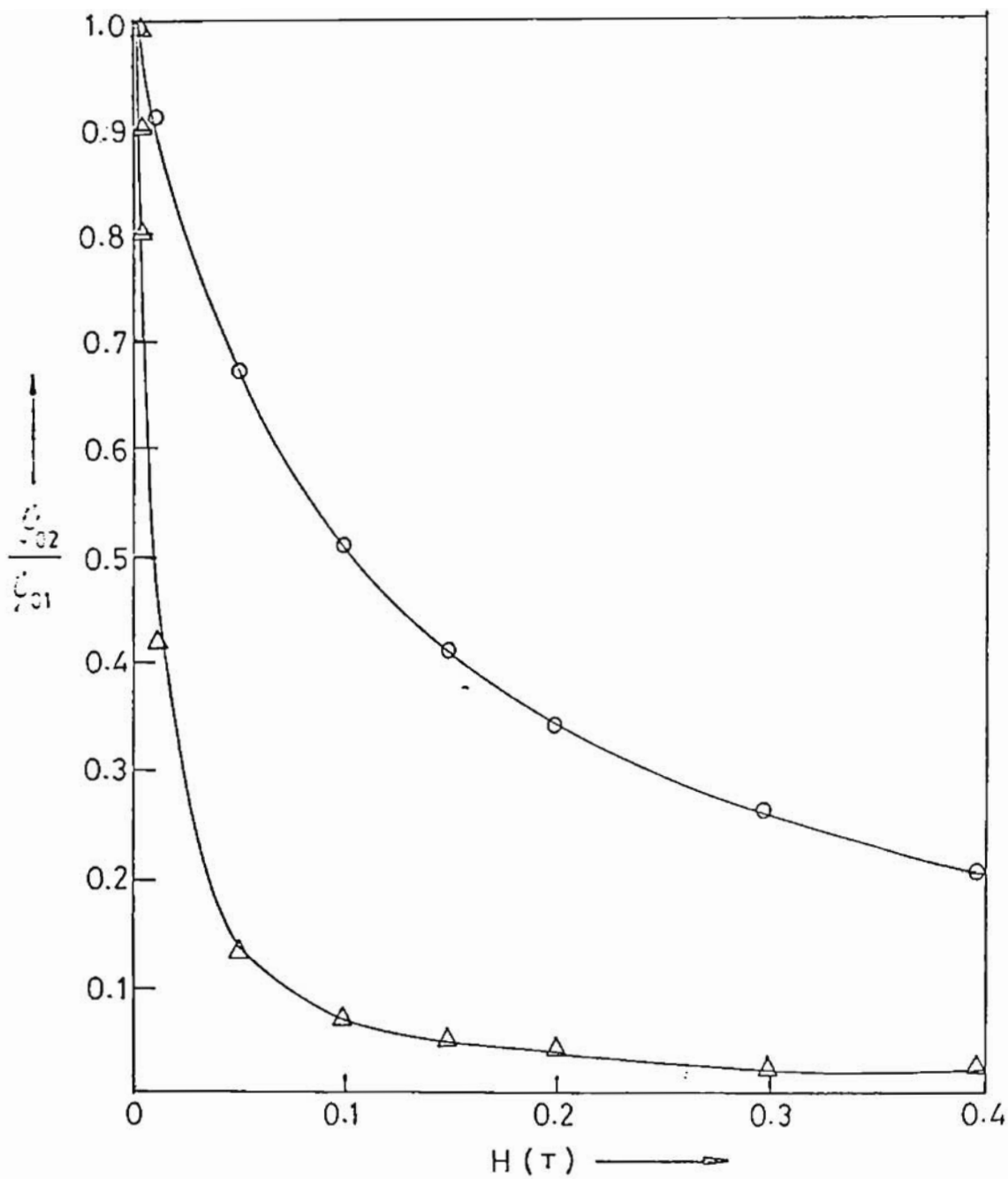


Figure 3.1 The ratio of the NSC to the SC orderparameter for field parallel to the c-axis. Triangles represent $YBa_2Cu_3O_7$ and circles represent $La_{1.57}Ca_{1.13}Cu_2O_6$.

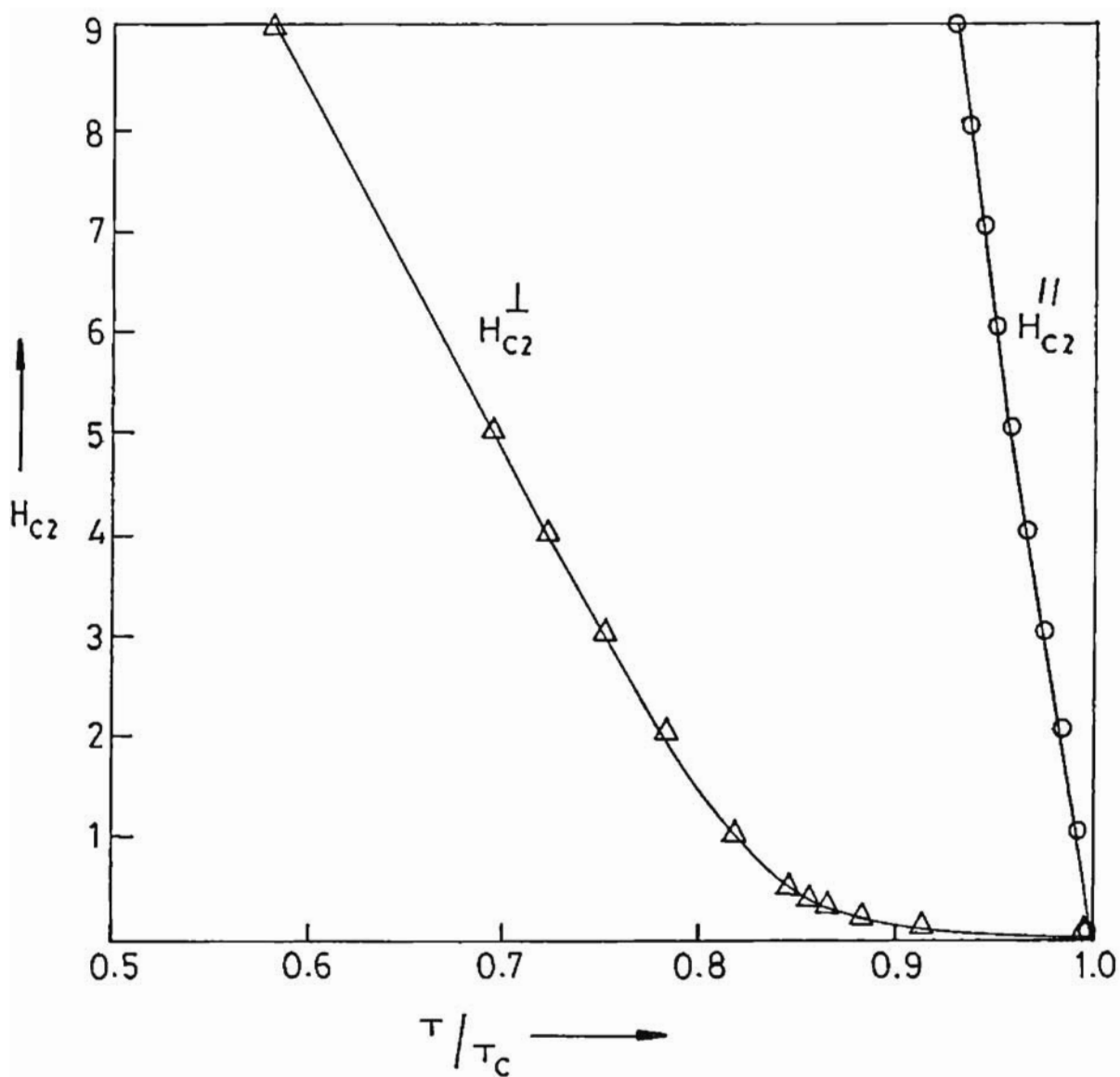


Figure 3.2 Graphical representation of $H_{c2}^{\perp}(T)$ and $H_{c2}^{\parallel}(T)$ for $YBa_2Cu_3O_7$.

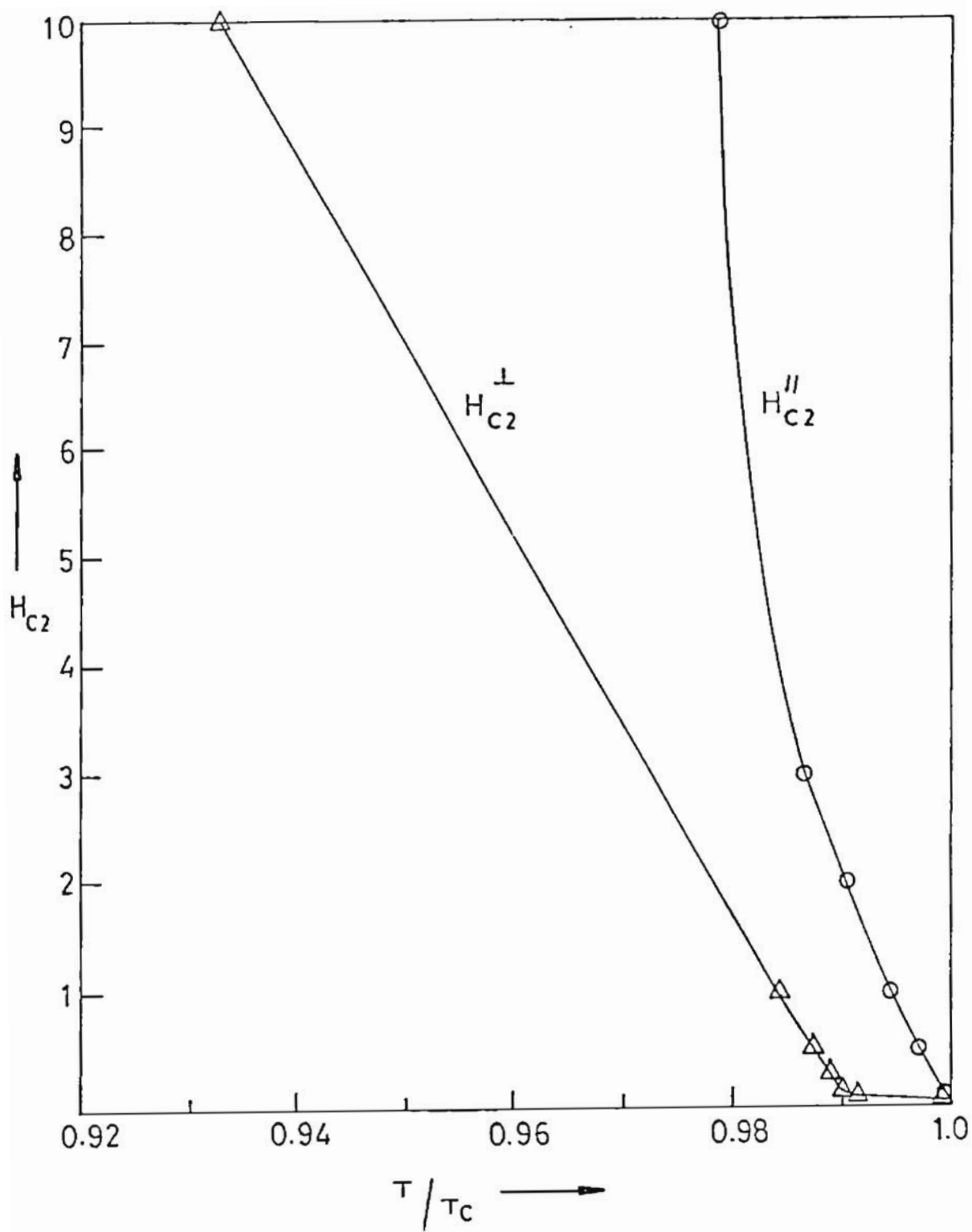


Figure 3.3 Graphical representation of $H_{C2}^{\perp}(T)$ and $H_{C2}^{\parallel}(T)$ for $La_{1.87}Ca_{1.13}Cu_2O_6$.

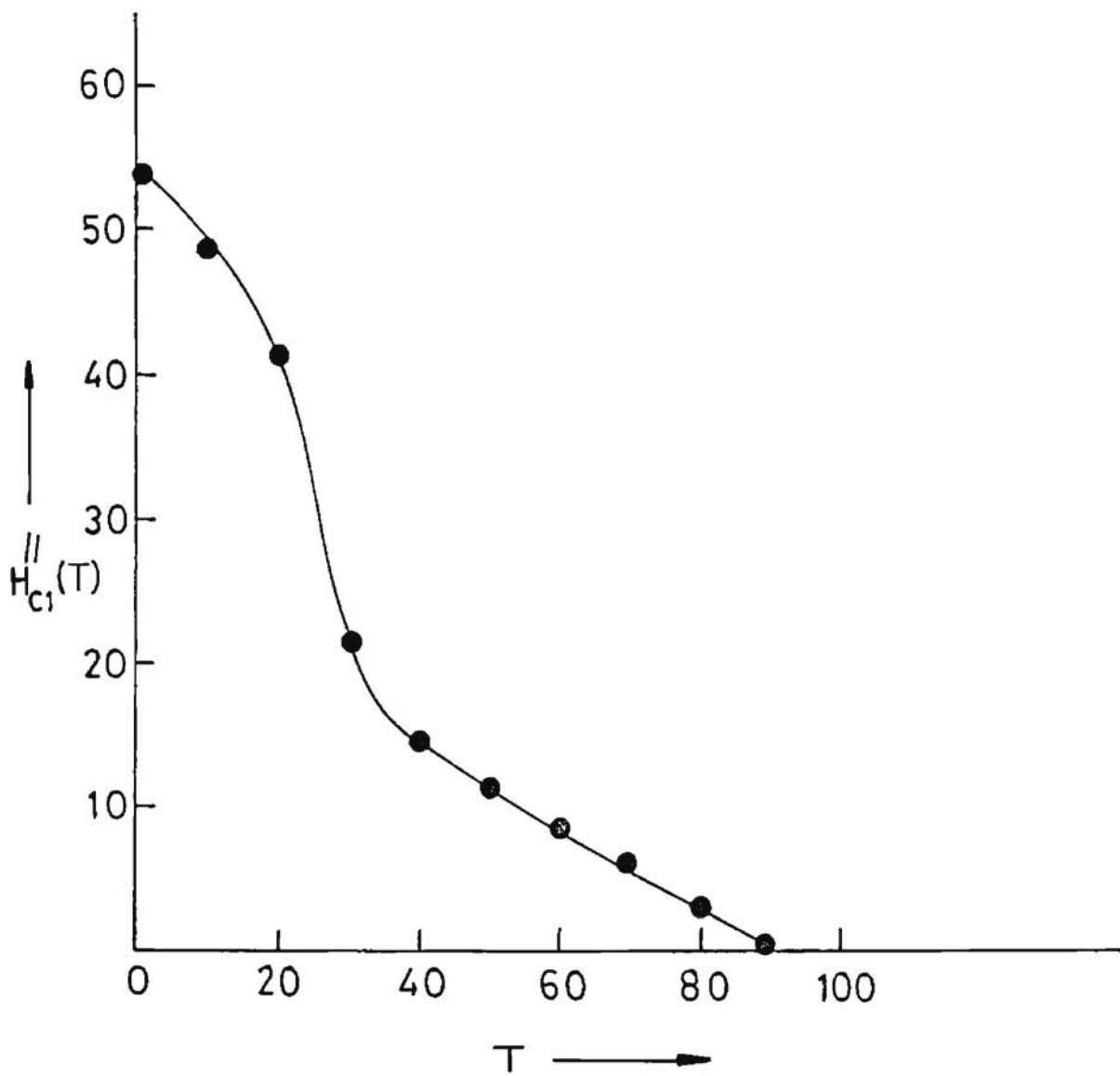


Figure 3.4 $H_{c1}^{\parallel}(T)$ for $YBa_2Cu_3O_7$.

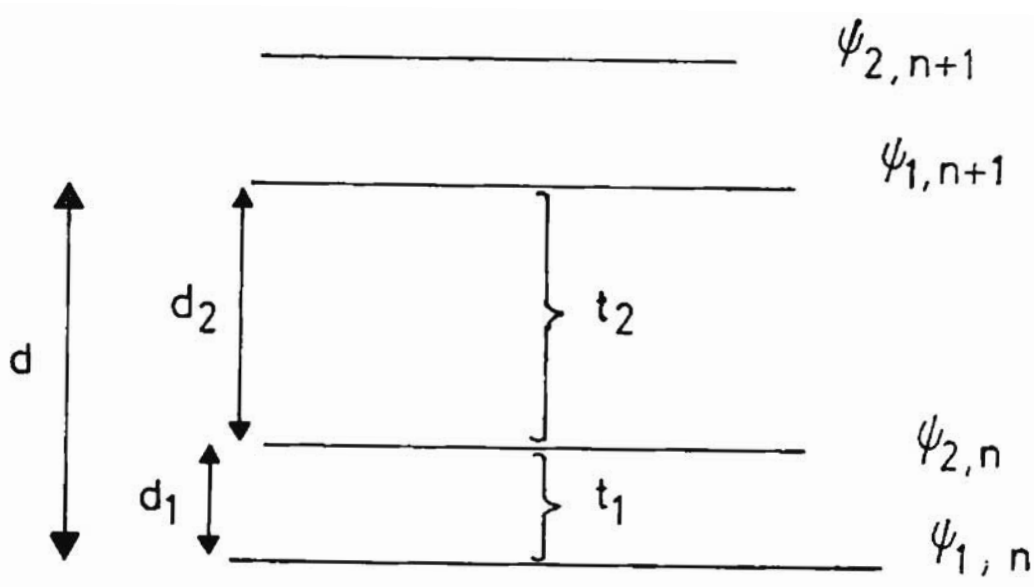


Figure 3.5 Alternate model for superconductors with inequivalent conducting layers described by the free energy functional (3.22).

CHAPTER IV

FLUCTUATION SPECIFIC HEAT

4.1 Introduction

Superconducting fluctuations have lately been a subject of considerable study. There are several reports of observation of superconducting fluctuations in the copper oxide materials. These fluctuations have been reported in specific heat [85], electrical conductivity [86] and magnetic susceptibility [87].

Thermodynamic fluctuations alter the properties of superconducting materials in the vicinity of the superconducting phase transition. Above T_c , fluctuations towards the superconducting state lead to the appearance of excess conductivity, specific heat, diamagnetism and tunneling currents. Below T_c , fluctuations towards the normal state lead to the appearance of resistance in thin wires and the break down of fluxoid quantization in small rings. The relevant length scale over which individual fluctuations are important is the GL coherence length which determines the dimensionality of a given sample geometry. Because the characteristic coherence length in conventional superconductors is quite long, these effects are in general small. But they can be measured experimentally in superconducting samples of reduced dimensionality such as thin films, whisker crystals and powders, because the thermal energy $k_B T$ leads to larger effects in smaller fluctuation volumes. Thus thermal fluctuation effects in high temperature superconductors are much more pronounced than in conventional superconductors because of their

very small correlation lengths, high transition temperatures and layered structures which effectively reduce the dimensionality.

The Ginzburg criterion defines the region of critical fluctuations. The critical region can be estimated from the specific heat jump ΔC [88]. The critical region lies within τ_G , where

$$|\tau_G| = \left| \frac{T_G}{T_c} - 1 \right| = \frac{1}{32\pi^2} \left(\frac{k_B}{\Delta C \xi(0)^3} \right)^2$$

For high- T_c superconductors, ΔC values from ref.[85] gives $\tau_G \sim 10^{-3}$. Thus critical fluctuations are absent outside of a 0.1K region above T_c in a 90K superconductor. This result is also obtained from magnetic field effects [89] using the expression

$$T_G = \frac{1.07 \times 10^{-9} \kappa^4 T_{c0}^8}{H_{c2}(0)} K.$$

These estimates imply that as long as $|\tau| \geq 10^{-3}$ critical fluctuations should not be important and it should be sufficient to consider Gaussian fluctuations or fluctuations of the mean field type.

Besides being strongly type II superconductors with extremely small coherence lengths the high- T_c materials possess layered structures. Since the highly anisotropic transport properties suggest that high- T_c superconductivity may be driven by coupling within the planes and since fluctuation effects are expected to be more pronounced in lower dimensions it is sensible to explore the dimensionality of these fluctuations in such layered superconductors. The fact that the transverse coherence length $\xi_c(0)$ in these materials is smaller than the interplane distance d brings about a cross-over between a three dimensional (3D) regime near T_c and a two dimensional (2D) regime for $|\frac{T_c - T}{T_c}| > r = \frac{2\xi_c(0)^2}{d^2}$. The cross-over temperature T^* defined by $|\frac{T_c - T^*}{T_c}| = r$ has a simple physical meaning: at $T = T^*$ the temperature

dependent coherence length $\xi_c(T) = \xi_c(0)(\frac{T_c}{T_c-T})^{\frac{1}{2}}$ becomes equal to the interplane distance d . The LD model predicts such a cross-over between the two regimes.

In addition to the intrinsic interest aroused by observing and understanding such fluctuation effects, the study of fluctuation effects has given important insights into the domains of validity of various theoretical approaches. In many cases the measurement of fluctuation effects has spurred the development and use of state-of-the-art experimental techniques, particularly SQUID magnetometers and voltmeters.

In this and the following chapters the fluctuation contribution to specific heat, conductivity and diamagnetism for copper oxide superconductors is studied based on the free energy functional (2.16) and the dimensional cross over (DCR) behaviour in the fluctuation regime is also examined in these materials.

4.2. Fluctuation specific heat (FSH)

The specific heat measurements in $YBa_2Cu_3O_7$ both with and without the presence of a magnetic field are rather interesting since historically fluctuations in the specific heat have been the most difficult to observe. A convenient theoretical foundation for understanding the basic phenomena of thermodynamic fluctuations near the superconducting phase transition is provided by the GL theory by virtue of its relatively simple mechanics and rich phenomenological insight.

The superconducting contribution to the specific heat of zero dimensional (0D) particles (the radius R is small compared to the magnetic penetration depth λ as well as the coherence length ξ) was calculated by Shmidt [90] using the thermo-

dynamic relation

$$C_V = -\frac{T}{V} \frac{\partial^2}{\partial T^2} \langle F \rangle$$

where $\langle F \rangle$ is the weighted average of the free energy $F = (a |\psi|^2 + \frac{b}{2} |\psi|^4)V$ over all values of the order parameter and V is the volume of the sample. For fluctuations effects above T_c , $|\psi|^2$ is small except in the narrow critical region near T_c . This smallness of $|\psi|^2$ allows us to drop the quartic term in the free energy expression. The fluctuations in small particles round off the behaviour expected from mean-field theory. The zero dimensional results have not been subjected to experimental test, because of the practical difficulties of achieving thermal equilibrium among a sufficient number of isolated small particles.

The result for bulk material is given by

$$C_V = \frac{k_B}{8\pi\xi^2(0)} \tau^{-\frac{1}{2}} \quad (4.1)$$

where additional terms have been included in the total free energy to represent the spatial variation of the order parameter. In typical conventional clean superconductors this would become comparable with the mean field jump in the specific heat at T_c only for $\tau \simeq 10^{-11}$. Even in very dirty materials with small $\xi(0)$ it should be unobservable. Cochran [91] has confirmed the absence of a $\tau^{-\frac{1}{2}}$ contribution in conventional bulk superconducting materials within the measurement precision. Expression (4.1) was also calculated from microscopic theory by Thouless [92] and Aslamazov and Larkin [93].

For two dimensional thin films of thickness d , Ferrel [94] has shown that expression (4.1) is enhanced by a factor $\xi(T)/4d$ so that

$$C_V \propto \tau^{-1} \quad (4.2)$$

Zally and Mochel [95] have been able to measure the heat capacity of individual

amorphous Bi-Sb alloy films using AC calorimetry techniques. The results for their films show good agreement with τ^{-1} dependence outside the critical region. However the magnitude of the fluctuation heat capacity observed is several times larger than that expected from the Aslamazov and Larkin calculation.

Gunther and Gruenberg [96] and Grossmann *et al.* [97] attempted to extend the theory into the critical region where the quartic term in the GL free energy becomes important in limiting the magnitude of the fluctuations. Other attempts to include the quartic term in various approximations [98] have all predicted a peak in the specific heat not observed experimentally.

The superconducting layered compounds with Josephson coupling of layers are described by the LD model and are intermediate between 3D and 2D systems and represent the two limits at $r = \frac{2\xi^2(0)}{d} \simeq 1$ and $r \ll 1$. We obtain cross-over from 2D fluctuations to 3D fluctuations in systems with $r \ll 1$ as we go down in temperature from $\tau = |T_c - T|/T_c \gg r$ to $\tau \ll r$ [99]. Such cross-over in Gaussian fluctuations is calculated as follows. First the free energy of the system taking into account the superconducting fluctuations is obtained by calculating the contribution of all the states described by order parameter $\psi_n(\rho)$ with statistical weights determined by the LD free energy functional (2.10).

$$F_s(T) = -T \ln \int D\psi_n(\rho) \exp[-F\{\psi_n(\rho)\}/T]$$

In the region of Gaussian fluctuations we take into account the quadratic terms only assuming that fluctuations are weak and $\psi_n(\rho)$ small. Omitting terms of the fourth order in $\psi_n(\rho)$ we get a functional which can be diagonalized by use of the Fourier representation for order parameter $\psi_{\mathbf{K}}$. Then taking $\psi_{\mathbf{K}} = \psi'_{\mathbf{K}} + i\psi''_{\mathbf{K}}$ and

performing the integration over the real and imaginary parts of $\psi_{\mathbf{K}}$ we get

$$\begin{aligned}
 F_s &= -T \ln \int \prod_{\mathbf{K}} D\psi'_{\mathbf{K}} D\psi''_{\mathbf{K}} \exp \sum_{\mathbf{K}} \left\{ -\frac{aT_c}{T} [\tau + \xi_{\parallel}^2(0) \mathbf{K}_{\parallel}^2 \right. \\
 &\quad \left. + r(1 - \cos K_z d)] [\psi_{1,\mathbf{K}}^2 + \psi_{2,\mathbf{K}}^2] \right\} \\
 &= -T \sum_{\mathbf{K}} \ln \left\{ \left(\pi \frac{T}{aT_c} [\tau + \xi_{\parallel}^2(0) \mathbf{K}_{\parallel}^2 + r(1 - \cos K_z d)] \right) \right\}
 \end{aligned}$$

The specific heat due to the superconducting fluctuations is given by

$$\begin{aligned}
 C_{fl} &= -\frac{\partial}{\partial T} \left(T \frac{\partial}{\partial T} F_s \right) \\
 &= \sum_{\mathbf{K}} \frac{1}{\tau + \xi_{\parallel}^2(0) \kappa_{\parallel}^2 + r(1 - \cos K_z d)} \\
 &= \frac{1}{4\pi \xi_{\parallel}^2(0) d \sqrt{\tau^2 + 2r\tau}}
 \end{aligned}$$

At $\tau \ll r$, $C_f(\tau) = [8\pi \xi_{\parallel}^2(0) \xi_z(0)]^{-1} \tau^{-\frac{1}{2}}$. In this temperature region fluctuation specific heat varies as $\tau^{-\frac{1}{2}}$ which is characteristic of 3D fluctuation regime. For $\tau \gg r$, $C_f(\tau) = [4\pi d \xi_{\parallel}^2(0)]^{-1} \tau^{-1}$. The τ^{-1} dependence of C_{fl} for large values of τ characterises a 2D fluctuation regime.

4.3 FSH of copper oxide superconductors

As seen in chapter 3, the modified LD model proposed in section 2.6 provides an adequate description of the superconducting properties of the layered high- T_c copper oxide superconductors. Hence in this section the fluctuation contribution to the specific heat is discussed within the framework of the modified LD model described by the free energy (2.16).

If we consider mean field or Gaussian fluctuations above T_c , the smallness of

$|\psi|^2$ allows us to drop the quartic terms in the free energy expression. In the zero field case $A = 0$ and equation (2.16) becomes

$$F_s = \sum_n \int \left[a_1 |\psi_{1,n}^{(\rho)}|^2 + \frac{\hbar^2}{2m_{\parallel}} |\nabla_{\parallel} \psi_{1,n}^{(\rho)}|^2 + a_2 |\psi_{2,n}^{(\rho)}|^2 + \frac{\hbar^2}{2} \sum_{l=x,y} \frac{1}{m'_l} \left| \frac{\partial}{\partial l} \psi_{2,n}^{(\rho)} \right|^2 + t |\psi_{1,n}^{(\rho)} - \psi_{2,n}^{(\rho)} e^{ix_n}|^2 + t |\psi_{1,n}^{(\rho)} - \psi_{2,n+1}^{(\rho)} e^{-ix_n}|^2 + \frac{\hbar_n^2}{8\pi} \right] d\rho. \quad (4.3)$$

We set

$$\psi_{j,n+1} = \psi_{j,n} \exp(ikd)$$

and

$$\psi_{j,n} = \sum_{\mathbf{q}} \psi_{j,\mathbf{K}} \exp(i\mathbf{q} \cdot \rho)$$

where $j = 1, 2$ and $\mathbf{K} = \mathbf{K}(\mathbf{q}, \mathbf{k})$. \mathbf{q} is the inplane wave vector and \mathbf{k} is the c-axis wave vector. The Fourier transform of equation (4.3) is performed using Parseval's identity. The order parameter ψ_2 of the NSC layers arises through a proximity effect. Let us therefore put $\frac{|\psi_{1,\mathbf{K}}|^2}{|\psi_{2,\mathbf{K}}|^2} = \delta^2$ where $\psi_{1,\mathbf{K}}$ and $\psi_{2,\mathbf{K}}$ are the Fourier transformed quantities of $\psi_{1,n}$ and $\psi_{2,n}$ respectively. We now get

$$F_s = \sum_{\mathbf{K}} \left[\varepsilon_1 |\psi_{1,\mathbf{K}}|^2 + \varepsilon_2 |\psi_{2,\mathbf{K}}|^2 \right]$$

where

$$\begin{aligned} \varepsilon_1 &= a_1 + \frac{\hbar^2 q^2}{2m_{\parallel}} + 2t(1 - \delta) - 2t\delta \cos kd \\ \varepsilon_2 &= a_2 + \frac{\hbar^2 q^2}{2M_{\theta}} + 2t \\ M_{\theta}^{-1} &= \left(\frac{\cos^2 \theta}{m'_x} + \frac{\sin^2 \theta}{m'_y} \right) \end{aligned}$$

θ is the angle which the inplane wave vector makes with the x-axis. Following Landau and Lifshitz [147], change in the thermodynamic potential can be written

as,

$$\begin{aligned}\Omega - \Omega_0 &= -T \ln \int \exp[-F_s(\psi_{1,\mathbf{K}}, \psi_{2,\mathbf{K}})] D\psi_{1,\mathbf{K}} D\psi_{2,\mathbf{K}} \\ &= -T \ln \int \exp[-\sum_{\mathbf{K}} \{\varepsilon_1 |\psi_{1,\mathbf{K}}|^2 + \varepsilon_2 |\psi_{2,\mathbf{K}}|^2\}] D\psi_{1,\mathbf{K}} D\psi_{2,\mathbf{K}}.\end{aligned}$$

Writing

$$\psi_{j,\mathbf{K}} = \psi'_{j,\mathbf{K}} + i\psi''_{j,\mathbf{K}}$$

and performing the integration over the real and imaginary parts of $\psi_{1,\mathbf{K}}$ and $\psi_{2,\mathbf{K}}$ using standard integrals [100],

$$\Omega - \Omega_0 = T_c \sum_{\mathbf{K}} \left[\ln \frac{4}{\pi T_c} + \frac{1}{2} \ln \varepsilon_1 + \frac{1}{2} \ln \varepsilon_2 \right] \quad (4.5)$$

Fluctuation specific heat is given by

$$C_{fl} = -T \frac{\partial^2 (\Omega - \Omega_0)}{\partial T^2}$$

In the fluctuation regime we assume the same temperature dependence for a_1 and a_2 and hence $a_1 = \alpha_1(T - T_c) = \alpha_1 \tau T_c$ and $a_2 = \alpha_2(T - T_c) = \alpha_2 \tau T_c$. Differentiating expression (4.5) twice with respect to T , we get

$$C_{fl} = \frac{T_c}{2} \sum_{\mathbf{K}} \left[\frac{\alpha_1^2}{\varepsilon_1^2} + \frac{\alpha_2^2}{\varepsilon_2^2} \right].$$

The sum over \mathbf{K} can be converted to an integration using the prescription

$$\sum_{\mathbf{K}} \longrightarrow \int \frac{d^3 K}{(2\pi)^3} \quad (4.6)$$

Now we get,

$$C_{fl} = \frac{1}{(2\pi)^3} \frac{T_c}{2} \int \left[\frac{\alpha_1^2}{\varepsilon_1^2} + \frac{\alpha_2^2}{\varepsilon_2^2} \right] d\mathbf{q} dk.$$

The k integration is carried out from 0 to $(2\pi/d)$ and the \mathbf{q} integration over the entire spectrum using standard integrals [100]. Thus

$$C_{fl} = \frac{T_c}{2\pi \hbar^2 d} \left[\frac{m_{\parallel} \alpha_1}{\sqrt{\tau^2 + 4r_1 \tau (1 - \delta)}} + \frac{\alpha_2 \sqrt{m'_x m'_y}}{\tau + 2r_2} \right] \quad (4.7)$$

where $r_1 = \frac{t}{\alpha_1 T_c}$ and $r_2 = \frac{t}{\alpha_2 T_c}$ are the Josephson coupling parameters.

In high- T_c superconductors the c-axis coherence length $\xi_c(0)$ is smaller than the interplanar distance d . But at temperatures close to T_c , $\xi_c(T) = \xi_c(0) |\tau|^{-\frac{1}{2}}$ will be large enough to justify a 3D Ginzburg-Landau approximation for such superconductors. For a system of Josephson coupled identical layers the 3D continuum approximation is replaced by 2D behaviour of the individual layers for temperature values $|\tau| > r = 2 \frac{\xi_c^2(0)}{d^2}$ where r is the Josephson coupling parameter. This brings about a cross over from a 3D regime near T_c to a 2D regime for $|\tau| > r$. In this context it is interesting to consider the contributions to the fluctuation specific heat in three different temperature regions. In the region close to T_c , $r_2 > r_1(1 - \delta) > \tau$, equation (4.7) becomes

$$C_{fl} = \frac{T_c}{2\pi\hbar^2 d} \left[\frac{\alpha_1 m_{\parallel}}{\sqrt{4r_1(1-\delta)}} \frac{1}{\sqrt{\tau}} + \frac{\alpha_2 \sqrt{m'_x m'_y}}{2r_2} \right]. \quad (4.8)$$

From this equation it is clear that C_{fl} varies as $\tau^{-\frac{1}{2}}$ which is the characteristic behaviour for a 3D fluctuation regime [101]. The 2D fluctuation regime is characterized by a τ^{-1} dependence for C_{fl} . For $r_2 > \tau > r_1(1 - \delta)$, we have

$$C_{fl} = \frac{T_c}{2\pi\hbar^2 d} \left[\frac{\alpha_1 m_{\parallel}}{\tau} + \frac{\alpha_2 \sqrt{m'_x m'_y}}{4r_2(\tau + r_2)^{\frac{1}{2}}} \right]. \quad (4.9)$$

In this region there is a 2D ($\sim \tau^{-1}$) as well as a 3D ($\sim \tau^{-\frac{1}{2}}$) contribution to the fluctuation specific heat. In fact this is a transitional region where DCR is taking place. For $\tau > r_2 > r_1(1 - \delta)$, equation (4.7) takes the asymptotic form

$$C_{fl} = \frac{T_c}{2\pi\hbar^2 d} [m_{\parallel} \alpha_1 + \sqrt{m'_x m'_y} \alpha_2] \frac{1}{\tau}. \quad (4.10)$$

This τ^{-1} dependence of C_{fl} shows that the fluctuation contribution becomes 2D in this temperature region. Thus fluctuation specific heat given by (4.7) exhibits

DCR from 3D behaviour near T_c to 2D behaviour further from T_c .

4.4 Conclusion

Equation (4.7) gives the fluctuation contribution to the specific heat for the modified Lawrence-Doniach type model of copper oxide superconductors described by the free energy functional (2.16). Dimensional cross over in the fluctuation regime from 3D for $r_2 > r_1(1 - \delta) > \tau$ to 2D for $\tau > r_2 > r_1(1 - \delta)$ is obtained as seen from equations (4.8), (4.9) and (4.10). These results explain the experimental observation of dimensional cross over in the Gaussian fluctuation regime for specific heat of $YBa_2Cu_3O_7$ superconductor by various authors [110]. The calculations point to the existence of a transitional temperature region, instead of a sharp 2D-3D transition, where the two regimes overlap. Such an overlapping region has also been obtained by Ghosh *et al.* [112] using a different procedure.

CHAPTER V

PARACONDUCTIVITY

5.1 Introduction

The first discovered and the most striking aspect of superconductors is their infinite DC conductivity below T_c . Historically and etymologically conductivity phenomena lies at the root of the subject. Therefore it is fitting that the first real progress in the study of fluctuation phenomena near the superconducting phase transition was made by studying the excess conductivity due to fluctuations above T_c , often called paraconductivity in analogy with paramagnetism.

Let us first consider the excess conductivity attributable to the direct acceleration of the superconducting pairs created by fluctuations above T_c . Without such fluctuations the normal DC conductivity is given by

$$\sigma_n = \frac{ne^2}{m} \tau_{tr}$$

where τ_{tr} is the mean scattering time of the normal electrons in transport properties and n is their number density per unit volume. By analogy, the superconducting fluctuations contribute an additional term

$$\sigma' = \frac{e^{*2}}{m^*} \sum_{\mathbf{K}} \langle |\psi_{\mathbf{K}}|^2 \rangle \frac{\tau_{\mathbf{K}}}{2}$$

The density and the life time of the superconducting fluctuation modes are given by [104]

$$\langle |\psi_{\mathbf{K}}|^2 \rangle = k_B T / a(1 + K^2 \xi^2)$$

and

$$\tau_K^{-1} = (1 + K^2\xi^2)/\tau_{GL}$$

where τ_{GL} is the characteristic relaxation time of the uniform ($K=0$) mode. The sum over \mathbf{K} can be converted into an appropriate integration depending on the dimensionality of the sample and the following results are obtained.

$$\sigma_{3D}^{AL} = \frac{1}{32} \frac{e^2}{\hbar\xi(0)} \tau^{-\frac{1}{2}} \quad (5.1a)$$

$$\sigma_{2D}^{AL} = \frac{1}{16} \frac{e^2}{\hbar d} \tau^{-1} \quad (5.1b)$$

and

$$\sigma_{1D}^{AL} = \frac{\pi}{16} \frac{e^2\xi(0)}{\hbar S} \tau^{-\frac{3}{2}} \quad (5.1c)$$

where the cross sectional area $S \ll \xi^2$. These results were first derived by Aslamazov and Larkin (AL) from microscopic theory [93] and then from GL theory by Abrahams and Woo [102] and Schmid [103]. For samples of intermediate thickness results which interpolate between these dimensional forms can be obtained.

In a 3D bulk sample of conventional superconductors the ratio $\sigma'_{3D}/\sigma_n \simeq (K_F^2/\xi(0))^{-1}\tau^{-\frac{1}{2}}$ is of the order of $10^{-7}\tau^{-\frac{1}{2}}$ in clean materials and at most $10^{-2}\tau^{-\frac{1}{2}}$ in extremely dirty materials where the mean free path is comparable with the interatomic spacing [104]. Thus even in the most favourable case σ'_{3D} is a very small fraction of σ_n except for $\tau \leq 10^{-4}$ *i.e.* except within at most a millidegree of T_c . Gittleman *et al.* [105] have observed the $\tau^{-\frac{1}{2}}$ temperature dependence characteristic of the bulk behaviour with approximately the above coefficient in thick films of extremely dirty aluminium.

For two dimensional thin films, equation (5.1b) predicts a universal dependence $\sigma'_{2D}d \equiv G'$, the excess conductance per square which is the quantity most easily determined experimentally. Since the magnitude of G' is sample independent, the

largest fractional changes are observed in very dirty thin samples with low normal conductance. Glover [106] observed an excess of conductivity proportional to τ^{-1} in amorphous bismuth films and the coefficient of proportionality was in excellent agreement with Glover's experimental value.

However, the predicted universal behaviour does not hold for cleaner films. The magnitude of the excess conductivity was observed to be larger than expected by upto an order of magnitude and its temperature dependence was anomalous in cleaner lead and aluminium films [107]. The origin of this anomalous conductivity has come to be understood as an indirect effect of fluctuations on the quasiparticle conductivity. The superconducting fluctuations decay into pairs of quasiparticles of nearly opposite momenta. By time-reversal symmetry, the quasiparticles remain in a state of small total momentum even after scattering from an impurity potential and continue to be accelerated much as they were while they were a superconducting fluctuation. The quasiparticle life time is limited in several ways ultimately including decay back into a superconducting fluctuation. This indirect contribution to conductivity known as Maki-Thompson (MT) term was obtained as [108],

$$\sigma_{2D}^{MT} = \frac{e^2}{8\hbar d} \frac{1}{\tau - \delta} \ln\left(\frac{\tau}{\delta}\right) \quad (5.2a)$$

and

$$\sigma_{1D}^{MT} = \sigma_{1D}^{AL} 4\left(\frac{\tau}{\delta}\right) \left[1 + \left(\frac{\tau}{\delta}\right)^{\frac{1}{2}}\right]^{-1} \quad (5.2b)$$

where $\delta = (T_{c0} - T_c)/T_c$ is the reduced shift of T_c due to pair breaking interactions. This combined theory (AL and MT) proved to be in good agreement with the experimental data for both the two dimensional thin films and one dimensional filaments. While the phenomenological GL theory with Gaussian fluctuations correctly reproduces the AL contribution to the conductivity it does not explain

the MT contribution.

It is difficult to measure the conductivity of zero-dimensional sub micron particles. Kirtley *et al.* [109] deposited a planar array of such particles by evaporating tin in an oxygen atmosphere. When the oxide coated particles are just barely touching, they observed an onset of extra conductivity above T_c which varies as τ^{-2} which is the temperature dependence of the AL term for zero dimensional particles. The τ^{-1} dependence expected for the MT term has not been observed.

Near T_c the direct (AL) contribution dominates the indirect (MT) term which may be neglected. In the linearized GL theory, the σ^{AL} term diverges at T_c . To cut off the divergence and to obtain a smooth variation of the conductivity through the transition, it is necessary to retain the $\frac{b}{2} |\psi|^4$ non linear term in the free energy density. Exact solutions for the conductivity including the non-linear term are not known. Therefore several approximations have been considered.

For superconducting layered compounds with Josephson coupling of the layers, the AL contribution to the parallel conductivity within the LD scheme [99] is given by

$$\sigma'_{ab}(\tau) = \frac{e^2}{16\hbar d} \frac{1}{\sqrt{\tau^2 + 2r\tau}} \quad (5.3)$$

The temperature dependence (5.3) of σ'_{ab} is similar to that of the fluctuation specific heat and exhibits DCR from 3D behaviour near T_c to 2D behaviour further from T_c .

5.2 Paraconductivity of copper oxide superconductors

In the recent past several authors have carried out paraconductivity measure-

ments on single crystals and poly crystalline samples of $YBa_2Cu_3O_7$ [86,110] which confirm a 2D to 3D cross over behaviour above T_c . In this section paraconductivity both parallel and perpendicular to the layers is calculated and the cross over behaviour explored within the modified LD scheme described by (2.16).

In the absence of an electric field, ψ undergoes equilibrium fluctuations and the average equilibrium fluctuation is given by [101]

$$\langle |\psi_{j,\mathbf{K}}^{(0)}|^2 \rangle = \frac{\int |\psi_{j,\mathbf{K}}|^2 \exp(-F_s/T) \prod_j D |\psi_{j,\mathbf{K}}|^2}{\int \exp(-F_s/T) \prod_j D |\psi_{j,\mathbf{K}}|^2} \quad (5.4)$$

where $j = 1, 2$. In the presence of a weak electric field \mathbf{E} , the equilibrium is perturbed and

$$\psi_{j,\mathbf{K}} = \psi_{j,\mathbf{K}}^{(0)} + \psi_{j,\mathbf{K}}^{(1)} \quad (5.5)$$

According to the Ginzburg-Landau theory [149], the average electric current in the zero field case ($\mathbf{A} = 0$) is given by

$$\begin{aligned} \mathbf{j}_{ab} &= -ie\hbar \left[\frac{1}{m_{\parallel}} \langle \psi_{1,n}^* \nabla_{\parallel} \psi_{1,n} - \psi_{1,n} \nabla_{\parallel} \psi_{1,n}^* \rangle + \sum_{\ell=1,2} \frac{1}{m_{\ell}} \langle \psi_{2,n}^* \frac{\partial \psi_{2,n}}{\partial \ell} - \psi_{2,n} \frac{\partial \psi_{2,n}^*}{\partial \ell} \rangle \hat{\ell} \right] \\ &= \sum_{\mathbf{K}} e\hbar \left[\mathbf{q}_1 |\psi_{1,\mathbf{K}}|^2 + \mathbf{q}_2 |\psi_{2,\mathbf{K}}|^2 \right] \end{aligned}$$

where $\mathbf{q}_1 = \mathbf{q}/m_{\parallel}$ and

$$\mathbf{q}_2 = \mathbf{q} \left(\frac{\cos \theta}{m'_x} \hat{x} + \frac{\sin \theta}{m'_y} \hat{y} \right)$$

If we substitute $\langle |\psi_{j,\mathbf{K}}^{(0)}|^2 \rangle$ given by (5.4) into this formula, we obtain zero and hence in the next approximation we get the fluctuation contribution to the current as

$$\delta \mathbf{j}_{ab} = \sum_{\mathbf{K}} e\hbar \sum_{j=1,2} \langle \psi_{j,\mathbf{K}}^{(0)} \psi_{j,\mathbf{K}}^{(1)*} + \psi_{j,\mathbf{K}}^{(1)} \psi_{j,\mathbf{K}}^{(0)*} \rangle \quad (5.6)$$

$\psi_{j,\mathbf{K}}^{(1)}$ is determined from the time dependent Ginzburg-Landau equation (TDGL)

$$-\frac{\pi\hbar\alpha}{4} \left[\frac{\partial \psi}{\partial t} + \frac{2ie}{\hbar} U\psi \right] = \frac{\delta F_s}{\delta \psi^*} \quad (5.7)$$

where U is the scalar potential. Since we are interested in the fluctuational correction to ψ that arises under the action of a constant electric field, it is assumed to be small and therefore to the first order the correction will be proportional to \mathbf{E} . But since \mathbf{E} does not depend on time, the correction to ψ will also be independent of time and hence $\frac{\partial\psi}{\partial t}$ can be neglected. As $\mathbf{A} = 0$, $\mathbf{E} = -\nabla U$. Since \mathbf{E} is homogenous $U = -\mathbf{E}\cdot\mathbf{r}$. With these substitutions equation (5.7) becomes

$$i\frac{\pi}{2}ea\mathbf{E}\cdot\mathbf{r}\psi = \frac{\delta F_s}{\delta\psi^*} \quad (5.8).$$

Changing equation (5.8) into momentum representation by the transformation $r \rightarrow -i\frac{\partial}{\partial\mathbf{q}}$ (when the electric field is parallel to the layers *i.e.* ab planes) and substituting for $\delta F_s/\delta\psi_{j,\mathbf{K}}$ from equation (4.4), we get

$$\frac{\pi}{2}ea_j(\mathbf{E}\cdot\frac{\partial}{\partial\mathbf{q}})\psi_{j,\mathbf{K}}^{(0)} + \epsilon_j\psi_{j,\mathbf{K}}^{(1)} = 0$$

and

$$\psi_{j,\mathbf{K}}^{(1)} = \frac{\pi ea_j}{2\epsilon}(\mathbf{E}\cdot\frac{\partial}{\partial\mathbf{q}})\psi_{j,\mathbf{K}}^{(0)} \quad (5.9)$$

Substituting (5.9) into (5.6), we get the parallel fluctuaton current

$$\delta\mathbf{j}_{ab} = \frac{\pi\hbar e^2}{2} \sum_{\mathbf{K}} \sum_{j=1,2} \frac{a_j\mathbf{q}_j}{\epsilon_j} (\mathbf{E}\cdot\frac{\partial}{\partial\mathbf{q}}) |\psi_{j,\mathbf{K}}^{(0)}|^2 \quad (5.10)$$

Substituting for $|\psi_{j,\mathbf{K}}^{(0)}|^2$ from equation (5.4),

$$\delta\mathbf{j}_{ab} = \frac{\pi\hbar^3 e^2 T_c}{2} \sum_{\mathbf{K}} \sum_{j=1,2} \frac{a_j\mathbf{q}_j}{\epsilon_j^3} (\mathbf{E}\cdot\mathbf{q}_j) \quad (5.11)$$

Converting the summation into integration using the prescription (4.6),

$$\delta\mathbf{j}_{ab} = \frac{\pi\hbar^3 e^2 T_c}{16\pi^3} \sum_j a_j I_j$$

where

$$I_j = \iiint \frac{\mathbf{q}_j(\mathbf{q}_j\cdot\mathbf{E})}{\epsilon_j^3} q dq d\theta dk$$

After performing the k and θ integrations as in section 4.3

$$I_1 = \frac{\pi^2}{2dm_{\parallel}^2} \int_0^{\infty} \frac{q^3 dq}{[Aq^4 + 2Bq^2 + C]^{\frac{3}{2}}}$$

and

$$I_2 = \frac{\pi^2}{2dm'^2} \int_0^{\infty} \frac{q^3 dq}{[A'q^2 + B']^3}$$

where

$$\begin{aligned} A' &= \frac{\hbar^2}{2m'}, & B' &= a_2 + 2t, \\ A &= \frac{\hbar^4}{4m_{\parallel}^2}, & B &= [a_1 + 2t(1 - \delta)] \frac{\hbar^2}{2m_{\parallel}} \end{aligned}$$

and

$$C = a_1^2 + 4t^2(1 - 2\delta) + 4a_1t(1 - \delta)$$

Since we are interested in studying the temperature dependence of paraconductivity it is convenient to set $m'_x = m'_y = m'$. After performing the q -integration, we get

$$\sigma'_{ab} = \frac{e^2}{16\hbar d} \left[\frac{1}{\sqrt{\tau^2 + 4r_1\tau(1 - \delta)}} + \frac{2}{(\tau + 2r_2)} \right] \quad (5.12)$$

The modified LD scheme considered here is only adequate to describe the AL contribution to the paraconductivity and does not include the anomalous MT contribution which is significant only for dirty superconductors. The high- T_c superconductors are treated as clean ones and hence the MT contribution can be ignored. The analysis of experimental data on paraconductivity in high- T_c superconductors [111] supports this contention.

Now let us consider the three temperature regions of interest. For temperatures close to T_c , $r_2 \gg r_1(1 - \delta) \gg \tau$ and

$$\sigma'_{ab} = \frac{e^2}{32\hbar d} \frac{1}{\sqrt{r_1(1 - \delta)}} \tau^{-\frac{1}{2}} \quad (5.13)$$

The $\tau^{-\frac{1}{2}}$ dependence of σ'_{ab} is characteristic of the 3D fluctuation regime. For $r_2 \gg \tau \gg r_1(1 - \delta)$,

$$\sigma'_{ab} = \frac{e^2}{16\hbar d} \left[\frac{1}{\tau} + \frac{1}{\sqrt{r_2}} \frac{1}{(\tau + r_2)^{\frac{1}{2}}} \right] \quad (5.14)$$

Equation (5.12) shows the existence of a transitional region where the paraconductivity has a 2D ($\sim \tau^{-1}$) as well as a 3D ($\sim \tau^{-\frac{1}{2}}$) contribution. For temperature regions further away from T_c , $\tau \gg r_2 \gg r_1(1 - \delta)$ and

$$\sigma'_{ab} = \frac{3e^2}{16\hbar d} \tau^{-1} \quad (5.15)$$

equation (5.13) represents the characteristic temperature dependence of 2D fluctuations. Thus here again, modified LD model (2.16) predicts DCR in the fluctuation contribution to paraconductivity. Additionally, as in the case of FSH, an overlapping region of 2D and 3D fluctuations is obtained.

When the electric field is perpendicular to the layers, the corresponding current density in the present model can be written as

$$\langle j_z \rangle = -\frac{2iet^2 d}{\hbar} \sum_n \left[\langle \psi_{1,n+1} \psi_{1,n}^* - \psi_{1,n} \psi_{1,n+1}^* \rangle + \langle \psi_{2,n+1} \psi_{2,n}^* - \psi_{2,n} \psi_{2,n+1}^* \rangle \right] \quad (5.16)$$

Performing the Fourier transformation,

$$\langle j_z \rangle = \frac{4et^2 d}{\hbar} \sum_{\mathbf{K}} \left[\langle |\psi_1(\mathbf{K})|^2 \rangle + \langle |\psi_2(\mathbf{K})|^2 \rangle \right] \sin 2kd$$

Proceeding as before

$$\sigma'_c = \frac{\pi e^2 d^2 t^2 T_c}{4\hbar} \sum_{\mathbf{K}} \left(\frac{a_1}{\varepsilon_1^3} + \frac{a_2}{\varepsilon_2^3} \right) \sin^2 kd.$$

Converting the summation into integration using the prescription (4.6), and performing the integrations using standard integrals [100],

$$\sigma'_c = \frac{e^2 d}{32\hbar^3} \left[\frac{\alpha_1 m_{\parallel} T_c}{4(1 - \delta)^2} \left(\frac{\tau + 2r_1(1 - \delta)}{\sqrt{\tau^2 + 4\tau r_1(1 - \delta)}} - 1 \right) + \alpha_2 \sqrt{m'_x m'_y} T_c \left(\frac{r_2}{\tau + 2r_2} \right)^2 \right] \quad (5.17)$$

Equation (5.17) shows that the specific temperature dependence of σ'_c is different from that of σ'_{ab} given by equation (5.12). For the temperature region close to T_c , $r_2 > r_1(1 - \delta) > \tau$ the specific temperature dependence of σ'_c is given by

$$\sigma'_c = \frac{e^2 dT_c}{32\hbar^3} \frac{\alpha_1 m_{\parallel}}{4\sqrt{r_1(1-\delta)^3}} \frac{1}{\sqrt{\tau}} \quad (5.18)$$

σ'_c varies as $\tau^{-\frac{1}{2}}$ which is the characteristic behaviour for a 3D fluctuation regime. Further away from T_c , $\tau > r_2 > r_1(1 - \delta)$,

$$\sigma'_c = \frac{e^2 dT_c}{32\hbar^3} \alpha_2 \sqrt{m'_x m'_y} \left(\frac{r_2}{\tau}\right)^2 \quad (5.19)$$

The τ^{-2} dependence of σ'_c in this region is indicative of 0D regime of fluctuations where superconducting electrons scarcely jump from plane to plane.

5.3 Conclusion

Foregoing calculations based on the modified LD free energy functional (2.16) explain the observation of dimensional cross over in paraconductivity measurements [110]. Both σ'_{ab} and the fluctuation specific heat C_f given by (4.7) have the same temperature dependence. An interesting feature of the calculations is the existence of an overlapping region of 2D and 3D fluctuations instead of a sharp 2D-3D transition. As mentioned in section (4.4) Ghosh *et al.* [112] have also predicted an overlapping region using a different procedure. Another important conclusion is that the temperature regime $\tau > r_2 > r_1(1 - \delta)$ shows a clear difference in the temperature dependence of σ'_{ab} and σ'_c . In the case of σ'_{ab} , the 2D nature of the fluctuations is well established. But for σ'_c , the τ^{-2} temperature dependence in this regime is reminiscent of 0D fluctuations expected of granular systems. Thus it is

appropriate to describe this temperature region as a 2D paraconductivity regime where conducting electrons scarcely jump from plane to plane.

CHAPTER VI

SUPERCONDUCTING FLUCTUATION DIAMAGNETISM

6.1. Introduction

We have seen in the foregoing chapters that above T_c , thermodynamic fluctuations towards the superconducting state contribute small but measurable amounts of characteristically superconducting properties like conductivity and specific heat. In conventional superconductors, even in the most favourable case, σ'_{3D} is very small fraction of σ_n except for $\tau \leq 10^{-4}$ which is in sharp contrast to the case of fluctuation diamagnetism where the coefficient of $\tau^{-\frac{1}{2}}$ is itself comparable with the normal state diamagnetism so that fractional changes are observable over a wide temperature range. In fact it is possible to measure the additional diamagnetism due to superconducting fluctuations even at twice its transition temperature. Fluctuation effects have also been observed in magnetic susceptibility measurements carried out in layered high- T_c copper oxide superconductors [87].

For a zero dimensional system like a particle whose radius R is small compared to ξ , the spatial variation of ψ over its volume V can be ignored. London [113] has shown that the diamagnetic susceptibility χ or induced magnetization per unit field H due to screening currents is given by

$$\chi = -\frac{1}{40\pi} \frac{R^2}{\lambda^2}. \quad (6.1)$$

Since the penetration depth is given by

$$\frac{1}{\lambda^2} = \frac{4\pi e^*{}^2}{m^*c^2} \langle |\psi|^2 \rangle, \quad (6.2)$$

the susceptibility is proportional to $R^2 \langle |\psi|^2 \rangle$. Fluctuations above T_c is the same order of magnitude as the fluctuations below T_c . Above T_c , ξ rises as τ^{-1} , but then rises more slowly as the critical region is reached. Well below T_c , ξ rises as τ after fluctuation effects are swamped by the mean field superconductivity [114]. Buhrman and Halperin [115] and Buhrman *et al.* [116] used SQUID magnetometers to measure diamagnetic susceptibility of aluminium powder formed by evaporating aluminium in an inert gas atmosphere and observed exactly this type of temperature behaviour predicted by GL theory providing conclusive proof for the validity of the GL theory both inside and outside the critical region so far as zero dimensional systems are concerned. However ξ fell below the predicted value for $T \geq 1.5T_c$ and this is not surprising as the GL theory is expected to be reliable only near T_c .

The zero field fluctuation diamagnetic susceptibility for bulk materials was calculated by Schmid [117] as

$$\chi' = -\frac{\pi k_B T}{6 \phi_0^2} \xi(T) \approx 10^{-7} \tau^{-\frac{1}{2}} \quad (6.3)$$

The susceptibility given by equation (6.3) formally diverges at T_c . However, in practice the enhancement factor never gets very large before being limited either by the first order transition in a magnetic field or by the width of the transition in a real sample. χ' is of the same order of magnitude as the London diamagnetism of normal metals, apart from the temperature dependent enhancement factor $\tau^{-\frac{1}{2}}$ and it is many order of magnitude smaller than the full diamagnetic susceptibility

in the Meissner state, $\chi = -\frac{1}{4\pi}$

Only small fields can be used without destroying the effect by shrinking and weakening the fluctuations. None-the-less the susceptibility is substantial compared with the background and it can be isolated by measuring the temperature dependent part of the magnetization in a magnetic field held absolutely constant by a superconducting coil in the persistent current mode. Such experiments were first carried out by Gollub *et al.* [118] using a SQUID magnetometer.

In larger magnetic fields, the fluctuations are smaller and weaker than in the zero field limit and the divergence temperature shifts below T_c to the nucleation temperature $T_{c2}(H)$ which is the temperature at which $H = H_{c2}(T)$. The Schmid result (6.3) was generalized by Prange [148] in the frame work of the GL theory to the case of finite fields. He found that the fluctuation magnetization M' should indeed diverge as $(T - T_{c2})^{-\frac{1}{2}}$ and that it should be a universal result if scaled variables were used. He obtained

$$\frac{M'}{H^{\frac{1}{2}}T} = f(x) \quad (6.4)$$

where f is a function of the single variable

$$x = \frac{(T - T_c)}{H(dH_{c2}/dT)T_c}$$

When data for several materials were plotted in terms of these variables, they did not fall on the theoretical universal curve, but instead fell systematically well below it especially for the higher field values. This disagreement was because of the two assumptions of the GL theory viz. (i) slow spatial variation of ψ and (ii) the theory is limited to reasonably weak fields. Thus the theory gives a poor account of the short wavelength ($\leq \xi(0)$) fluctuations which dominate far above T_c and in strong magnetic fields. An explanation for the disagreement between theory and experiment was first suggested by Patton, Ambegaokar and Wilkins [119] who

proposed the introduction of a cut-off energy for short wavelength fluctuations. This implied that fluctuations would be greatly suppressed for $H > H^* \approx H_{c2}(0)$ and H/H^* would govern the fall-off of the magnetization with field, independent of the material *i.e.* Prange's universal function $f(x)$ would have to be replaced by a new function $f(x, H/H^*)$. Gollub *et al.* [120,121] found that such a scaling procedure could indeed eliminate the material dependence of their results.

However, in clean materials with long mean free path, the scaling field H_s was much smaller than that predicted by Patton *et al.* [119]. Lee and Payne [123] and Kurkijarvi *et al.* [124] found that the effect of non-locality becomes important at much lower fields than $H_{c2}(0)$ and therefore account for the smaller scaling field. In contrast, the experimental values of $H_s/H_{c2}(0)$ in alloys approach a limiting value of ~ 0.5 [133]. This is in good agreement with the dirty limit microscopic calculation of Maki and Takayama [123] and Usadel [126] for which non-locality is unimportant.

The study of fluctuation diamagnetism in bulk samples has not only demonstrated the existence of superconducting fluctuations above T_c , but has also proved useful for exploring the limits of the GL theory.

Schmid [117] showed that the zero field susceptibility of a 2D system should change as τ^{-1} compared with the $\tau^{-\frac{1}{2}}$ dependence of bulk materials. If the film thickness d is much less than the coherence length $\xi(T)$, then

$$\chi'_{\perp} \simeq -k_B T \xi^2(T) / \phi_0^2 d = \frac{\xi}{d} \chi'_{3D} \propto \tau^{-1}$$

and

$$\chi'_{\parallel} \simeq -k_B T d / \phi_0^2 \quad (6.5)$$

For the parallel field, the fluctuation effects are very small and weakly temperature

dependent and therefore essentially unobservable. For the perpendicular field, the susceptibility is enhanced by a factor of ξ/d over the bulk value. Probes *et al.* [127] studied the superconducting layered compound TaS_2 intercalated with pyridine molecules and suggested that over a limited temperature range well above T_c the fluctuation susceptibility could be fitted by the form (6.5) suggesting the existence of 2D fluctuations within the superconducting layers.

Within the framework of the Lawrence-Doniach model [69], the layered compounds are modelled with Josephson coupling between the layers. Tsuzuki [128], Klemm *et al.* [129] and Gerhardtts [130] extended the previous treatment of bulk fluctuations to this model and the fluctuation contribution to the perpendicular susceptibility in this model is

$$\chi'_{\perp}(\tau) = \frac{\pi T_c \xi_{\parallel}^2(0)}{3\phi_0^2 d \sqrt{\tau^2 + 2r\tau}} \quad (6.6)$$

Much smaller effect is obtained for the parallel susceptibility on the lines of equation (6.5). Equation (6.6) allows the cross over from 3D to 2D behaviour. Mun-Seog Kim *et al.* [131] have observed fluctuation induced magnetization above T_c in $HgBa_2Ca_3Cu_4O_{10+\delta}$ and a dimensional cross over at $T^* = 121.7K$.

Since diamagnetic susceptibility for superconductors is proportional to λ^{-2} by virtue of equation (6.1), we have attempted in section 6.2 to calculate the fluctuation contribution to the London penetration depth both parallel and perpendicular to the layers of high- T_c copper oxide superconductors within the framework of the modified Lawrence-Doniach model described by the free energy (2.16). The calculations are an extension of the work done by Buzdin and Vuyichit [132] in the context of the GL theory.

6.2. Fluctuation contribution to the London penetration depth

In order to calculate the fluctuation contribution to the London penetration depth we consider the Helmholtz free energy F_s corresponding to the modified LD expression (2.16).

$$\begin{aligned}
 F_s = \sum_n \int & \left[a_1 |\psi_{1,n}^{(\rho)}|^2 + \frac{b_1}{2} |\psi_{1,n}^{(\rho)}|^4 + \frac{\hbar^2}{2m_{\parallel}} \left| \left(\nabla_{\parallel} - \frac{2ie}{\hbar c} A_{\parallel,n} \right) \psi_{1,n}^{(\rho)} \right|^2 \right. \\
 & + a_2 |\psi_{2,n}^{(\rho)}|^2 + \frac{b_2}{2} |\psi_{2,n}^{(\rho)}|^4 + \frac{\hbar^2}{2} \sum_{\ell=x,y} \frac{1}{m'_{\ell}} \left| \left(\frac{\partial}{\partial \ell} - \frac{2ie}{\hbar c} A_{\ell,n} \right) \psi_{2,n}^{(\rho)} \right|^2 \\
 & \left. + t |\psi_{1,n}^{(\rho)} - \psi_{2,n}^{(\rho)} e^{i\chi_n}|^2 + t |\psi_{1,n}^{(\rho)} - \psi_{2,n+1}^{(\rho)} e^{-i\chi_n}|^2 + \frac{\hbar^2}{8\pi} \right] d\rho. \quad (6.7)
 \end{aligned}$$

In the calculation of the fluctuations in high- T_c superconductors for which $\xi \ll \lambda(T)$, we may treat the vector potential A as constant. This is because the characteristic length scale for changes in A is of the order of $\lambda(T)$ whereas the same for ψ fluctuations is of the order of $\xi(T)$. The magnetic field fluctuations can also be neglected for such superconductors. For calculating the fluctuation contribution to the London penetration depth below T_c , we may write the order parameters as

$$\begin{aligned}
 \psi_{1,n} &= \psi_{10,n} + \phi_{1,n} \\
 \psi_{2,n} &= \psi_{20,n} + \phi_{2,n}
 \end{aligned} \quad (6.8)$$

where $\psi_{10}^2 = |a_1|/b_1$ and $\psi_{20}^2 = |a_2|/b_2$ represent the equilibrium values of the order parameters for $T < T_c$ and ϕ represents the contributions from fluctuations. Using (6.7) and (6.8) we calculate the fluctuation contribution δF_s to the free energy in the quadratic approximation over ϕ .

$$\begin{aligned}
 \delta F_s = \sum_n \int & \left\{ \frac{|a_1|}{2} [2 |\phi_{1,n}|^2 + \phi_{1,n}^2 + \phi_{1,n}^{*2}] + \frac{|a_2|}{2} [2 |\phi_{2,n}|^2 + \phi_{2,n}^2 + \phi_{2,n}^{*2}] \right. \\
 & \left. + \frac{\hbar^2}{2m_{\parallel}} \left| \left(\nabla_{\parallel} - \frac{2ie}{\hbar c} A_{\parallel,n} \right) \phi_{1,n} \right|^2 + \frac{\hbar^2}{2} \sum_{\ell=x,y} \frac{1}{m'_{\ell}} \left| \left(\frac{\partial}{\partial \ell} - \frac{2ie}{\hbar c} A_{\ell,n} \right) \phi_{2,n} \right|^2 \right.
 \end{aligned}$$

$$\begin{aligned}
& + t \left[2 |\phi_{1,n}|^2 + |\phi_{2,n}|^2 - \phi_{1,n} \phi_{2,n}^* e^{-i\chi_n} - \phi_{1,n}^* \phi_{2,n} e^{i\chi_n} \right. \\
& \left. + |\phi_{2,n-1}|^2 - \phi_{1,n} \phi_{2,n-1}^* e^{i\chi_n} - \phi_{1,n}^* \phi_{2,n-1} e^{-i\chi_n} \right] d\rho \quad (6.9)
\end{aligned}$$

Fourier transformation of equation (6.9) is performed using the identities

$$\sum_n \int |\phi_n|^2 d\rho = \sum_{\mathbf{K}} |\phi_{\mathbf{K}}|^2, \quad \sum_n \int \phi_n^2 d\rho = \sum_{\mathbf{K}} \phi_{\mathbf{K}} \phi_{-\mathbf{K}}$$

and

$$\sum_n \int \left| \left(\nabla_{\parallel} - \frac{2ie}{\hbar c} A_{\parallel,n} \right) \phi_n \right|^2 d\rho = \sum_{\mathbf{K}} \left(\mathbf{q} - \frac{2e}{\hbar c} A_{\parallel,n} \right)^2 |\phi_{\mathbf{K}}|^2$$

The fluctuation contribution to the free energy can now be written as

$$\begin{aligned}
\delta F_s = \sum_{\mathbf{K}} \left[\frac{a_1}{2} (\phi_{1,\mathbf{K}} \phi_{1,-\mathbf{K}} + \phi_{1,\mathbf{K}}^* \phi_{1,-\mathbf{K}}^*) + C_1 |\phi_{1,\mathbf{K}}|^2 \right. \\
\left. + \frac{a_2}{2} (\phi_{2,\mathbf{K}} \phi_{2,-\mathbf{K}} + \phi_{2,\mathbf{K}}^* \phi_{2,-\mathbf{K}}^*) + D_1 |\phi_{2,\mathbf{K}}|^2 \right] \quad (6.10)
\end{aligned}$$

where

$$C_1 = a_1 + \frac{\hbar^2}{2m_x} \left[\mathbf{q} - \frac{2e}{\hbar c} A_{\parallel} \right]^2 + 2t \left\{ 1 - \gamma \cos \left[\chi_n + \frac{kd}{2} \right] \right\},$$

$$D_1 = a_2 + \frac{\hbar^2}{2m'_x} \left[\mathbf{q} \cos \theta - \frac{2e}{\hbar c} A_{x,n} \right]^2 + \frac{\hbar^2}{2m'_y} \left[\mathbf{q} \sin \theta - \frac{2e}{\hbar c} A_{y,n} \right]^2 + 2t \left\{ 1 - \frac{1}{\gamma} \cos \left[\chi_n + \frac{kd}{2} \right] \right\}$$

and $\mathbf{K} = \mathbf{K}(\mathbf{q}, k)$. \mathbf{q} is the inplane wave vector and k is the c-axis wave vector. θ is the angle which the inplane wave vector makes with the x-axis.

We have set $\gamma^2 = \frac{|\phi_{2,\mathbf{K}}|^2}{|\phi_{1,\mathbf{K}}|^2}$. This introduces an additional phase term which does not affect the derivation of the final result. The general expression for the fluctuation free energy is

$$F_{fl} = -T \ln \int \exp[-\delta H_{eff}(\phi, A)/T] D\phi. \quad (6.11)$$

Taking δF_s as an effective hamiltonian,

$$F_{fl} = -T \ln \int \exp[-\delta F_s(\phi_{1,\mathbf{K}}, \phi_{2,\mathbf{K}}, \mathbf{A})/T] D\phi_{1,\mathbf{K}} D\phi_{2,\mathbf{K}}. \quad (6.12)$$

Writing

$$\phi_{\mathbf{K}} = \phi'_{\mathbf{K}} + i\phi''_{\mathbf{K}},$$

the functional integration in (6.12) is performed over the real and imaginary parts of $\phi_{1,\mathbf{K}}$ and $\phi_{2,\mathbf{K}}$. This gives

$$F_{fl} = -\frac{T_c}{2} \sum_{\mathbf{K}} \left[\ln \frac{\pi^2 T_c^2}{(C_1 C_2 - a_1^2)} + \ln \frac{\pi^2 T_c^2}{(D_1 D_2 - a_2^2)} \right]. \quad (6.13)$$

where

$$C_2 = a_1 + \frac{\hbar^2}{2m_{\parallel}} \left[\mathbf{q} + \frac{2e}{\hbar c} A_{\parallel} \right]^2 + 2t \left\{ 1 - \gamma \cos \left[\chi_n - \frac{kd}{2} \right] \right\}$$

and

$$D_2 = a_2 + \frac{\hbar^2}{2m'_x} \left[\mathbf{q} \cos \theta + \frac{2e}{\hbar c} A_{x,n} \right]^2 + \frac{\hbar^2}{2m'_y} \left[\mathbf{q} \sin \theta + \frac{2e}{\hbar c} A_{y,n} \right]^2 + 2t \left\{ 1 - \frac{1}{\gamma} \cos \left[\lambda_n - \frac{kd}{2} \right] \right\}$$

The additional superconducting current due to fluctuations is

$$\mathbf{j}_{fl} = -c \frac{\delta F_{fl}}{\delta \mathbf{A}}. \quad (6.14)$$

Since we are interested in finding the linear response only, the vector potential \mathbf{A} is considered to be small. Neglecting terms in second and higher powers of \mathbf{A} , we get

$$\frac{\delta F_{fl}}{\delta A_x} = -\frac{T_c}{2} A_x \sum_{\mathbf{K}} \left[\frac{B + C \cos \frac{kd}{2}}{a + b \cos \frac{kd}{2}} + \frac{B' + C' \cos \frac{kd}{2}}{a' + b' \cos \frac{kd}{2}} \right] \quad (6.15)$$

where

$$\begin{aligned} B &= -\frac{4\hbar^2 e^2 q^2}{m_{\parallel}^2 c^2} + \frac{8e^2}{m_{\parallel} c^2} (a_1 + 2t) & C &= -\frac{16e^2 t \gamma}{m_{\parallel} c^2} \\ a &= \frac{\hbar^4 q^4}{4m_{\parallel}^2} + \frac{\hbar^2 q^2}{m_{\parallel}} (a_1 + 2t) + 4a_1 t & b &= -[4a_1 \gamma t + 2q^2 \frac{\hbar^2 \gamma t}{m_{\parallel}}] \\ B' &= -\frac{4\hbar^2 e^2 q^2}{m_x'^2 c^2} \left(-\frac{\cos^2 \theta}{m'_x} + \frac{\sin^2 \theta}{m'_y} \right) + \frac{8e^2}{m_x' c^2} (a_2 + 2t) & C' &= -\frac{16e^2 t}{m_x' \gamma c^2} \\ a' &= \frac{\hbar^4 q^4}{4M_{\theta}^2} + \frac{\hbar^2 q^2}{M_{\theta}} (a_2 + 2t) + 4a_2 t & b' &= -\left[\frac{4a_2 t}{\gamma} + 2q^2 \frac{\hbar^2 t}{\gamma M_{\theta}} \right]. \end{aligned}$$

A similar expression can also be obtained for $\delta F_{fl}/\delta A_y$ by changing the suffix from x to y in equation (6.15). The summation over \mathbf{K} in (6.15) is converted to integration using the prescription (4.6). The integrals are evaluated using standard integrals [100] and the terms in second and higher powers of t are neglected. As suggested by Patton, Ambegaokar and Wilkins [119], we have introduced a cut off energy for short wavelength fluctuations by carrying out the q -integration upto $\frac{1}{\xi_{\parallel}}$. The London penetration depth is given by the expression

$$\lambda_i^{-2} = -\frac{4\pi j_i}{cA_i}. \quad (6.16)$$

The fluctuation contribution to the London penetration depth parallel to the layers can be calculated from equations (6.14), (6.15) and (6.16) as,

$$\delta\lambda_{\ell}^{-2} = \frac{4e^2 T_c}{\hbar^2 c^2 d} \sum_{j=1,2} \left(\frac{M}{m_{\ell}}\right)^{j-1} \left[\ln\left(\frac{2r_j}{3|\tau|}\right) + \gamma^{2i} \left(\frac{1}{4} - \frac{r_j}{2|\tau|}\right) + 2\frac{(|\tau| + r_j)}{|\tau|} \ln\frac{2(r_j + |\tau|)}{3r_j} \right]. \quad (6.17)$$

$$\ell = x, y, \quad M = \frac{1}{\pi} \int_0^{\pi} M_{\theta} d\theta, \quad M_{\theta}^{-1} = \left[\frac{\cos^2 \theta}{m_x'} + \frac{\sin^2 \theta}{m_y'} \right], \quad i = (-1)^{j-1} \text{ and } r_j = \frac{2t}{\alpha_j T_c}.$$

Similarly

$$\frac{\delta F_{fl}}{\delta A_x} = -\frac{4e^2 d^2}{\hbar^2 c^2} \sum_{\mathbf{K}} \left[\frac{b}{a + b \cos \frac{kd}{2}} + \frac{b'}{a' + b' \cos \frac{kd}{2}} \right] \cos \frac{kd}{2}$$

and the fluctuation contribution to the London penetration depth perpendicular to the layers is given by

$$\delta\lambda_c^{-2} = \frac{8te^2 d T_c}{\hbar^4 c^2} \sum_{j=1,2} \gamma^j m_j \left[|\tau| + r_j \ln \frac{2|\tau| + r_j}{r_j} \right]. \quad (6.18)$$

where $m_1 = m_{\parallel}$ and $m_2 = M$. For $|\tau| \ll r_j$,

$$\delta\lambda_{\ell}^{-2} = \frac{4e^2 T_c}{\hbar^2 c^2 d} \sum_{j=1,2} \left[\frac{2|\tau|}{r_j} - \left(2\ln \frac{2}{3} - \frac{\gamma^{2i}}{2}\right) \frac{|\tau|}{r_j} + \ln \frac{|\tau|}{r_j} + \left(3\ln \frac{2}{3} + \frac{\gamma^{2i}}{4}\right) \right] \quad (6.19a)$$

and

$$\delta\lambda_c^{-2} = \frac{24te^2 d T_c}{\hbar^4 c^2} \sum_{j=1,2} \gamma^j m_j |\tau|. \quad (6.19b)$$

At large $|\tau|$ values ($\tau \gg r$),

$$\delta\lambda_{\ell}^{-2} = \frac{4e^2 T_c}{\hbar^2 c^2 d} \sum_{j=1,2} \left(\frac{M}{m_{\ell}}\right)^{j-1} \left[\ln \frac{8|\tau|}{27r_j} + \frac{\gamma^{2j}}{4} \right] \quad (6.20a)$$

and

$$\delta\lambda_c^{-2} = \frac{8te^2 d T_c}{\hbar^4 c^2} \sum_{j=1,2} \gamma^j m_j \left[|\tau| + r_j \ln \frac{2|\tau|}{r_j} \right]. \quad (6.20b)$$

6.3. Conclusion

Our results (6.17) and (6.18) give the fluctuation contribution to the London penetration depth below T_c of copper oxide superconductors described by the modified LD free energy (2.16). Since diamagnetic susceptibility is proportional to λ^{-2} , equations (6.17) and (6.18) which describe the temperature dependence of the fluctuation contribution to λ^{-2} also give the temperature dependence of the superconducting fluctuation diamagnetic susceptibility. $\delta\lambda_c^{-2}$ exhibits $|\tau|$ -linear dependence near T_c as expected [114], but at temperatures further removed from the critical temperature in addition to the linear term a logarithmic contribution also appears. In the case of $\delta\lambda_{\perp}^{-2}$, for $\tau \ll r_j$ in addition to the linear term there appears a $|\tau|^{-1}$ term as well as a logarithmic term. At $\tau \gg r_j$, only the logarithmic term is present. This change in temperature dependence from (6.19) to (6.20) could be the result of dimensional cross over in the fluctuation regime. Comparison of these results show that $\delta\lambda_{\parallel}^{-2}$ has a temperature dependence which is different from that for $\delta\lambda_c^{-2}$. For the parallel field, the fluctuation effects ($\delta\lambda_c^{-2}$) are weakly temperature dependent near T_c where as $\delta\lambda_{\parallel}^{-2}$ diverges logarithmically at T_c .

The ratio of the amplitudes of these fluctuations for applied field perpendicular to the layers to that parallel to the layers is $\hbar^2/2td^2m_{\parallel} = m_{\perp}/m_{\parallel}$ where m_{\perp} is the transverse effective mass. In the GL limit $m_{\perp} = m_{\parallel}$ and the magnitudes become

equal as should be expected. Since $m_{\parallel} \ll m_{\perp}$ for copper oxide superconductors, the fluctuation effect is much smaller for the parallel susceptibility *i.e.* when the field is applied parallel to the layers than that for the perpendicular susceptibility. This conclusion is in agreement with the observations in refs.[128,129,130].

CHAPTER VII

SUMMARY AND CONCLUSIONS

Experimental observations by Kleiner *et al.* [75] and also by Briceno and Zettl [74] indicate a scenario where copper oxide superconductors can be modelled as a superlattice of two dimensional superconducting (SC) sheets consisting of multiple CuO_2 planes sandwiched between non-superconducting (NSC) sheets consisting of multiple metallic planes like the CuO chain layers in $YBCO$. The strongly superconducting layers induce a finite order parameter in weakly superconducting metallic layers through a proximity effect, thus leading to the existence of different order parameters in the two type of layers. This necessitates a modification of the Lawrence-Doniach model on the lines suggested by Bulaevskii and Vagner [143] to describe the observed properties of high- T_c superconductors. This modification of the LD model has been done in section 2.6.

Studies have been carried out in chapter III on the temperature dependence of the critical magnetic fields of cuprates using the modified LD free energy functional (2.16). For temperatures close to T_c , $H_{c2}^{\perp}(T)$ has a positive curvature and becomes a straight line with negative slope further away from T_c . There is qualitative and quantitative agreement with the experimental data for $YBa_2Cu_3O_7$ and $La_{1.87}Ca_{1.13}Cu_2O_4$. Present calculations also predict positive curvature for $H_{c2}^{\parallel}(T)$ graph. D.C.magnetization measurements of the upper critical field of single crystals of $YBa_2Cu_3O_7$ support these predictions. Comparison of models (2.16) and

(3.22) shows conclusively that the non-zero value of the order parameter on the NSC layers which are structurally different from the SC layers is essential to explain the positive curvature of $H_{c2}^{\perp}(T)$ whereas the positive curvature of $H_{c2}^{\parallel}(T)$ can be explained even on the standard LD model. Angular dependence of H_{c2} obtained in this model agrees with experimental observations.

Calculations carried out in section (3.5) shows that the temperature dependence of $H_{c1}^{\parallel}(T)$ changes from a τ -linear dependence near T_c to a $\tau^{\frac{1}{4}}$ dependence further away from T_c . Equations (3.32) and (3.35) giving the temperature dependence of H_{c1}^{\parallel} when fitted to available experimental data explain the upturn in $H_{c1}^{\parallel}(T)$ graph observed experimentally for copper oxide superconductors. The temperature dependence of $H_{c1}^{\perp}(T)$ has also been studied in this section, but could not be compared with experiment due to lack of relevant data.

Thermal fluctuation effects in high- T_c superconductors are much more pronounced than in conventional superconductors. Experimentally fluctuation contribution has been observed in conductivity, specific heat and magnetic susceptibility measurements in *YBCO* superconductors. Fluctuation contribution to the specific heat calculated in chapter IV within the framework of the modified LD model explains the experimentally observed dimensional cross over in the Gaussian fluctuation regime from 3D near T_c to 2D further away from T_c . The calculations point to the existence of a transitional temperature region, instead of a sharp 2D-3D transition, where the two regimes overlap.

Paraconductivity calculations in chapter V show that both σ'_{ab} and the fluctuation specific heat C_f have the same temperature dependence and have an overlapping region of 2D and 3D fluctuations. However, the temperature dependence of σ'_c is different from that of σ'_{ab} . For temperature regions further away from

T_c , σ'_c has a τ^{-2} dependence characteristic of 0D fluctuations instead of the τ^{-1} dependence shown by σ'_{ab} in this region. This observation is appropriate for a 2D regime.

Since diamagnetic susceptibility is proportional to λ^{-2} , the fluctuation contribution below T_c to the London penetration depth both parallel and perpendicular to the layers has been calculated in chapter VI. $\delta\lambda_{ab}^{-2}$ has a temperature dependence which is different from that for $\delta\lambda_c^{-2}$. For the parallel field the fluctuation effects ($\delta\lambda_c^{-2}$) are weakly temperature dependent near T_c whereas $\delta\lambda_{ab}^{-2}$ diverges logarithmically at T_c . Fluctuation effect is seen to be much smaller for the parallel susceptibility than for the perpendicular susceptibility. $\delta\lambda_{ab}^{-2}$ also exhibits a dimensional cross over in the fluctuation regime.

The modified LD model is thus capable of explaining the experimentally observed temperature dependence of the magnetic critical fields and the fluctuation effects of copper oxide superconductors.

References

- [1] H.Kammerling Onnes, Akad van Wetenschappen (Amsterdam) **14**, 113, 818 (1911).
- [2] F.B.Meissner and R.Ochsenfeld, Naturwissen **21**, 787 (1933).
- [3] F.B.Silsbee J.Wash.Acad.Sci.**6**, 597 (1916).
- [4] L.W.Shubnikov, V.I.Khotkevich, J.D.Shepelev and J.N.Rjabinin, Zh.Eksperim.i Theor.Fiz.**7**, 221 (1937).
- [5] A.W.Sleight, A.L.Gillsan and D.E.Bierstedt, Solid state Commun.**17**, 27 (1975).
- [6] J.G.Bednorz and K.A.Mueller, Z.Phys.B; Condensed Matter **64**, 189 (1986).
- [7] M.K.Wu *et al.*, Phys.Rev.Lett.**58**, 908 (1987).
- [8] H.Maeda, Y.Tanaka, M.Fukutomi and T.Asano, Jpn.J.Appl.Phys.**27** L209 (1988).
- [9] Z.Z.Sheng, A.M.Herman, A.El Ali *et al.* Nature **332**, 138 (1988); *ibid*, Phys.Rev.Lett.**60**, 937 (1988); *ibid*, Appl.Phys.Lett.**52** 1738 (1988).
- [10] S.S.Parkin, V.Y.Loe, A.I.Nazzed *et al.* Phys.Rev.**B38**, 6531 (1988).
- [11] R.J.Cava *et al.*, Nature **332**, 814 (1988).
- [12] A.Schilling *et al.*, Nature **363**, 56 (1993).
- [13] S.N.Putlin *et al.*, Nature **362**, 226 (1993).
- [14] L.Gao *et al.*, Physica **C213**, 213 (1993).

- [15] T.Ikemoto, K.Kikuchi, K.Saito, S.Suzuki, Y.Achiba, A.Ugawa and K.Yakushi, JJAP Series 7: Mechanism of Superconductivity 1992; p.367.
- [16] K.Holczer, O.Klein, G.Gurner, J.D.Thompson, F.Diederich and R.J.Wetten, Phys. Rev. Lett.**67**, 271 (1991).
- [17] C.J.Gorter and H.B.G.Casimir, Physica**1**,306 (1934).
- [18] F. and H. London, Proc.Roy.Soc.(London)**A149**, 71 (1935).
- [19] A.B.Pippard, Proc.Roy.Soc.(London)**A216**, 547 (1953).
- [20] V.L.Ginzburg and L.D.Landau, Zh.Eksperim.i Theor.Fiz.**20**, 1064 (1950).
- [21] L.P.Gorkov, Zh.Eksperim.i Theor.Fiz.**36**, 1918 (1959); **37**, 1407 (1959).
- [22] J.Bardeen, L.N.Cooper and J.R.Schrieffer, Phys.Rev.**108**, 1175 (1957).
- [23] A.A.Abrikosov, Dokl.Akad.Nauk.USSR,**86**, 489 (1952).
- [24] A.A.Abrikosov, Zh.Eksperim.i Theor.Fiz.**32**, 1442 (1957).
- [25] H.Frolich, Phys.Rev.**79**, 845 (1950).
- [26] C.A.Reynolds, B.Serin, W.H.Wright and L.B. Nesbitt, Phys.Rev.**78**, 487 (1950).
- [27] E.Maxwell, Phys.Rev.**78**, 477 (1950).
- [28] L.N.Cooper, Phys.Rev.**104**, 1189 (1956).
- [29] I.Giaver, Phys.Rev.Lett.**5**, 147 (1960).
- [30] B.D.Josephson, Phys.Lett.**1** 251 (1962).

- [31] P.W.Anderson and J.M.Rowell, *Phys.Rev.Lett.***10**, 230 (1963).
- [32] S.Uchida, H.Takagi, K.Kitazawa and S.Tanaka, *Jpn.J.Appl.Phys.***26**, L1 (1987).
- [33] H.Takagi, S.Uchida, K.Kitazawa and S.Tanaka, *Jpn.J.Appl.Phys.***26**, L123 (1987).
- [34] D.Vaknin, S.K.Sinha, D.E.Moncton, D.C.Johnston, J.M.Newsam, C.R.Safinya and H.E.King, Jr., *Phys.Rev.Lett.***58**, 2802 (1987).
- [35] Robert N.Shelton in *High Temperature Superconductivity*, Ed., Jeffrey W.Lynn, Springer-Verlag, New York (1990).
- [36] J.M.Tarascon, P.Barboux, B.G.Bagley, L.H.Greene, W.R.Mckinnon and G.W.Hull, in *Chemistry of High Temperature Superconductors*, Ed., D.L.Nelson, M.S.Whittingham and T.F.George (American Chemical Symposium Series, 351 , pp.198-210 (1987).
- [37] S.Uchida, *Physica***C185-189**, 28 (1991); M.Cardona, *Physica C* **185-189**, 65 (1991); C.N.R.Rao and P.Ganguly, *Curr.Sci.***56**, 47 (1987); P.Ganguly, R.A. Mohan Ram, K.Sreedhar and C.N.R.Rao, *J.Phys.***28**, L321 (1987).
- [38] T.Siegrist, S.Sunshine, D.W.Murphy, R.J.Cava and S.M.Zahurak, *Phys. Rev.* **B35**, 7137 (1987).
- [39] F.Beech, S.Miragha, A.Santoro and R.S.Roth, *Phys.Rev.***B35**, 8778 (1987).
- [40] R.J.Cava, B.Batlogg, C.H.Chen, E.A.Rietman, S.M.Zahurak and D.Werder, *Nature***329**, 423 (1987).

- [41] P.Marsh, R.M.Fleming, M.L.Mandich, A.M.Santobo, J.Kwo, M.Hong and L.J.Martinez-Miranda, *Nature***334**, 141 (1988).
- [42] M.Kikuchi, S.Nakajima, Y.Syono, K.Hiraga, T.Oka, D.Shindo, N.Kobayashi, H.Iwasaki and Y.Muto, *Physica* **C158** 79 (1989).
- [43] S.Nakajima, M.Kikuchi, Y.Syono, T.Oka, D.Shindo, K.Hiraga, N.Kobayashi, H.Iwasaki and Y.Muto, *Physica* **C158** 471 (1989).
- [44] T.P.Orlando, K.A.Deliu, S.Foner, E.J.McNiff,Jr., J.M.Tarascon, L.H.Greene, W.R.Mckinnon and G.W.Hull, *Phys. Rev.* **B36**, 2394 (1987).
- [45] Y.Hidaka, M.Oda, M.Suzuki, A.Kutsui, T.Murakami, N.Kobayashi and Y.Muto, in *Superconductivity in Highly Correlated Fermion Systems*, Eds. M.Tachiki, Y.Muto and S.Maekawa (North Holland, Amsterdam, 1987), pp 329-331; W.J.Gallagher, T.K.Worthington, T.R.Dinger, F.Holtzberg, D.L.Kaiser and R.L.Sandstrom, *ibid*, pp 228-232.
- [46] T.R.Dinger, T.K.Worthington, W.J.Gallagher and R.L.Sandstrom, *Phys. Rev. Lett.* **58**, 2687 (1987).
- [47] J.Niemeyer, M.R.Dietrich, C.Politis, *Z.Phys.* **B67**, 155 (1987).
- [48] M.F.Hundley, A.Zettl, A.Stacy and M.L.Cohen, *Phys. Rev.* **B35**, 8000 (1987); N.P.Ong, Z.Z.Wang, J.Clayhold, J.M.Tarascon, L.H.Greene and W.R.Mckinnon, *Phys. Rev.* **B35**, 8807 (1987); M.W.Shafter, T.Penney and B.Olson, *Phys. Rev.* **B36**, 4047 (1987); M.W.Shafter, T.Penney and B.Olson, in *Novel Superconductivity*, Eds. S.A.Wolf and V.Z.Kresin (Plenum, New York, 1987) pp 771-779.

- [49] Z.Z.Wang, J.Clayhold, N.P.Ong, J.M.Tarascon, L.H.Greene, W.R.Mckinnon and G.W.Hull, *Phys. Rev.* **B36**, 7222 (1987); H.Takagi, S.Uchida, H.Iwabuchi, S.Tajima and S.Tanaka, *Jpn. J.Appl. Phys. Series1: Superconducting materials*, p37 (1988).
- [50] L.Forro, M.Raki, C.Ayache, P.C.E.Stamp, J.Y.Henry and J.Rossat-Mignod, *Physica C***153-155**, 1357 (1988).
- [51] J.E.Crow and N.P.Ong in *High-Temperature Superconductivity*, Ed. J.W.Lynn (Springer-Verlag, New York, 1990), pp202-267.
- [52] D.Esteve *et al.*, *Europhys. Lett.* **3**, 1237 (1987).
- [53] C.E.Gough *et al.*, *Nature* **326**, 855 (1987); R.H.Koch *et al.*, *Appl. Phys. Lett.* **51**, 200 (1987); P.Gammel *et al.*, *Phys. Rev. Lett.* **59**, 2592 (1987).
- [54] H.F.C.Hoevers *et al.*, *Physica C***152**, 105 (1988).
- [55] G.M.Eliashberg, *Soviet Phys. JETP* **7**, 696 (1960).
- [56] W.A.Little, *Science* **242**, 1390 (1988).
- [57] O.S.Akhtyamov, *Sov. Phys. JETP Lett.* **3**, 183 (1966).
- [58] W.N.Hardy *et al.*, *Phys. Rev. Lett.* **70**, 3999 (1993); D.A.Bonn *et al.*, *Phys. Rev.* **B47**, 11314 (1993).
- [59] J.E.Somer *et al.*, *Phys. Rev. Lett.* **72**, 744 (1994).
- [60] D.A.Wollman, D.J.Van Harlingen, W.C.Lee, D.M.Ginsberg and A.J.Legget, *Phys. Rev. Lett.* **71**, 2134 (1993); D.A.Wollman, D.J.Van Harlingen, J.Giapintzakis and D.M.Ginsberg, *Phys. Rev. Lett.* **74**, 797 (1995); D.J.Van

Harlingen, Rev. Mod. Phys. **67** 515 (1995); C.C.Tsuei, J.R.Kirtley, C.C.Chi, L.S.Yu-Jahnes, A.Gupta, T.Shaw, J.Z.Sun and M.B.Ketchen, Phys. Rev. Lett. **73**, 593 (1994); A.Mathai, Y.Gim, R.C.Black, A.Amar and F.C.Wellstood, Phys. Rev. Lett. **74**, 4523 (1995).

- [61] A.Junod, A.Bezinge, J.Muller, Physica **C152**, 50 (1988).
- [62] D.J.Scalapino, R.T.Scalettar, and N.E.Bickers, in *Novel Superconductivity*, Eds. S.A.Wolf and V.Z.Kresin (Plenum, New York, 1987) p.475.
- [63] G.Chen and W.A.Goddard, Science **239**, 899 (1988).
- [64] J.R.Schrieffer, X.G.Wen and S.C.Zhang, Phys. Rev. Lett. **60**, 944 (1988).
- [65] I.Furo *et al.*, Phys. Rev. **B36**, 5690 (1987).
- [66] K.B.Lyons *et al.*, Phys. Rev. Lett. **60**, 732 (1988).
- [67] V.L.Ginzberg, Zh. Eksp. Teor. Fiz. **23**, 236 (1952).
- [68] M.Tinkham, *Introduction To Superconductivity*, (McGraw Hill Inc., 1996), Chapt. 4.
- [69] W.E.Lawrence and S.Doniach, in *Proc. of the 12th Int. Conf. on Low-Temperature Physics, Kyoto, 1970*, Ed. E.Kanda (Keigaku, 1970) p.361.
- [70] Byung Deok Yu, Hanchil Kim and J.Ihm, Phys. Rev. **B45**, 8007 (1992).
- [71] J.Yu, S.Massidda and A.J.Freeman, Physica **C152**, 273 (1988); D.R.Hamann and L.F.Mattheiss, Phys. Rev. **B36**, 7248 (1987).
- [72] P.A.Sterne and C.S.Wang, J.Phys. **C21**, L949 (1988).

- [73] P.G. de Gennes, *Superconductivity of Metals and Alloys* (Benjamin, New York, 1966), p.234.
- [74] G.Briceno and Z.Zettl, *Solid State Commun.* **70**, 1055 (1989).
- [75] R.Kleiner, F.Seinmeyer, G.Kunkel and P.Muller, *Phys. Rev. Lett.* **68**, 2394 (1992); R.Kleiner and P.Muller, *Phys. Rev.* **B49**, 1327 (1994).
- [76] U.Welp, W.K.Kwok, G.W.Crabtree, K.G.Vandervoort and J.Z.Liu, *Phys. Rev. Lett.* **62**, 1908 (1989).
- [77] D.Prober, R.Schwall and M.Beasley, *Phys. Rev.* **B21**, 2717 (1980); Y.Yeshurn and A.Malozemoff, *Phys. Rev. Lett.* **60**, 2202 (1988).
- [78] H.Claus, G.W.Crabtree, J.Z.Liu, W.K.Kwok and A.Umezawa, *J.Appl. Phys.* **63**, 4170 (1988).
- [79] Kyoichikinoshita and Azusa Matsuda, *Physica C* **179**, 39 (1991).
- [80] U.Welp, W.K.Kwok, G.W.Crabtree, K.G.Vandervoort and J.Z.Liu, *Phys. Rev.* **B40**, 5263 (1989).
- [81] H.Adrian, W.Assmus, A.Hohr, J.Kowalewski, H.Spille and F.Steglich, *Physica C* **163-163**, 329 (1989).
- [82] A.Schilling, F.Hulliger and H.R.Ott, *Z.Phys.B-Condensed Matter* **82**, 9 (1991); A.Schilling, F.Hulliger and H.R.Ott, *Physica C* **168**, 272 (1990); V.G.Fleisher, R.Laiho, E.Lahderanta, Yu P. Stepanov, K.B.Traito, *Physica C* **264**, 295 (1996).
- [83] T.Shibauchi, N.Katase, T.Tamegai and K.Uchinokura, *Physica C* **264** 227 (1996).

- [84] J.P.Strobel, A.Thoma, B.Hensel, H.Adrian and G.Saemann-Ischenko, *Physica C* **153-155**, 1537 (1988); V.V.Moshchalkov, J.Y.Henry, C.Marin, J.Rossat-Mignod and J.F.Jacquot, *Physica C* **175**, 407 (1991).
- [85] S.E.Inderhees, M.B.Salamon, N.Goldenfeld, J.P.Rice, B.G.Pazol, D.M.Ginsberg, J.Z.Liu, G.W.Crabtree, *Phys. Rev. Lett.* **60**, 1178 (1988); E.Bonjour, R.Calemczuk, J.Y.Henry and A.F.Khoder, *Phys. Rev.* **B43**, 106 (1991).
- [86] B.Oh *et al.*, *Phys. Rev.* **37**, 7861 (1988); A.Kapitulnik, *Physica C* **153-155**, 520 (1988); J.A.Veira and F.Vidal, *Phys. Rev.* **B42**, 8743 (1990); A.V.Pogrebnyakov, L.D.Yu, T.Freltoft and P.Vase, *Physica C* **183**, 27 (1991).
- [87] E.C.Lee, R.A.Klemm and D.C.Johnston, *Phys. Rev. Lett.* **63**, 1012 (1989); K.Kanoda *et al.*, *J.Phys. Soc. Jpn.* **57**, 1554 (1988).
- [88] Khandker F. Quader and Elihu Abrahams, *Phys. Rev.* **B38**, 19977 (1988).
- [89] C.J.Lobb, *Phys. Rev.* **B36**, 3930 (1987).
- [90] V.V.Shmidt, *Zh. Exp. Teor. Phys. Pis Red.* **3**, 141 (1966).
- [91] J.F.Cochran, *Ann. Phys. NY* **19**, 186 (1962).
- [92] D.J.Thouless, *Ann. Phys. NY* **10**, 553 (1960).
- [93] L.G.Aslamazov and A.I.Larkin, *Phys. Lett.* **26A**, 238 (1968); L.G.Aslamazov and A.I.Larkin, *Fiz. Tverd. Tela* **10**, 1104 (1968).
- [94] R.A.Ferrell, *J.Low. Temp. Phys.* **1**, 241 (1969).
- [95] G.D.Zally and J.M.Mochel, *Phys. Rev. Lett.* **27**, 1710 (1971); G.D.Zally and J.M.Mochel, *Phys. Rev.* **B6**, 4142 (1972).

- [96] L.Gunther and L.W.Gruenberg, *Solid State Commun.* **10**, 567 (1972).
- [97] S.Grossmann, P.H.Richter and C.Wissel, *Solid State Commun.* **11**, 433 (1972).
- [98] W.E.Masker, S.Marcelja and R.D.Parks, *Phys. Rev.* **188**, 745 (1969); A.J.Bray and G.Rickayzen, *J.Phys. F: Metal Phys.* **2**, L109 (1972); G.Rickayzen and A.J.Bray, *J.Phys. F: Metal Phys.* **3**, L134 (1973).
- [99] L.N.Bulaevskii, *Int.J. Mod. Phys.* **B4**, 1849 (1990).
- [100] I.S.Gradshteyn and I.M.Ryzhik, *Table of Integrals, Series and Products*, (Academic Press, New York, 1965).
- [101] A.A.Abrikosov, *Fundamentals of the Theory of Light* (North Holland, Amsterdam, 1988).
- [102] E.Abrahams and J.W.F. Woo, *Phys. Lett.* **27A**, 117 (1968).
- [103] A.Schmid, *Z.Phys.* **215**, 210 (1968).
- [104] W.J.Skocpol and M.Tinkham, *Rep. Prog. Phys.* **38**, 1049 (1975).
- [105] J.I.Gittleman, R.W.Cohen and J.J.Hanak, *Phys. Lett.* **29A**, 56 (1969).
- [106] R.E.Glover, *Phys. Lett.* **25A**, 542 (1967).
- [107] M.Strongin, O.F.Kammerer, J.Crow, R.S.Thompson and H.L.Fine, *Phys. Rev. Lett.* **20**, 922 (1968); A.K.Bhatnagar, P.Kahn and T.J.Zammit, *Solid State Commun.* **8**, 79 (1970).
- [108] K.Maki, *Prog. Theor. Phys.* **39**, 897 (1968); K.Maki, *Prog. Theor. Phys.* **40**, 193 (1968); R.S.Thompson, *Phys. Rev.* **B1**, 327 (1970); R.S.Thompson, *Physica* **55**, 296 (1971).

- [109] J.Kirtley, Y.Imry and P.K.Hansma, *J.Low. Temp. Phys.* **17**, 247 (1974).
- [110] B.Oh,K.Char,A.D.Kent,M.Naito,M.R.Beasley,T.H.Geballe, R.H.Hammond and A.Kapitulnik, *Phys. Rev.* **B37**, 7861 (1988); T.A.Friedmann, J.P.Rice, John Giapintzakis and D.M.Ginsberg, *Phys. Rev.* **B39**, 4258 (1989).
- [111] L.Reggiani, R.Vagho and A.A.Varlamov, *Phys. Rev.* **B44**, 9541 (1991).
- [112] A.K.Ghosh, S.K.Bandyopadhyay and A.N.Basu, *Mod. Phys. Lett.* **B11**, 1013 (1997).
- [113] F.London, *Superfluids Vol.1* (Wiley, New York, 1950).
- [114] M.Tinkham, *Introduction to Superconductivity, 2nd Ed.* (McGraw Hill Inc., New York, 1996).
- [115] R.A.Buhrman and W.P.Halperin, *Phys. Rev. Lett.* **30**, 692 (1973).
- [116] R.A.Buhrman, W.P.Halperin and W.W.Webb, *Proc. 13th Int. Conf. on Low Temp. Phys.* (1974).
- [117] A.Schmid, *Phys. Rev.* **180**, 527 (1969).
- [118] J.P.Gollub, M.R.Beasley, R.S.Newbower and M.Tinkham, *Phys. Rev. Lett.* **22**, 1288 (1969).
- [119] B.R.Patton, V.Ambegaokar and J.W.Wilkins, *Solid State Commun.* **7**, 1287 (1969).
- [120] J.P.Gollub, M.R.Beasley and M.Tinkham, *Phys. Rev. Lett.* **25**, 1646 (1970).
- [121] J.P.Gollub, M.R.Beasley and M.Tinkham, *Proc. 12th Int. Conf. on Low Temperature Physics, Kyoto (Keigaku, Tokyo)*, 271 (1970).

- [122] NIL
- [123] P.A.Lee and M.G.Payne, Phys. Rev. Lett. **26**, 1537 (1971); P.A.Lee and M.G.Payne, Phys. Rev. **B5**, 923 (1972).
- [124] J.Kurkijarvi, V.Ambegaokar and G.Eilenberger, Phys. Rev. **B5**, 868 (1972).
- [125] K.Maki and H.Takayama, J.Low Temp. Phys. **5**, 313 (1971).
- [126] K.P.Usadel, Solid State Commun. **11**, 1699 (1972).
- [127] D.E.Prober, M.R.Beasley and M.Tinkham, Proc. 13th Int. Conf. on Low Temperature Physics, Boulder, Vol.III, Ed. W.S.O'Sullivan (Plenum, New York), 428 (1972).
- [128] T.Tsuzuki, J.Low Temp. Phys. **9**, 525 (1972).
- [129] R.A.Klemm, M.R.Beasley and A.Luther, Phys. Rev. **B11**, 5072 (1973).
- [130] R.R.Gerhardts, Phys. Rev. **B9**, 2945 (1974).
- [131] Mun-Seog Kim, Wan-Seon Kim, Sunk-Ik Lee, Seong-Cho Yu, E.S.Itskevich and I.Kuzemskaya, Physica **C282-287**, 1987 (1997).
- [132] A.Buzdin and B.Vuyichit, Mod. Phys. Lett. **B4**, 485 (1990).
- [133] H.L.Kaufman and F.de la Cruz, Solid State Commun. **9**, 1729 (1971); H.L.Kaufman, F.de la Cruz and G.Seidel, Proc. 13th Int. Conf. on Low Temp. Phys., Boulder, 1972, Vol.III, Ed. W.S.O'Sullivan (Plenum, New York) pp 673-6.
- [134] W.S.Corak, B.B.Goodman, C.B.Satterthwaite and A.Wexler, Phys. Rev. **96**, 1442 (1954); Phys. Rev. **102**, 656 (1956).

- [135] C.C.Torardi, M.A.Subramaniam, J.C.Calabrese, J.Gopalakrishnan, K.J.Morrissey, T.R.Askew, R.B.Flippen, U.Chowdhry and A.W.Sleight, *Science*, **240**, 631 (1988).
- [136] C.P.Bean, *Phys. Rev. Lett.* **8**, 250 (1962).
- [137] L.C.Bourne, A.Zettl, T.W.Barbee, III and M.L.Cohen, *Phys. Rev.* **B36**, 3990 (1987); Q.Li *et al.*, *Solid State Commun.* **65**, 869 (1988).
- [138] D.R.Harshman *et al.*, *Phys. Rev.* **B36**, 2386 (1987).
- [139] B.Pumpin *et al.*, *Phys. Rev.* **B42**, 8019 (1990).
- [140] W.C.Lee and D.M.Ginsberg, *Phys. Rev.* **B44**, 2815 (1991); L.Krusin-Elbaum, R.L.Greene, F.Holtzberg, A.P.Malozemoff and Y.Yeshurun, *Phys. Rev. Lett.* **62**, 217 (1989); J.Schoener, J.Karpinski, E.Kaldis, J.Keller and P.de la Mora *Physica* **C166**, 145 (1990).
- [141] Shi-Min Cui and Chien-Hua Tsai, *Phys. Rev.* **B44**, 12500 (1991).
- [142] Ching-ping S. Wang in *High Temperature Superconductivity*, Ed. Jeffrey W. Lynn (Springer Verlag, New York, 1990), pp 122-161.
- [143] L.N.Bulaevskii and I.D.Vagner, *Phys. Rev.* **B43**, 8694 (1991).
- [144] Jeffrey W. Lynn in *High Temperature Superconductivity*, Ed. Jeffrey W. Lynn (Springer Verlag, New York, 1990), pp 268-296.
- [145] S.Theodorakis and Z.Tesanovic, *Phys. Lett.* **A132**, 372 (1988); *Phys. Rev.* **B40**, 6659 (1989).
- [146] N.Boccaro, J.P.Carton and G.Sarma, *Phys. Lett.* **A49**, 165 (1974).

- [147] Landau and Lifshitz, *Statistical Physics Part I* (Pergamon Press, 1989), Sec.147.
- [148] R.E.Prange, Phys Rev.**B1**, 2349 (1970).
- [149] D.Saint James, G.Sarma and E.J.Thomas, *Type II Superconductivity* (Pergamon Press, 1969), p.23.
- [150] C.Baraduc and A.Buzdin, Phys. Lett. **A171**, 408 (1992).